MODELLING THE ECOLOGY AND EVOLUTION OF MICROORGANISMS

by

ROBERT JAMES CLEGG

A thesis submitted to the University of Birmingham

for the degree of DOCTOR OF PHILOSOPHY

Centre for Systems Biology
School of Biosciences
College of Life and Environmental Sciences
University of Birmingham
August 2014
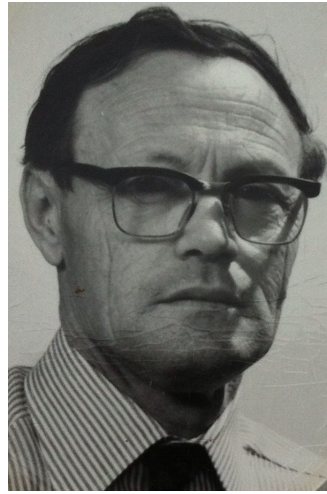
UNIVERSITY OF BIRMINGHAM

ABSTRACT

Theoretical models in microbiology have a relative short but successful history. Research presented in this thesis explores the evolutionary origin of aging and the methods used to quantify syntrophic cooperation between microbial species that are distantly related. The mathematical and computational tools used in doing so are developed and discussed in detail.

Microorganisms were long thought to be capable of immortality until recent evidence demonstrated otherwise. Theoretical models suggest that aging strategies sacrificing repair for segregation of damage have highest evolutionary fitness, but this is not reflected in nature. The model developed here corrects this view of aging through more realistic assumptions regarding repair.

Many estimates of the rate of interspecies metabolite transfer are based on spatial point pattern statistics and assumptions regarding cell surface concentrations. These are shown to be very inaccurate, but proposed alternatives required greater parameterisation. The system is sensitive to difficulties in determining consumption affinity constants, an issue also raised by previous authors.

Dedicated to my late grandfather, Leonard Clough (1924-2014)

Grandad, your love and support will always be remembered

ACKNOWLEDGEMENTS

CONTENTS

LIST OF FIGURES

LIST OF TABLES

LIST OF ABBREVIATIONS & SYMBOLS

CV   Coefficient of variation

EPS   Extracellular Polymeric Substances

FEM   Finite Element Method

IbM   Individual-based Model

iDynoAge   Individual-based Dynamics of microbial Aging

iDynoMiCS   Individual-based Dynamics of Microbial Communities Simulator

IMT   Interspecies metabolite transfer

ODE   Ordinary Differential Equation

PDE   Partial Differential Equation

ND   Not determined

R-D   Reaction-Diffusion

SD   Standard deviation

XFP   Expressing fluorescent protein

CHAPTER 1: SYNOPSIS

With his now famous essay, "Nothing makes sense in biology except in the light of evolution", Theodosius Dobzhansky aimed to persuade American biology teachers that the theory of evolution by natural selection posed no threat to any religious beliefs they might hold (Dobzhansky 1973). His success in this is impossible to quantify, although it is fair to say that it was incomplete. Nevertheless, the title itself has achieved a measure of fame, both within the educational debate and among biologists primarily concerned with the progress of their subject. This is desirable in the sense that the statement is largely true, especially when compared to the anti-scientific ideas that Dobzhanksy argued against, and yet unfortunate that many have accepted such a simplification as the whole truth.

The title first appeared in the text of an essay he wrote a decade earlier, discussing the differing approaches of molecular and organismic biology (Dobzhansky 1964). Addressed to an academic audience, whose acceptance of evolution he could assume, Dobzhansky expanded on his understanding of what Darwin and Wallace's theory entailed:

> "Organic diversity is necessary because no single genotype can possess a superior adaptedness in all physical environments… The more different organisms inhabit a territory, the greater becomes the variety of ecological niches."

Dobzhansky appreciated that evolution requires adaptation not only to the physical environment, but also to the biological environment; competitors, co-operators, predators, prey and parasites may all play a role in the evolution of a species (Dawkins 1988; Yoshida et al. 2003; Johnson and Stinchcombe 2007; Cavender-Bares et al. 2009; Evans, Bithell, et al. 2013; Soyer and O'Malley 2013).

However, separating ecology and evolution is often necessary when trying to unravel the intricacies of life. Stay true to reality by including both in a model, be it physical or theoretical, and the problem often becomes intractable. Assume however that one stays the same while the other changes, and one begins to make progress. The effect of complexity on the difficulty of a problem, it would seem, is greater than additive (Adami 2002; C. Koch 2012).

Researchers have long justified this separation by pointing to the differences in time-scale: evolution is best observed over many generations, whereas the ecological interactions between species may change rapidly over an individual's lifespan. Evolution is often seen as too slow to have a noticeable effect on ecology, and ecology fluctuates so much that only its overall trend is considered relevant to evolution. Time-scale separation has been hugely successful in biology, but voices of caution should be heard and healthy scepticism applied (Gunawardena 2014a).

Nowhere is this more apparent than in the world of microorganisms, where short generation times have made their use in studies both of evolution (Elena and Lenski 2003; Adams 2004) and of ecology (Jessup et al. 2004; Benton et al. 2007) particularly interesting. The prevalence of horizontal gene transfer (HGT) between microbes, mediated by plasmids and phages, also means that genes can evolve faster than their cellular hosts are able to reproduce (Levin 2010). Such is the effect of HGT on the evolution of microbes that it has sparked a lively debate on what constitutes a microbial species (see e.g., Rosselló-Mora and Amann 2001; Boucher et al. 2003; Kurland, Canback, and Berg 2003; Barberán, Casamayor, and Fierer 2014)

Microbes are fascinating organisms to study in their own right: the importance of their roles in digestion, disease, wastewater treatment, global nutrient cycles, and many other processes is difficult to overstate. Yet a number of researchers have pointed out that, as in much of biology, the ecology of microbes has been neglected when studying their evolution, and vice versa (Feldgarden et al. 2003; Jessup et al. 2004; Haruta et al. 2009; Cordero and Polz 2014)

Haruta et al. (2009) reason that, as studying isolated microbial cultures is equivalent to the purification and *in vitro* examination of proteins, so we should attempt to knock-out (or add) individual species in mixed communities in much the same way that genes encoding proteins of interest are often knocked-out during *in vivo* experiments (Galli-Taliadoros et al. 1995). They

identify defined mixed cultures in chemostats as a useful setting in which to first develop this field (Haruta et al. 2009), and researchers have already made progress (e.g., Miller et al. 2010). Sharon Walker's group have even developed an *in vitro* model of effluent flow through a human colon, into a septic tank, and finally ending up in groundwater. This system was monitored with and without a pathogenic strain of *Escherichia coli* and assessed it in a number of ways, including phenotypic characterisation and short-chain fatty acid production. Although the abundance of Proteobacteria (including the pathogen) barely changed, Firmicutes replaced Bacteriodes as the dominant phylum as a result of the pathogen's presence. Furthermore, acetic acid and butyric acid productions changed significantly in a manner that may aid the pathogen to produce virulence factors and establish an ecological niche (Marcus et al. 2013).

In addition to laboratory models, theoretical models have long played a role in biological research (Miller et al. 2010). Theoretical models are easily confused with statistical models due to their shared reliance on mathematical – and more recently, computational – techniques. The difference between them is fundamentally one of approach: a statistical model examines data to discover patterns and relationships within them, whereas a theoretical model derives conclusions logically from assumptions made by the researcher.

Just as the conclusions of a statistical model are only as good as the quality of the data provided, the conclusions of a theoretical model are only as good as the assumptions made in forming it. An overlap in this fallibility occurs when the theoretical model requires input from the statistical: one must always take care to check how sensitive the accuracy of a theoretical model is to errors in parameter values. Yet there is a growing acceptance that the sensitivity of theoretical models should not only be checked with regard to parameters, but to structural changes also (Adamson and Morozov 2013)

A decision must also be made about how generally applicable a particular model should be. Generality itself is beneficial, yet it often involves simplifications that detract from realism and/or precision in a model (Levins 1966). A number of researchers have argued that this cost is too great (Evans, Grimm, et al. 2013a), but others have pointed out that lack of data availability often constrains the development of complex models (Lonergan 2014). A reasonably complex model, thoroughly explored for sensitivity to differences in parameters or structure that may well exist between the particular systems being modelled, seems the best compromise in many situations.

In any case, detailing the simplifying assumptions made in the development of a model is standard practice (Grimm et al. 2006); justifying these through evidence and persuasive argument is, however, often seen as only an optional extra. I organised a one-day workshop on this subject, held on the 7th May 2014: researchers from a variety of different scientific backgrounds shared their experiences in making and justifying the simplifying assumptions of their theoretical models. Similar difficulties arise when modelling systems in different subjects, and yet there was much to be learnt from others' approaches to solving these.

It is tempting to draw a parallel between the questions in biology that have characterised its progress in the 20th Century and the problems listed by David Hilbert, which largely set the mathematical agenda over that period (Hilbert 1902). Among these mathematical problems is the question of how densely spheres can be packed: the solution, conjectured by Johannes Kepler in 1611, was not proven until recently (T. C. Hales 1992). This result will be of use in Chapter 2, where the packing of spheres in space is compared to circles on a plane.

Several lists of questions in specific fields of biology have been proposed (see e.g., Maynard Smith and Szathmáry 1995) but many of the questions on these have been open for far longer. Some of the questions on a hypothetical list from over a century ago, such as the

mechanism of genetic inheritance (Watson and Crick 1953), may have since been answered whereas the solutions to others, such as the molecular origin of life (Pross and Pascal 2013) and the transition from unicellularity to multicellularity (Bonner 1998; Grosberg and Strathmann 2007; Ratcliff et al. 2012), have proved far harder.

In this thesis I make small contributions to our understanding of two major problems in (micro)biology, not listed above. In Chapter 3 the evolutionary origin of aging is investigated and in Chapter 4 a form of cooperation is explored. Mathematical techniques are employed throughout this research, and this approach is discussed beforehand in Chapter 2.

CHAPTER 2: MODELLING MICROBES AS INDIVIDUAL CELLS

While traditionally considered as homogenous populations, the view that microbes should be treated as individual cells has gained traction in recent years (Maynard Smith et al. 1993; Davidson and Surette 2008; Ferrer, Prats, and Lopez 2008; Ackermann 2013). This widening acceptance of the individuality of microbes is largely thanks to the technological advances allowing science to study them as such, both in the laboratory and in computer simulations (Lencastre Fernandes et al. 2011; Kreft et al. 2013). This chapter focuses on the latter approach and its recent progress, but naturally, experimental findings are discussed where they have aided or inspired theoretical understanding.

Growth models are fundamental to many models of microbial communities, especially where there is competition over growth-limiting resources. Since growth depends on reactions, it is inevitable that many of these growth models bear a striking resemblance to models of reaction kinetics; the justification for this approach is discussed.

Both are used extensively in the research presented in this this thesis: the growth model Monod kinetics is used in Chapter 3, where aging cells are modelled competing for resources against competing strategies; and reaction kinetics form the basis of Chapter 4, where syntrophic communities exchange hydrogen produced and consumed by reactions they catalyse. The research presented in Chapter 3 was performed using the software iDynoMiCS, and so this is introduced in some detail here. A minor result, comparing simulations in two and in three dimensions, is also given using this software.

2.1. Reactions leading to growth

The key process leading to evolutionary fitness is reproduction (Darwin 1859; Dawkins 1988; Roff 2008), as this gives greater abundance to a particular species or gene. The process of reproduction can itself be broken down into sub-processes, chiefly survival and growth. An organism that is killed, say by predation or disease, before it is ready to reproduce will not be directly represented in the next generation. Likewise, reproduction without growth is impossible;

even ignoring the material required for genome duplication, it is easy to imagine the fate of a population whose numbers increase but whose total mass remains constant.

Growth requires the uptake of mass from the environment in order to increase the size of the organism. However, this mass is rarely structured in chemical compounds suitable for the organism's composition, and so the organism must produce enzymes catalysing reactions in order to obtain the compounds that are, a process known as anabolism (see Box 1). Many of these anabolic reactions will be endergonic, and so it will be necessary to couple these with exergonic reactions consuming abiotic sources such as sunlight or organic molecules produced by other organisms (Russell and Cook 1995). Given the complexity of metabolism, this section revisits enzyme kinetics before looking at how these are incorporated into models of microbial growth.

Box 1. Terms Commonly Used in Describing Chemical Processes.

- **Affinity** inclination for molecules to bind in order to react, i.e. the reaction rate will be approximately proportional to the substrate concentration when it is low; note that a *greater* affinity constant typically signifies *lower* affinity
- **Anabolism** constructing complex molecules
- **Catabolism** breaking down chemical compounds in order to release free energy and/or smaller molecules
- **Endergonic** requiring the input of free energy from an external source, e.g. a separate exergonic reaction (Gibb's free energy $\Delta G > 0$)
- **Exergonic** producing excess free energy that may be absorbed by an endergonic reaction, dissipated as heat, etc (Gibb's free energy $\Delta G < 0$)
- **Gibb's free energy** (G) formally defined in terms of enthalpy (H), entropy (S) and temperature (T), such that $G = H - TS$; quantifies the maximum energy available for gain or loss when performing a reaction (see Endergonic, Exergonic)
- **Metabolism** all chemical processes occurring within an organism; combines anabolism and catabolism

2.1.1. Enzyme kinetics

The family of enzyme kinetics models under consideration supposes a reaction converting substrate S into a product P to be catalysed by a single (or rate-limiting) enzyme E via a enzyme-substrate complex ES. The reaction should be split into two pairs of elementary steps:

$$E + S \underset{k_{-1}}{\overset{k_{+1}}{\rightleftharpoons}} ES \underset{k_{-2}}{\overset{k_{+2}}{\rightleftharpoons}} E + P \qquad (2.1)$$

where k_{+1}, k_{+2}, k_{-1}, and k_{-2} are rate constants. A more comprehensive model would include the enzyme-product complex EP; known as Langmuir-Hinshelwood kinetics (Table 2.1), they are commonly used in surface chemistry but deemed unnecessary elsewhere (Moser 1985).

By assuming substrate to be far more abundant than enzyme or product, k_{-2} to be zero (i.e. an irreversible reaction from ES to $E + P$) and that substrate-binding and -unbinding was much faster than product formation (a technique known as timescale-separation), Leonor Michaelis and Maud Menten derived the differential expression

$$\frac{d[P]}{dt} = \frac{r_{max}[S]}{K_M + [S]} \qquad (2.2)$$

where [...] denotes molar concentration, $r_{max} = k_{+2}E_{tot}$ is the upper bound on the reaction rate and $K_M = k_{-1}/k_{+1}$ the affinity constant (Michaelis and Menten 1913; Gunawardena 2014a). Briggs and Haldane suggested a decade later that a quasi-steady state where $\frac{d[ES]}{dt} = 0$ was a more appropriate assumption than time-scale separation but this did not change the form of the equation, merely the definition of the affinity constant: $K_M = (k_{-1} + k_{+2})/k_{+1}$. In their words, "Michaelis and Menten's analysis... still holds good" (G. E. Briggs and Haldane 1925).

It is interesting to note that, from a historical viewpoint, Michaelis-Menten kinetics hit a "sweet spot" in terms of complexity. The Van Sylke-Cullen model assumes both steps to be irreversible (i.e. $k_{-1} = k_{-2} = 0$) and is now largely confined to textbooks and historical reviews (Van Sylke and Cullen 1914; Chen, Niepel, and Sorger 2010). On the other hand, assuming

product formation to be reversible doubles the number of parameters needed from two to four, deterring use of reversible Michaelis-Menten kinetics, also known as the Haldane Equation (Moser 1985; Gunawardena 2012):

$$\frac{d[P]}{dt} = \frac{V_{f,max}\left(\frac{[S]}{K_{f,M}}\right) - V_{r,max}\left(\frac{[P]}{K_{r,M}}\right)}{1 + \left(\frac{[S]}{K_{f,M}}\right) + \left(\frac{[P]}{K_{r,M}}\right)}$$

(2.3)

where $V_{f,max} = k_{+2}E_{tot}$ denotes the maximum forward reaction rate, $V_{r,max} = k_{-1}E_{tot}$ the maximum reverse reaction rate, $K_{f,M} = (k_{-1} + k_{+2})/k_{+1}$ the forward affinity constant, and $K_{r,M} = (k_{-1} + k_{+2})/k_{-2}$ the reverse affinity constant.

Since accumulation of P causes the rate of its own production to decline it will not be completely consumed by the reaction, but instead $[S]$ and $[P]$ will reach an equilibrium. Note that Equation 2.3 can be rearranged, as in Table 2.1; while the form given there is neater, the symmetry of the form above emphasizes the fact that S and P are essentially interchangeable.

Table 2.1. Summary of kinetics models for a simple reaction catalyzed by an enzyme.

A summary of the enzyme kinetics used that do not involve branching, i.e. the reaction can be described linearly, as in Equation 2.1, and has no alternate pathways. An enzyme E binds to a substrate S in order to produce a product P. Table adapted and corrected from Moser (1985). Note that for all five models the form of the rate expression, but not the definition of the parameters, is the same when $[P] = 0$.

Mechanism	Rate	Parameters
$E + S \xrightarrow{k_{+1}} ES \xrightarrow{k_{+2}} E + P$ Van Sylke-Cullen	$r([S]) = \dfrac{r_{max}[S]}{K_S + [S]}$	$r_{max} = k_{+2}[E_{tot}]$ $K_S = k_{+2}/k_{+1}$
$E + S \underset{k_{-1}}{\overset{k_{+1}}{\rightleftharpoons}} ES \xrightarrow{k_{+2}} E + P$ Michaelis-Menten (Briggs-Haldane)	$r([S]) = \dfrac{r_{max}[S]}{K_S + [S]}$	$r_{max} = k_{+2}[E_{tot}]$ $K_S = (k_{-1}+k_{+2})/k_{+1}$
$E + S \underset{k_{-1}}{\overset{k_{+1}}{\rightleftharpoons}} ES \underset{k_{-2}}{\overset{k_{+2}}{\rightleftharpoons}} E + P$ reversible Michaelis-Menten (Haldane)	$r([S],[P]) = \dfrac{r_{max}\left([S] - v\dfrac{[P]}{K_{eq}}\right)}{K_S + [S] + \dfrac{[P]}{K_{eq}}}$	$r_{max} = k_{+2}[E_{tot}]$ $K_S = (k_{-1}+k_{+2})/k_{+1}$ $K_{eq} = k_{+1}/k_{-2}$ $v = k_{-1}/k_{+2}$
$E + S \underset{k_{-1}}{\overset{k_{+1}}{\rightleftharpoons}} ES \xrightarrow{k_{+2}} EP \underset{k_{-3}}{\overset{k_{+3}}{\rightleftharpoons}} E + P$ Langmuir-Hinshelwood	$r([S],[P]) = \dfrac{r_{max}[S]}{K_S + [S] + K_P[P]}$	$r_{max} = k_{-1}k_{+2}[E_{tot}]/k_{+1}$ $K_S = (k_{-1}+k_{+2})/k_{+1}$
$E + S \underset{k_{-1}}{\overset{k_{+1}}{\rightleftharpoons}} ES \underset{k_{-2}}{\overset{k_{+2}}{\rightleftharpoons}} EP \underset{k_{-3}}{\overset{k_{+3}}{\rightleftharpoons}} E + P$ reversible Langmuir-Hinshelwood	$r([S],[P]) = \dfrac{r_{max}\left([S] - v\dfrac{[P]}{K_{eq}}\right)}{K_S + [S] + \dfrac{[P]}{K_{eq}}}$	$r_{max} = \dfrac{k_{+2}k_{+3}[E_{tot}]}{(k_{-2}+k_{+2}+k_{+3})}$ $K_S = \dfrac{(k_{-2}k_{-1}+k_{-1}k_{+3}+k_{+2}k_{+3})}{k_{+1}(k_{-2}+k_{+2}+k_{+3})}$ $K_{eq} = \dfrac{k_{+1}(k_{-2}+k_{+2}+k_{+3})}{k_{-3}(k_{-2}+k_{-1}+k_{+2})}$ $v = \dfrac{k_{-2}k_{-1}(k_{-2}+k_{+2}+k_{+3})}{k_{+2}k_{+3}(k_{-2}+k_{-1}+k_{+2})}$

2.1.2. Growth dependence on substrate

For a time, living cells were considered by many to be little more than "bags of enzymes" performing metabolism in order to grow, guided by the instructions encoded in the genome. While this line of thinking is long out-dated (Mathews 1993; L. Shapiro, McAdams, and Losick 2009), a vestige exists in the modelling of microbial metabolism:

> "Microbial activities like growth and product formation can be regarded as a sequence of enzymatic reactions… This metabolic network including autocatalysis, however, can be simplified with the aid of the rate-determining-step concept."
>
> (Moser 1985).

Following the success of Michaelis and Menten in providing a mathematical framework to enzyme kinetics, the contribution of Jacques Monod giving microbial growth an equivalent foundation was warmly received (Monod 1949; Ferenci 1999). According to Monod kinetics, growth rate is dependent on the concentration of a single, limiting substrate, S, such that:

$$\frac{dX}{dt} = \frac{\mu_{max}[S]}{K_S + [S]} X \qquad (2.4)$$

where X denotes biomass, μ_{max} the maximum growth rate, and K_S the affinity constant (also known as the half-saturation constant). The similarity of Equation 2.4 to irreversible Michaelis-Menten kinetics (Equation 2.2) is clear, the assumption being that the growth rate is limited by consumption of one substrate at one point in the metabolic pathway, usually uptake (Button 1978). μ_{max} can then be naively considered equivalent to r_{max}, scaled by the fraction of biomass X that is the enzyme E catalysing this rate-determining step in the overall reaction.

Monod was not the first to advise against the automatic assumption of a rate-determining step (Monod 1949) and determining the relative contributions of steps along a metabolic pathway has since matured into Metabolic Control Theory (see e.g., Fell 1992). Similarly, assuming that growth is limited by a single substrate may also be an oversimplification (Egli, Lendenmann, and Snozzi 1993). As in reversible Michaelis-Menten kinetics, metabolic products may also inhibit reactions leading to growth (Levenspiel 1980). It is also worth noting that, whereas Michaelis-

Menten kinetics have a mechanistic basis, the evidence for Monod growth kinetics derives from empirical correlation, a reason for caution that Monod was keen to emphasize (Monod 1949). Despite the commendable *post hoc* efforts to give Monod kinetics a firmer footing (Wirtz 2002; Yu Liu 2006; 2007), there are still reasonable concerns about the seductive simplicity of the overall approach (Button 1983; Ferenci 1999; Button 2000).

Despite these shortcomings, Monod kinetics has remained popular among those modelling populations of microbes, especially where growth is not the primary research focus. The basic premise of Monod kinetics, that growth first increases approximately linearly with increasing availability of nutrients before saturating as these become relatively high, is essentially the same as other growth kinetics (e.g. Blackman kinetics: Dabes, Finn, and Wilke 1973). Where the finer details of growth are not necessary, common usage of Monod kinetics makes for easier comparison between models (D. Hales, Rouchier, and Edmonds 2003). It is also worth noting that, although the non-linearity of Monod kinetics can make analytic approaches difficult at times, it is continuous and easily differentiable.

At the opposite end of the spectrum are recent efforts to model every aspect of a cell (N. Ishii et al. 2004; Karr et al. 2012; Monk and Palsson 2014), including its interior spatial structure (L. Shapiro, McAdams, and Losick 2009). While this approach is admirable for its comprehensiveness and adherence to reality, it is computationally expensive, suffers from a difficulty in determining parameters, and is so complex that the model produced may be as difficult to understand as the organism itself (Oberhardt and Ruppin 2013). It is difficult to predict when we will have the capability to incorporate such complex models into population models of evolutionary and ecological dynamics. For reference, the most recent studies combine metabolic pathway reconstructions with spatial grids coarse enough to contain a number of species in each grid element (Harcombe et al. 2014).

When the precise workings of an individual are not the primary focus of a study, capturing all essential elements may be sufficient; the difficulty lies in determining which elements are essential (Brooks and Tobias 1996; Evans, Grimm, et al. 2013b). When doing so, one must take care when manipulating mathematical expressions that are non-linear: a common pitfall is to take the average of too early in the calculation, as demonstrated in Figure 2.1.
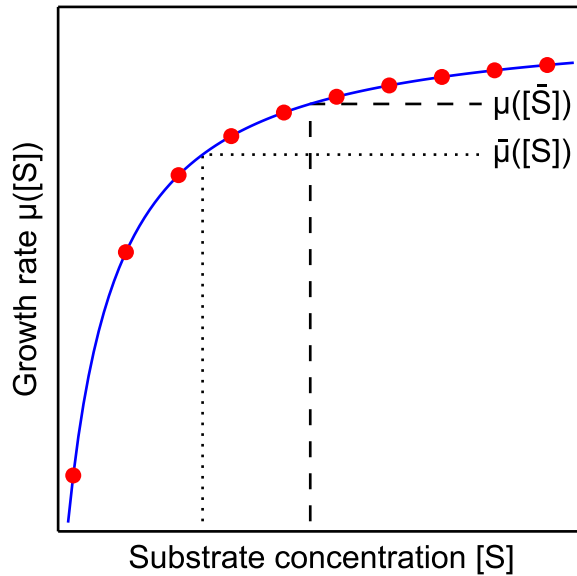
Figure 2.1. Calculating an average response.

In this example, the growth rate $\mu([S])$ dependence on substrate concentration $[S]$ is known to follow Monod kinetics (blue line). The (arithmetic mean) average growth rate (dotted line) of a number of samples (red circles) is different to the growth rate that would come from an average substrate concentration (dashed line). This can be an issue, e.g. when spatial homogeneity of substrate concentration is incorrectly assumed. That there will be a difference between the two has been known for over a century ("Jensen's Inequality", see Jensen 1906) and yet the mistake is still made often.

2.1.3. Determining parameter values

Michaelis-Menten enzyme kinetics are described by two parameters; Monod growth kinetics also. This increases to three for irreversible Langmuir-Hinshelwood kinetics, and then to four for reversible Michaelis-Menten/Langmuir-Hinshelwood kinetics. Determining the values of these is not straightforward.

For Michaelis-Menten type kinetics, Hans Lineweaver and Dean Burk suggested transforming Equation 2.2 to

$$\left(\frac{d[P]}{dt}\right)^{-1} = \frac{1}{r_{max}} + \frac{K_M}{r_{max}} \cdot \frac{1}{[S]} \quad\quad\quad (2.5)$$

so that by plotting $\left(\frac{d[P]}{dt}\right)^{-1}$ against $\frac{1}{[S]}$ the maximum reaction rate, r_{max}, can be determined from the intercept and then the affinity constant, K_M, from the slope (Lineweaver and Burk 1934). Known as the double-reciprocal plot or Lineweaver-Burk plot, it is cited as the most widely-used method of determining these parameter values (Price 1985; Cornish-Bowden 2004). Given its simplicity this is perhaps unexpected, but the problems with this approach have been long known (Dowd and Riggs 1965; Cornish-Bowden 2004). Measurement errors when $[S]$ and $\frac{d[P]}{dt}$ are small are magnified, whereas those when they are large are greatly reduced. Lineweaver and Burk called for caution when proposing this approach but, as with Michaelis-Menten kinetics and Monod kinetics, their concerns have been largely forgotten. This has become less excusable since the advances in computational power have made non-linear regression widely accessible (J A Robinson and Tiedje 1983).

A key difference between the enzymes modelled by Michaelis-Menten kinetics and microbes modelled by Monod kinetics is that the latter adapt to their environment. Adaptation on a short time-scale involves recalibration of cellular machinery in response to changing conditions: synthesis of substrate-specific uptake proteins, for example, is thought to be part of the reason a 'lag phase' of negligible growth are observed when microbial populations are first exposed to a new growth medium (e.g., Gottschalk 1979). Evolutionary adaptation over many generations may bring about further changes in microbial metabolism, in ways we are only beginning to understand (Elena and Lenski 2003).

In terms of the parameters defining Monod kinetics, the affinity constant is much more susceptible to change than maximum growth rate (Kovárová-Kovar and Egli 1998). There may be a trade-off between the two (Kreft and Bonhoeffer 2005), meaning that microbes adapted to environments poor in nutrients (oligotrophic) will tend to sacrifice maximum growth rate for higher affinity by producing a greater fraction of uptake mechanisms (e.g. surface bound

proteins, siderophores) than growth machinery (ribosomes, chaperone proteins, etc). Conversely, those adapted to environments rich in nutrients (eutrophic) will tend to do the opposite (Kovárová-Kovar and Egli 1998). This pattern is often observed when chemostat and repeated batch experiments are compared. A typical chemostat environment is steadily oligotrophic, leading to greater fitness for microbes that maintain sufficient growth at lower substrate concentration, whereas in batch cultures a large amount of nutrients is rapidly consumed in the early stages, leading to greater fitness for those than can reproduce quickest.

The lessons of this variability in Monod parameters are: first, to try to find estimates from environments similar to the one being modelled; when this is not possible, or one cannot predict the environment that will emerge, to treat such parameter estimates with caution and perform a robust sensitivity analysis. A number of researchers have attempted to incorporate this adaptation into the Monod growth model (Senn et al. 1994; Y. Tan et al. 1994; Wirtz 2002; Yu Liu 2006; Yu Liu 2007) but so far none of these seems to have reached maturity and general acceptance.

The greatest difficulty when estimating parameter values for the more complex reversible kinetics (Equation 2.5) is in determining the relationship between the maximum forward and reverse reaction rates, $V_{f,max}$ and $V_{r,max}$. Previous authors have simply assumed the two to be equal, i.e. $v = 1$ (Hoh and Cord-Ruwisch 1996; Mösche and Jördening 1999) but there is no reason why this should be so. Equality seems to be the least-bad option until a more appropriate solution is found.

2.2. Modeling spatial structure

While often studied in well-mixed environments in the laboratory, microbes in the natural environment are frequently observed in spatially structured habitats. The diffusion of cells and metabolites may be restricted by non-microbial material, such as soil particles or mucus produced by an animal host, or microbial material, such as the extracellular polymeric substances (EPS)

produced by many species of microorganism to bind themselves to surfaces and other microbes (Flemming and Wingender 2010).

Spatial structure may facilitate direct intercellular interactions such as plasmid transfer that are already present in well-mixed populations (Krone et al. 2007). Unique to spatially structured environments however, are the metabolite concentration gradients resulting from diffusion limitation: should a metabolite be produced by one cell and consumed by another, the concentration of that metabolite will differ along the space between them (see e.g., Stams 1994). The rates of many reactions will be concentration-dependent, and microbial growth will depend on these reactions, leading to tightly coupled feedback loops between the reactions producing/consuming metabolites and diffusion transporting them from areas of high to low concentration.

iDynoMiCS (individual-based Dynamics of Microbial Communities Simulator) is an Individual-based Model (IbM) software package developed for the purpose of simulating the population dynamics of microbes (Lardon et al. 2011). Microbial cells are modelled explicitly as unique and discrete entities; the population-level behaviour emerges from the low-level interactions of the individuals. All processes occur within discrete time-steps. For evaluation of the effect of spatial structure on growth dynamics, iDynoMiCS allows simulation of both spatially structured biofilm and well-mixed chemostat environments.

The biomass in cells can be structured (composing, for example, of active and inert proportions) and can catalyse reactions that depend on local solute concentration levels and/or other biomass components within the same cell. Cell division is triggered once the radius of a cell exceeds a pre-set division-radius; a daughter cell is then created, inheriting approximately half the biomass (some stochasticity is typically allowed) so that the total post-division biomass of the two cells equals that of the pre-division mother cell. Similarly, a cell dies if its radius falls below the death-radius and its biomass is converted back into nutrients in the local environment.

In the biofilm setting, microbes are confined to a cuboid computational domain representative of a small subset of the macro-scale environment. The boundaries of this domain may be planktonic bulk compartments (of either constant or variable solute concentrations; cells may detach into this compartment, but not back across), solid (impermeable to cells and solutes), membranous (impermeable to cells and some solutes; others may diffuse across to a bulk compartment), or periodic (cells and solutes crossing out over one boundary cross in via the opposite boundary).

Within this domain, microbes are modelled as incompressible spheres that displace any others whose volume overlaps with theirs. Each described by their radius and centre position, the volumes of cells may change within a time step according to the reactions they (auto)catalyse. New cells may also be added to the population through reproduction. Following this recalculation of all cell volumes, the shoving algorithm cycles through the populations to resolve any conflicts that may have arisen. Where two neighbouring cells overlap, they are displaced in opposite directions; however, this displacement may cause new conflicts with other neighbouring cells. As such, the shoving algorithm may need to cycle through the population multiple times until the population contains no overlaps. Methods to improve the computational efficiency of this process are described in Section 2.2.1.

Note that it is also possible to model biofilms in two-dimensional space, the chief distinction being that cells are instead considered cylindrical. 2D simulations typically require much less computational power/time than 3D simulations: while it is usually feasible to run a small number of 3D simulations, running a large number (e.g. as part of a sensitivity analysis) may be very inefficient. Consistency between these two methods is discussed in Section 2.2.1.

The computational domain is split into cubic grid elements that store local concentrations of the solutes present in the system. These solutes are subjected to Fickian diffusion and microbe-mediated reactions (see above). The combined Reaction-Diffusion (R-D) system is

solved using by a multigrid method, which accurately and efficiently models long-distance (coarser grids) and short-distance (finer grids) interactions (see e.g. W. L. Briggs, Henson, and McCormick 2000). Since R-D is assumed to occur much more quickly than cellular processes (growth, division, etc), timescale separation allows us to solve the R-D system to steady-state while assuming the population to be fixed.

Liquid within the biofilm and a boundary layer above is assumed to be unaffected by convection; shear stress cannot be directly modelled, and so detachment of cells from the top of the biofilm is instead approximated by an erosion-speed function.

2.2.1. Consistency between 2D and 3D simulations

When simulating microbial communities growing in three dimensions (3D), or in a well-mixed chemostat, iDynoMiCS considers cells to be hard spheres; in two-dimensional (2D) simulations they are modelled as hard cylinders, with axes aligned and of length equal to the grid resolution. In 2D this approach ensures that the cell radii, and consequently the overall size and shape of the biofilm, are unaffected by the choice of grid resolution. Furthermore, the thresholds in cell radius that trigger events such as division and death are consistent between simulations. The disadvantages of this approach are that the total masses of cells of a given radius can differ greatly between the two types of simulations, and that cylinders tend to pack more densely than spheres (Visscher and Bolsterli 1972) leading to an overall biomass density that is higher in 2D simulations.

To achieve (approximately) equal overall biomass density in the two simulation types we adjust the cell (dry) biomass density of cells in the 2D simulations by the packing density. Following the standard definition of packing as the fraction of the space that is filled by the objects:

$$\rho_2 \eta_2 = \rho_3 \eta_3 \quad \Rightarrow \quad \rho_2 = \frac{\rho_3 \eta_3}{\eta_2} \qquad\qquad (\ 2.6\ )$$

where ρ denotes cell biomass density (g L^{-1}), η the packing density (dimensionless, between 0 and 1) and subscripts indicate the dimensionality of the simulation being considered.

The densest possible packing of spheres in a volume is $\eta_{kepler} = \frac{\pi}{3\sqrt{2}} \approx 0.74$ (T. C. Hales 1992) whereas the densest possible packing of circles in a plane is $\eta_{honeycomb} = \frac{\pi}{2\sqrt{3}} \approx 0.91$ (Figure 2.2A). While we cannot expect cells simulated in a biofilm to reach this, it is reasonable to expect that the packing observed will fall short of the optimum by a similar degree in 2D and 3D (Visscher and Bolsterli 1972).

However, calculating the appropriate cell biomass density in 2D is not as simple as multiplying that used in 3D by $\frac{\eta_{kepler}}{\eta_{honeycomb}} = \frac{\sqrt{2}}{\sqrt{3}}$. In each iterative step iDynoMiCS's shoving algorithm eliminates any overlap between cells due growth, etc. It is computationally expensive to set all cell surfaces touching exactly, so for the purposes of the shoving algorithm the radii of cells are increased by a "shove factor" and the precision required of the algorithm relaxed slightly (Figure 2.2B). The value of this shove factor, s_f, is chosen heuristically; values of around 1.05 or 1.10 are typical.

Therefore, even if cells were arranged perfectly we would have to adjust for this shove factor. In 2D this would mean

$$\eta_2 = \eta_{honeycomb} \frac{\pi r^2}{\pi (s_f r)^2} = \frac{\eta_{honeycomb}}{(s_f)^2} \qquad (2.7)$$

and in 3D

$$\eta_3 = \eta_{kepler} \frac{\left(\frac{4}{3}\right)\pi r^3}{\left(\frac{4}{3}\right)\pi (s_f r)^3} = \frac{\eta_{kepler}}{(s_f)^3}. \qquad (2.8)$$

As a result, Equation 2.6 becomes

$$\rho_2 = \frac{\rho_3 \, \eta_{kepler}}{s_f \, \eta_{honeycomb}} \approx \frac{0.82}{(s_f)} \rho_3. \qquad (2.9)$$
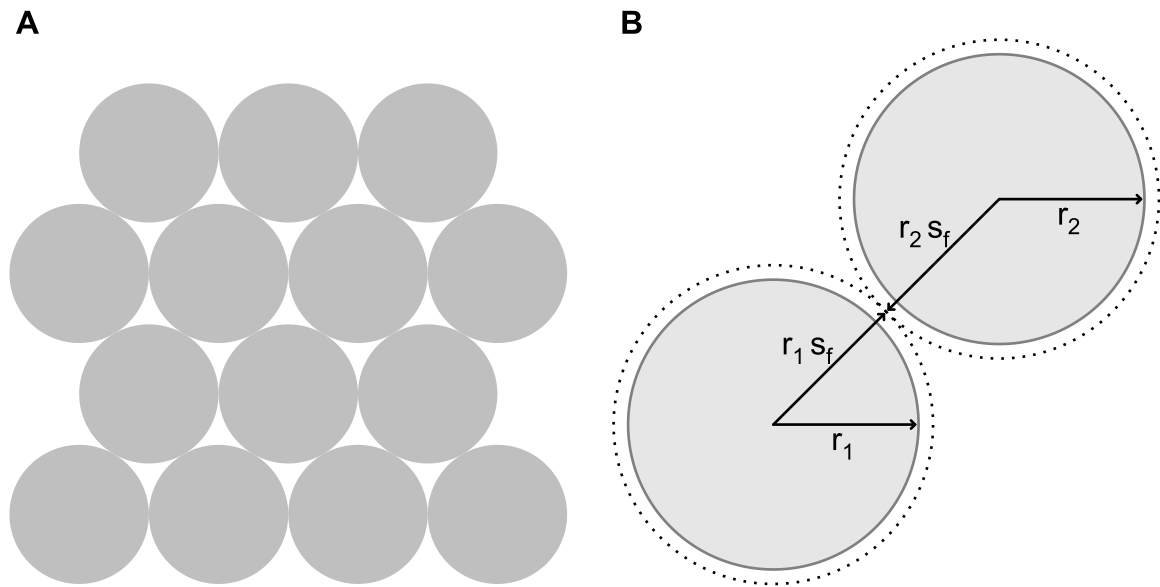
Figure 2.2. Packing cells in two dimensional space.

(A) The hexagonal lattice gives the density possible packing of circles. Bees are known to use this arrangement in their hives, giving it the name *honeycomb* packing. **(B)** For the purposes of the shoving algorithm, the radii of the cells are scaled by a shove factor s_f. This means that a small overlap between cells of these scaled radii (dotted lines) can be permitted for computational efficiency, without risking overlap of the actual cells (solid lines).

To test this, a single-species *Escherichia coli* biofilm is simulated growing on a flat surface, limited by glucose. Model parameters are given in Table 2.2 and detachment is ignored here. Simulations stop once the top of the biofilm crosses the maximum thickness threshold, T_{max}. Since the growth and reaction kinetics are not of primary interest here, growth on glucose is assumed to follow Monod kinetics with maximum rate μ_{max} and affinity K_S. Figure 2.3 shows the results for these simulations. Adjusting for both dimension and shove factor gives results that are closer to those for 3D than adjusting for dimension alone or not at all.

Table 2.2. Model parameters for packing simulations.

Symbol	Name	Units
μ_{max}	Maximum specific growth rate (A. L. Koch and Wang 1982)	1.2 h^{-1}
K_S	Growth affinity constant (A. L. Koch and Wang 1982)	0.00234 g L^{-1}
S_B	Glucose concentration in the bulk	0.001 g L^{-1}
s_f	Shove factor	1.10
T_{max}	Maximum biofilm thickness threshold	48 µm
b_L	Boundary layer thickness	12 µm
D	Diffusivity of glucose (Chang 1977)	0.57 x 10^{-9} m^2 s^{-1}
r_{div}	Threshold radius triggering to division	0.8 µm
Y_μ	Growth yield, the efficiency of converting glucose to biomass (Neijssel, de Mattos, and Tempest 1996)	0.444 g g^{-1}
ρ_3	Cell biomass density in 3D and naïve 2D (Shuler, Leung, and Dick 1979)	290 g L^{-1}
ρ_2^*	Cell biomass density in 2D, adjusting for dimension only	237 g L^{-1}
ρ_2	Cell biomass density in 2D, adjusting for dimension and shove factor	215 g L^{-1}
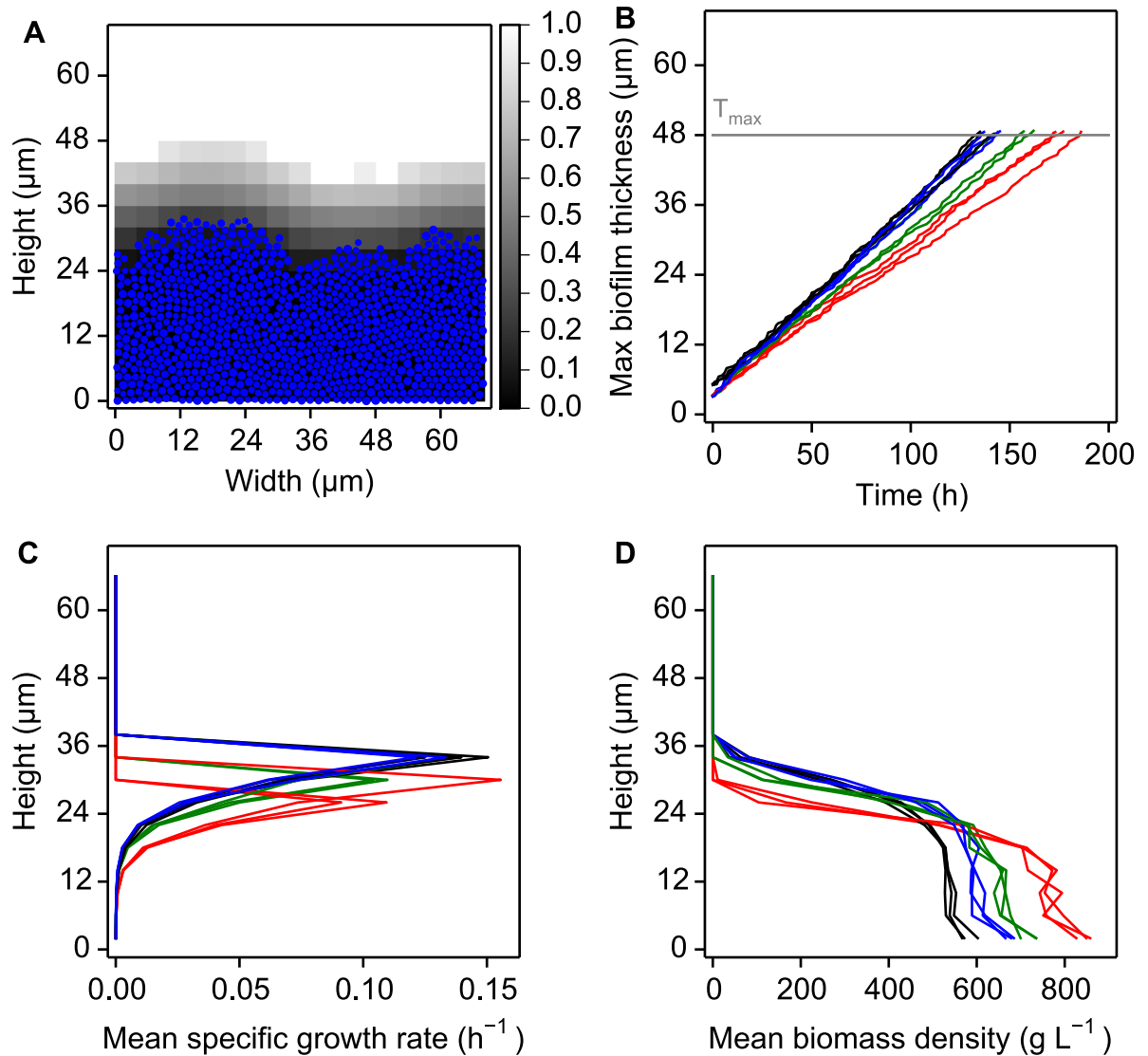
Figure 2.3. Adjusting for both dimension and shove factor is necessary.

(A) Typical 2D biofilm structure using the parameters given in Table 2.2. Cells are shown in blue and the glucose concentration in greyscale (mg L^{-1}). Biomass density adjusted for dimension and shove factor. Time is 100 h after initialisation with 16 cells placed randomly on the solid surface. **(B)** Maximum biofilm thickness through time of simulations in 3D (biomass density ρ_3, black), in 2D without adjustment (biomass density ρ, red), in 2D with adjustment for dimension only (biomass density ρ_2^*, green), in 2D with adjustment for dimension and shove factor (biomass density ρ_2, blue). **(C)** Average growth rate of cells against height above the solid surface. **(D)** Average overall biomass density against height above the solid surface. **(B-D)** Three replicate simulations are shown for each set of parameters. **(C-D)** Colour scheme as in (B). Averages are taken over layers 4 μm thick, the grid resolution in all simulations.

CHAPTER 3: REPAIR RATHER THAN SEGREGATION OF DAMAGE IS THE OPTIMAL UNICELLULAR AGING STRATEGY

A version of this chapter has been published by BMC Biology (Clegg, Dyson, and Kreft 2014).

Aging is detrimental; it is therefore hard to explain why it evolved (Kirkwood 2005). Aging clearly occurs in those multicellular organisms that evolved a division of labour between germline and soma, rendering the soma disposable (Kirkwood 2005; Kirkwood and Cremer 1982). Due to extrinsic mortality, natural selection may favour early reproduction at the cost of a reduced chance of reproduction later in life (Medawar 1952); similarly early reproduction is also favoured when populations expand (Ratcliff et al. 2009; Rashidi, Kirkwood, and Shanley 2012). This leads to a trade-off in resource allocation between maintaining and repairing the disposable soma versus investing in reproduction, suggesting that evolution selects for an optimal investment in repair and hence optimal longevity, at least in multicellular organisms with a germline (Kirkwood 2005).

3.1. Background

For unicellular bacteria in particular, it was commonly believed that such a division of labour into germline and soma and therefore aging does not occur, although in fact aging was long known to occur in a eukaryotic unicellular organism, the budding yeast *Saccharomyces cerevisiae* (Mortimer and Johnston 1959). Budding yeast may have been seen as a special case not relevant to bacteria, although budding and other forms of asymmetric division also occur in bacteria (Angert 2005). Moreover, regarding the evolutionary benefits of aging, it should not matter whether the organism is eukaryotic (e.g. a yeast) or prokaryotic (e.g. a bacterium); it should only matter whether it is unicellular – including cancer cell lines – or multicellular. Regarding molecular mechanisms, aging would also require some form of asymmetric division in unicellular organisms. Whatever the reason, the idea of aging as a universal hallmark of life, even affecting bacteria, was considered but dismissed in the 1950's and 60's (Hughes 1955; E. O. Powell 1956; E. O. Powell 1958; Schaechter et al. 1962; E. O. Powell and Errington 1963; Marr, Harvey, and Trentini 1966).

It was the discovery of aging in the fission yeast *Schizosaccharomyces pombe* (Barker and Walmsley 1999), which divides apparently symmetrically by binary fission like many bacteria, and then the discovery of aging in the asymmetrically dividing bacterium *Caulobacter crescentus* (Ackermann, Stearns, and Jenal 2003) that rejuvenated the idea that aging may be a universal hallmark of life. This view was cemented further by the discovery of a limited degree of aging in the model bacterium *Escherichia coli* by Stewart and coworkers in 2005 (Stewart et al. 2005). They showed that while cell division in *E. coli* was morphologically symmetric, it was not functionally symmetric: the old-pole cell, i.e. the daughter cell inheriting the older pole of the mother cell, grew more slowly and the new-pole cell grew faster than the mother cell, suggesting that the older pole was associated with more damage. This demonstrated the possibility of division of labour between daughter cells even if cells appear to divide symmetrically.

Box 2. Definitions of aging and senescence.
Aging research is troubled by a difficulty in defining commonly-used terms (Hayflick 2007). While these definitions may not be universally accepted, they will aid the reader to understand the work presented.

- **Aging** the deterioration of individual fitness due to the accumulation of damage, whether this be caused internally (e.g. toxic metabolic by-products) or externally (e.g. Ultra-Violet radiation)
- **Aging strategy** a set of genotypic responses to aging. Selection acts upon the reproductive success of organisms employing a particular strategy when in competition against those employing other strategies.
- **Chronological senescence** the deterioration of individual fitness with time. This term is mostly applicable to so-called higher organisms, such as mammals, many of which appear to have a finite lifespan regardless of environmental conditions.
- **Clonal senescence** the deterioration of fitness for a population of clones, i.e. individuals identical both in terms of their age and of their aging strategy.
- **Conditional senescence** the deterioration of individual fitness due to damage caused by the environment. In a constant environment, where the individual is unable to reproduce, this is equivalent to chronological senescence.
- **Replicative senescence** the deterioration of individual fitness triggered by reproduction. One individual may inherit more damage than the other, giving the latter an advantage at the expense of the former.

Throughout this work, the term **age** will be assumed to mean the current fitness of an individual due solely to the accumulation of damage, i.e. the fraction of biomass in an individual that is damaged. Any reduction in fitness due to the costs of an aging strategy will be treated separately.

Since then, the evidence for aging in unicellular organisms in the sense of reduced growth rate of the old-pole cell has become less clear: some further studies supported a limited degree of aging in the bacteria *E. coli* (Lindner et al. 2008), *Bacillus subtilis* (Veening et al. 2008), *Mycobacterium* spp. (Aldridge et al. 2012), and the diatom *Ditylum brightwellii* (Laney, Olson, and Sosik 2012), while others found no evidence of aging in *E. coli* (Wang et al. 2010; Bergmiller and Ackermann 2011; Aldridge et al. 2012) and other bacteria (Bergmiller and Ackermann 2011) or the unicellular eukaryotic alga *Euglena gracilis* (Goto and Beneragama 2010). Chao and coworkers (Chao 2010; Rang, Peng, and Chao 2011) pointed out that age in the sense of the damaged fraction of cells could reach a steady state in growing cells where damage accumulation would be balanced by damage dilution such that 'age' would not increase with time, and that this was the case in the studies of Stewart et al. (2005) and Wang et al. (2010). Repair was not considered, but could be an additional process that removes damage. In such a steady state age, damage would keep being formed, but the growth rate and condition of the cell would not deteriorate over time, nor would lifespan be reduced. This differs strongly from what is observed in the budding yeast (Mortimer and Johnston 1959; Egilmez and Jazwinski 1989) and in *C. crescentus* (Ackermann, Stearns, and Jenal 2003). However, Wang et al. (2010) found that growth rates of *E. coli* old-pole cells grown in channels of a microfluidic device did not change over 200 generations, suggesting lifespan to be long. On the other hand, they also found that the probability of sudden events such as death or filamentation (elongation into long filaments due to growth without cell division) increased with age, suggesting that at least some kind of damage accumulated during this apparent steady state. This is difficult to reconcile with the interpretation that these cells grew in a steady state of age. Moreover, different experimental conditions such as the presence of damaging agents or the expression of fluorescent proteins might also explain differences between studies (Rang et al. 2012). Adding a further note of caution, we know nothing of aging in archaea, multicellular bacteria, or those spherical bacteria that do not conserve the 'old pole' over consecutive divisions since their division plane cycles through orthogonal directions (Turner et al. 2010).

Most recently, the fission yeast was shown not to age under benign conditions in a study that included following individual cells for at least 30 consecutive divisions (Coelho et al. 2013). The two studies following cells for a large number of generations under benign conditions suggest that the growth rates of old-pole cells of *E. coli* (Wang et al. 2010) and of the fission yeast (Coelho et al. 2013) may fluctuate but do not decline. Rather, death may become more likely with age in wild-type *E. coli* approaching the probability of death of an SOS repair deficient *lex*A3 mutant (Wang et al. 2010). In the fission yeast, death also appears to be a sudden and random event triggered by accidental partitioning of protein aggregates during cell division, rather than an active mechanism of damage segregation (Coelho et al. 2013).

In the wake of Ackermann et al. (2003) and Stewart et al. (2005), some mathematical models have been specifically developed to address the evolutionary question of the fitness benefits of aging in unicellular organisms (Watve et al. 2006; Ackermann, Chao, et al. 2007; Erjavec et al. 2008; Chao 2010; Rashidi, Kirkwood, and Shanley 2012). These models differ in their assumptions and their treatment of key processes, making it difficult to describe them and their predictions briefly yet accurately; see Table 3.1 for an attempt to summarise them.

The differences and extent of experimental support for the various assumptions are summarised in Table 3.2 and discussed in more detail later. Taken together, these models predicted asymmetric division and absence of repair to be the fittest strategy, placing unicellular organisms into the division of labour terrain just as multicellular organisms. Note, however, that these models predicted complete asymmetry combined with complete absence of repair to be the fittest strategy. Neither predictions are correct (Chao 2010; Rang et al. 2012): asymmetry is often very limited (Stewart et al. 2005; Lindner et al. 2008; Veening et al. 2008; Aldridge et al. 2012; Laney, Olson, and Sosik 2012) or absent (Wang et al. 2010; Bergmiller and Ackermann 2011; Rang et al. 2012; Aldridge et al. 2012; Coelho et al. 2013) whilst dedicated molecular systems for the repair of damage are ubiquitous. Further, these repair mechanisms are inducible and deletions reduce fitness (Tyedmers, Mogk, and Bukau 2010; Winkler et al. 2010).

Table 3.1. Summary of assumptions and predictions of various aging models.

Assumptions				Predictions
Growth & Division	Effect of damage	Removal of damage	Environ-ment	
Watve et al. (2005): Leslie Matrix model with multiple cellular components of different age				
Growth rates of cellular components decline with their age. Cells divide after a fixed time without any restriction on daughter cell sizes. Cells die if they are in the oldest age class and no longer contribute to population growth	'Toxicity' considered by assuming oldest and slowest growing components to be growth rate limiting	Repair converts oldest into newest components without growth rate cost	Constant	Asymmetric division increases population growth rate over the symmetric case if older components in the latter are 'toxic' and decline of growth rate with age above minimal. Repair increases population growth rate since repair turns old into new components at no growth rate cost
Ackermann et al. (2007): evolutionary model where survival depends on damage and repair				
Cells do not grow, yet divide after a fixed time	Damage decreases survival probability	Repair removes damage, at cost of decreased survival probability	Constant, extrinsic mortality	Repair is only beneficial in symmetrically dividing cells. The best strategy is complete asymmetry without any repair
Erjavec et al. (2008): metabolic model of growing cells				
Growth of cells linear; cells divide once active protein reaches a threshold	Damage toxic	No repair but decay of active and damaged protein; decay without cost, no recycling of damaged into active protein	Constant	Asymmetry of damage partitioning beneficial, the stronger the asymmetry, the higher the benefit. Symmetry beneficial if offspring are smaller unless damage accumulation rate too high
Chao (2010): damage affects time between divisions				
Cells acquire active and damaged protein at linear rates; cells divide once active protein reaches a threshold.	Damage toxic by linearly decreasing growth rate	Repair absent	Constant, extrinsic mortality	Complete asymmetry has highest mean fitness apart from a narrow region of intermediate damage accumulation rates where the fittest strategy is slightly below complete asymmetry
Rashidi et al. (2012): energy budget model				
Cells grow and prevent damage accumulation depending on energy allocated to growth and prevention, with a fixed total energy budget for the cell	No effect on growth or division, but can trigger instant cell death if above threshold	Damage is degraded but not repaired (recycled)	Constant	Asymmetry ensures survival of the population at high damage accumulation rates in the absence of degradation. Symmetrically dividing cells invest just enough into damage prevention to avoid instant death
UnicellAge: metabolic model of growing and repairing cells competing for resources				
Cells grow exponentially by consuming resource; cells divide once total protein reaches a threshold	Damage inert or toxic	Repair by active protein that does not contribute to growth; repair recycles material with a certain efficiency	Constant or dynamic, extrinsic mortality	Repair better than asymmetry unless damage accumulation rate high, damage toxic, and efficiency of repair low

Table 3.2. Summary of experimental evidence.

Phototrophic organisms have been excluded from this table since they are less well studied whilst their diurnal life cycle is more complicated. Cells growing in the absence of external stresses and damaging agents such as streptomycin and not expressing fluorescent proteins (XFP) were considered to grow under benign conditions. Any other conditions are indicated explicitly.

Organism			Key experimental findings
Name	Phylogeny	Ecology	
Cell division by budding facilitating damage segregation			
Saccharomyces cerevisiae	Ascomycota (Eukaryote)	Spoils environment	Limited number of generations of mother cell, sharp increase of generation time of mother cell starting a few generations before death (**benign**) (Egilmez and Jazwinski 1989), protein aggregates tethered to organelles that remain in mother cell enabling segregation of unrepaired damage (Spokoini et al. 2012).
Caulobacter crescentus	α-Proteobacteria (Gram-negative)	Attached to short-lived surfaces	Marked decline of growth rate of mother cell over time (**benign**) (Ackermann, Stearns, and Jenal 2003; Ackermann, Chao, et al. 2007; Ackermann, Schauerte, et al. 2007).
Cell division by binary fission			
Schizo-saccharomyces pombe	Ascomycota (Eukaryote)	Spoils environment	No apparent decline of growth rate over ≥ 30 generations (**benign**), sudden death of mother cell when aggregates accumulate under stress (Coelho et al. 2013).
Methylobacterium extorquens	α-Proteobacteria (Gram-negative)	Plant leaves, relatively long-lived but seasonal	No decline of growth rate over 5 generations (**benign**) (Bergmiller and Ackermann 2011).
Escherichia coli	γ-Proteobacteria (Gram-negative)	Grows in relatively long-lived colon, survives outside host	No decline of growth rate over 3 generations (**benign**) (Bergmiller and Ackermann 2011). No difference in growth rates between old and new-pole siblings (**benign**) (Lele, Baig, and Watve 2011). No decline of growth rate (**benign**) but decline in the presence of streptomycin (Rang et al. 2012). Slow decline of growth rate over 7 generations in the presence of XFP (Stewart et al. 2005; Lindner et al. 2008). No decline of growth rate over ~200 generations in microfluidic device in the presence of XFP, but increased probability of sudden death (Wang et al. 2010). Stronger aging after mild heat shock or in a repair mutant (chaperone *clpB* deletion) (in presence of XFP) (Winkler et al. 2010). Reduced protein aggregate formation if superoxide dismutase overexpressed (Maisonneuve, Ezraty, and Dukan 2008).
Bacillus subtilis	Firmicutes (Gram-positive)	Grows in soil while nutrients present, then sporulates	Similar to *E. coli*: slow decline of growth rate over 4 generations using fluorescence microscopy (Veening et al. 2008).
Mycobacterium spp.	Actinobacteria (Gram-positive)	Pathogen remaining inside host cells for years	Complex growth pattern: alternating polar growth of cell wall, cycling between fast and slow growth, age of pole different from age of side-wall and rest of cell, minimal decline of growth rate with age of side-wall in the presence of XFP (Aldridge et al. 2012).

Given the confusing experimental evidence and the incorrect predictions of previous mathematical models developed to explore consequences of aging, this question is revisited using iDynoMiCS, a generic individual-based model of the growth of unicellular organisms (Lardon et al. 2011). iDynoMiCS and its precursors have been applied to a range of problems and its aging-independent elements, such as the simulation of the chemostat environment as well as growth and cell division, have thereby been validated. By adding the processes of accumulation, repair, and segregation of damage, where the damage is either inert or toxic, iDynoMiCS has been extended to develop UnicellAge. Three differences from previous models are central: (i) inclusion of costly repair, (ii) continuous growth of individual cells catalysed by undamaged components of the cell, making any decrease of these catalytically active components by damage accumulation or increase by repair immediately effective, and (iii) growth rate dependence on resource concentration, leading to resource competition in dynamic environments.

UnicellAge predicts that repair is always beneficial when damage accumulation is above a baseline rate. Further, there is an optimal investment in repair. In contrast, damage segregation is only beneficial in addition to damage repair if the damage accumulates at a high rate and is toxic and repair is inefficient. This suggests that repair should occur in all unicellular organisms, while damage segregation should be limited to toxic damage that cannot be repaired at reasonable cost. This is well in line with experimental evidence in many unicellular organisms where aging is either absent or minimal, at least under benign conditions. However, the predictions of UnicellAge are in contrast to the considerable degree of aging found in the budding bacterium *C. crescentus* and the budding yeast. Budding may well function as a mechanism of cell division that facilitates damage segregation. The evolution of aging in these budding organisms can be explained by their ecology, as they are living in transient habitats where longevity is of little advantage: rapid initial growth, producing as many offspring as possible before the environment is destroyed, will be more successful than the approach that maximises fitness over the long term. Overall, taking account of all experimental evidence in the light of the predicted fitness benefits clearly shows

that the idea that aging is beneficial for unicellular organisms and therefore universal is overly simplistic.

3.2. Model development

The three aging-related processes of damage accumulation, repair and segregation have been embedded in iDynoMiCS (Lardon et al. 2011), a general individual-based model of the growth of microbial cells immersed in a given environment. Together with its predecessors, iDynoMiCS has been applied to colony (Kreft, Booth, and Wimpenny 1998) and biofilm growth (Kreft et al. 2001; Picioreanu, Kreft, and van Loosdrecht 2004), evolution of cooperation (Kreft 2004), lag phase (Dens et al. 2005), metabolic switching (Lardon et al. 2011) and plasmid transfer (Merkey et al. 2011), and thereby tested relatively well. The new iDynoMiCS-based aging model is referred to as UnicellAge as it is a general model for aging in all unicellular organisms, or unicells for short. iDynoMiCS and UnicellAge are open-source programs that are freely available from www.idynomics.org. An overview of UnicellAge is given in Figure 3.1 and the model equations introduced step by step in the following subsections.

In UnicellAge, cells grow by taking up nutrients from the environment, which automatically leads to competition for limiting resources. For example, cells with a strategy of damage repair can compete against cells with a strategy of damage segregation. Fitness emerges from this interaction rather than being defined by some arbitrary measure such as population size after a certain time. The fitter strategy wins the competition significantly more frequently.

A   Biomass & Volume Growth   **B**   Cell Division

Uptake/Growth

S P_{act} $(1-\beta)$ β

[Toxicity]

Repair
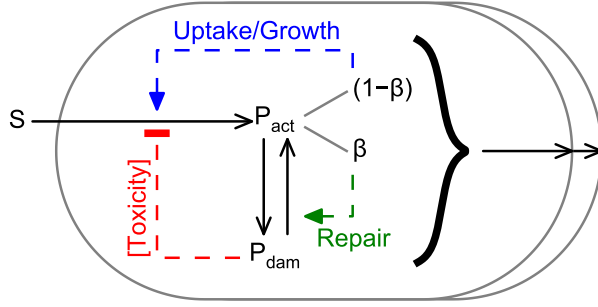
P_{dam}

$$\frac{dP_{act}}{dt} = (1-\beta)\mu(S)\,P_{act}\left[\frac{P_{act}}{P_{act}+P_{dam}}\right] - aP_{act} + Y_r\,r(\beta P_{act}, P_{dam})$$

$$\frac{dP_{dam}}{dt} = \qquad\qquad\qquad\qquad aP_{act} \;-\; r(\beta P_{act}, P_{dam})$$

Symmetric $\alpha=0$

P_{dam}^{old} P_{act}^{old} P_{act}^{new} P_{dam}^{new}

Asymmetric $\alpha=1$

P_{dam}^{old} P_{act}^{old} P_{act}^{new}
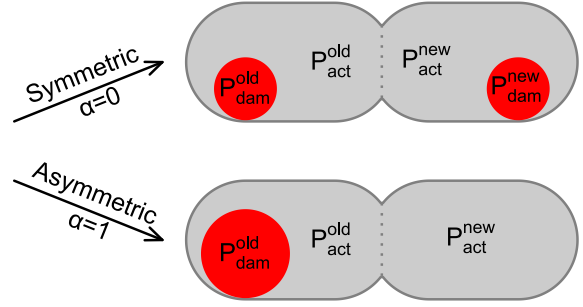
$$P_{act}^{old} = (1-\theta)P_{act} - \alpha\theta P_{dam}, \quad P_{act}^{new} = \theta P_{act} + \alpha\theta P_{dam}$$

$$P_{dam}^{old} = (1-\theta)P_{dam} + \alpha\theta P_{dam}, \quad P_{dam}^{new} = \theta P_{dam} - \alpha\theta P_{dam}$$

C   Constant Environment   **D**   Dynamic Environment
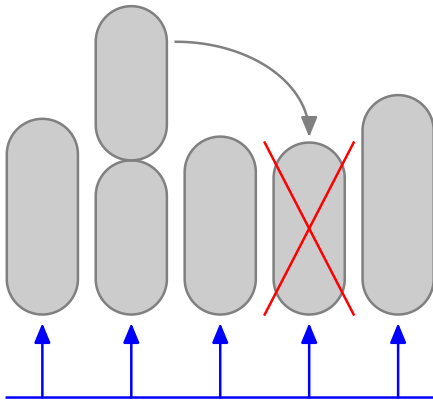
S_{in} S

Constant substrate concentration (S)
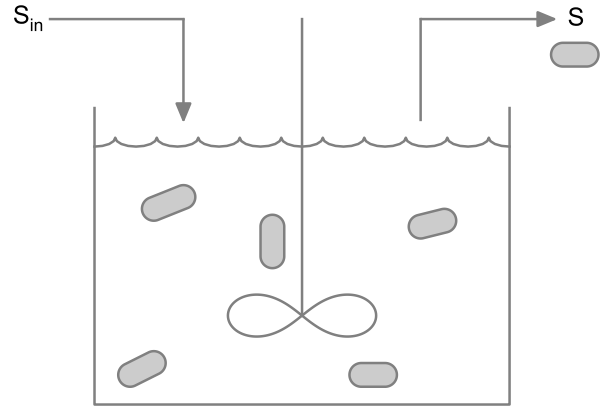
$$\frac{dS}{dt} = D(S_{in}-S) - \sum_{cells}(1-\beta)\mu(S)P_{act}\left[\frac{P_{act}}{P_{act}+P_{dam}}\right]$$

Figure 3.1. Schematic of the model.

(A) The continuous processes of growth, damage accumulation and repair. Substrate (S) is taken up and converted into active protein (P_{act}). The substrate concentration may be either constant or dynamic, depending on the environment. This autocatalytic growth process is catalysed by the 'growth machinery', a fraction ($1-\beta$) of active protein, producing more active protein. Active protein is converted at damage accumulation rate a into damaged protein (P_{dam}), which may inhibit the growth process if it is toxic. Damaged protein may also be repaired according to Equation 3.6 by the 'repair machinery', the other fraction of active protein (β). Protein represents the entire biomass. **(B)** The discontinuous process of cell division. Both daughter cells inherit the same amounts of total biomass on average, specified by the variable θ that is chosen from a truncated normal distribution with mean 0.5, SD 0.025. They may acquire the same proportions of active and damaged protein (symmetric division) or the old-pole cell may take on all (or as much as possible) of the damaged protein (asymmetric division). These are the two extreme cases of a continuum denoted by the variable α. **(C)** In the constant environment, a cell is randomly replaced by a new cell formed upon cell division; this models external mortality. Substrate is

34

taken up by the cells but its concentration does not change. **(D)** In the dynamic environment, substrate at concentration S_{in} is fed into the system, and cells and substrate at concentration S are leaving the system, all in proportion to the dilution rate D. Removal of cells is a form of extrinsic mortality.

3.2.1. Modelling growth

Each individual cell in the model is composed of just two types of biomass, referred to simply as 'protein' (Lindner and Demarez 2009): intact, active protein P_{act} and damaged protein P_{dam} (Figure 3.1A). Only active protein catalyses biomass growth: the consumption of substrate resulting in the production of more catalytically active biomass. Note that this autocatalytic nature of growth leads to an exponentially increasing rate of biomass growth of a damage free cell. Such exponential growth of single cells during their cell cycle is empirically well supported by most studies of unicellular organisms (A. L. Koch 1993; Godin et al. 2010; Wang et al. 2010; Mir et al. 2011; Cooper 2013). However, some studies of the fission yeast (Baumgärtner and Tolić-Nørrelykke 2009; Horváth et al. 2013) and *E. coli* (Reshes et al. 2008) provided evidence for bilinear growth, i.e. a growth pattern composed of two distinct stages, each linear but with markedly different rates. Nevertheless, bilinear growth can be approximated by exponential growth. Linear growth has also been examined for comparison with previous models that make this assumption (Erjavec et al. 2008; Chao 2010; Rashidi, Kirkwood, and Shanley 2012) To describe the dependence of growth rate on substrate concentration, S, Monod kinetics were chosen (Figure 3.2B) as appropriate for a non-toxic, sole growth limiting substrate, e.g. growth of *E. coli* on glucose (Lendenmann, Snozzi, and Egli 1999):

$$\mu(S) = \frac{\mu_{max} S}{K_S + S} \tag{3.1}$$

where μ_{max} is the maximum growth rate and K_S the affinity constant. Values for these are given in Table 3.3.

Table 3.3. List of variables and parameters used.

The parameter values were taken from measurements of *Escherichia coli* growing on glucose as the limiting nutrient wherever possible. *The protein amount triggering division is based on total protein, i.e. $P_{act} + P_{dam}$. Note that 621 fg is equivalent to a spherical radius of 0.8 μm (volume ~2 μm^3) as dry biomass density is 290 g L^{-1} (Shuler, Leung, and Dick 1979).

Symbol	Name	Units
a	Aging or damage accumulation rate	h^{-1}
α	Asymmetry (damage segregation) factor	Dimensionless, between 0 (symmetric) and 1 (asymmetric)
β	Proportion of active protein invested in repair	Dimensionless, between 0 and 1
D	Dilution rate in the chemostat	0.3 h^{-1}
θ	Baby Mass Fraction: proportion of total protein inherited by new-pole cell (drawn from Normal distribution with mean 0.5 and SD 0.025)	Dimensionless, between 0 and 1
K_S	Half-saturation constant (A. L. Koch and Wang 1982)	0.00234 g L^{-1}
$\mu(S)$	Specific growth rate as a function of substrate concentration S (Monod kinetics)	h^{-1}
μ_{max}	Maximum specific growth rate (A. L. Koch and Wang 1982)	1.2 h^{-1} or 3.0 h^{-1} for Figures 5, S6, S7
P_{act}	Active protein	fg
P_{dam}	Damaged protein	fg
P_{div}	Threshold protein mass triggering division*	621 fg
S	Substrate concentration	g L^{-1}
S_{in}	Chemostat inflow substrate concentration (determines biomass density in chemostat)	0.00324 g L^{-1}
$r(\beta P_{act}, P_{dam})$	Repair rate	h^{-1}
t	Time	h
Y_μ	Growth yield, the efficiency of converting glucose to active protein (Neijssel, de Mattos, and Tempest 1996)	0.444 g g^{-1}
Y_r	Repair yield, the efficiency of converting damaged protein to active protein (assumed to be between Y_μ and 1)	0.8 g g^{-1}
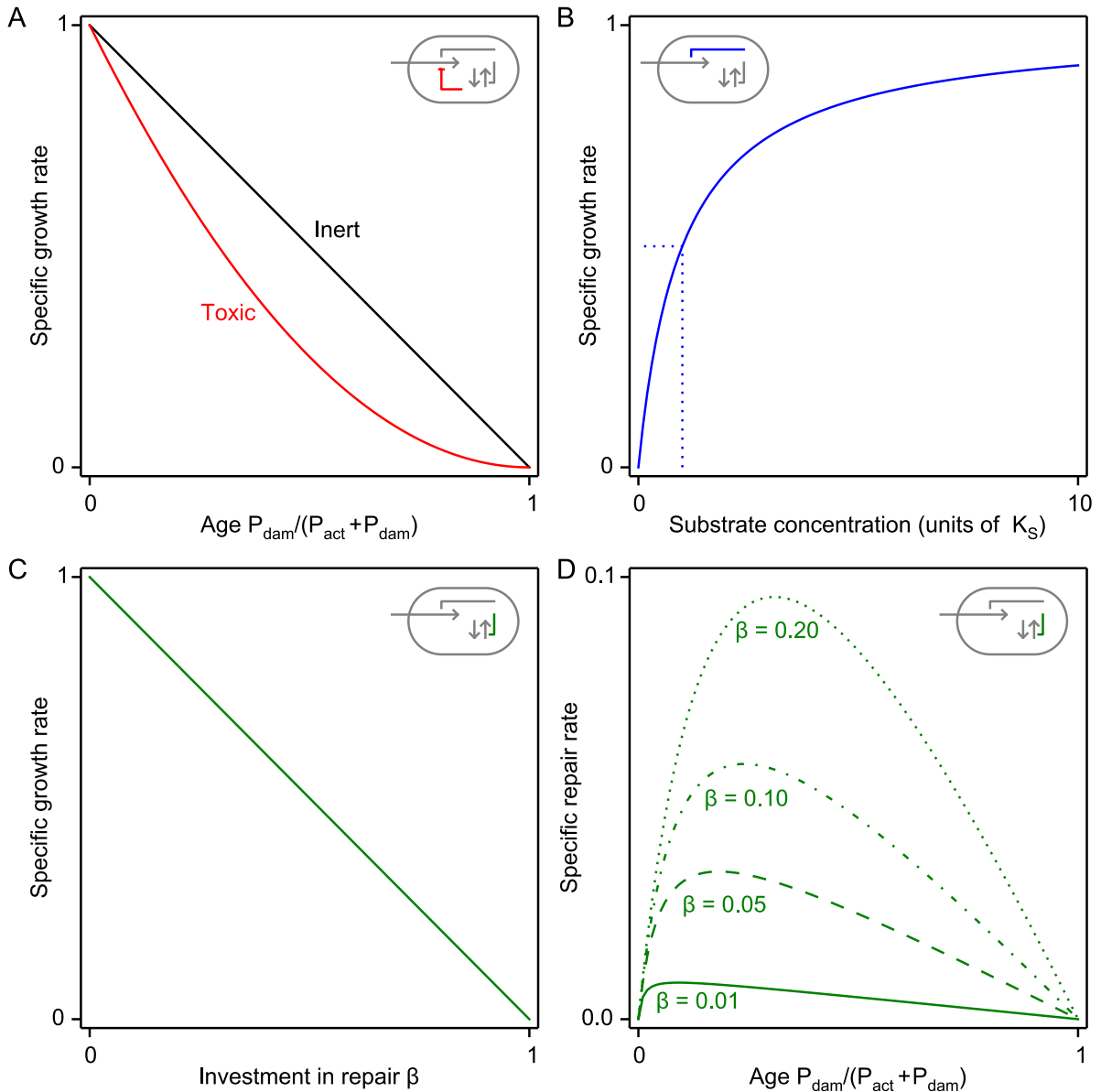
Figure 3.2. Explaining the qualitative behavior of various elements of the model equations.

(A) Specific growth rate declines with age, defined as the fraction of damaged material. This decline is either linear for inert damage (black) or concave-quadratic for toxic damage (red). **(B)** Specific growth rate increases with substrate concentration, $\mu(S)$, following saturation (Monod) kinetics (solid line), reaching half its maximal rate at a substrate concentration of K_S (dotted line). **(C)** Specific growth rate decreases linearly with investment into repair since the fraction of protein involved in repair does not contribute to growth. **(D)** The specific repair rate is Equation 3.6 divided by total protein, making it a function of β and age. The specific repair rate initially increases with increasing age since damaged protein is the "substrate" of the repair process, but since the amount of "enzyme" for the repair process is proportional to active protein, the specific repair rate then declines as age tends to one. Increasing investment in repair increases the specific rate of repair and also increases the age at which this rate peaks.

3.2.2. Modelling damage accumulation and repair

Active protein is converted to damaged protein at an environmentally determined, constant rate of damage accumulation a, in line with those previous models based on continuous time processes (Erjavec et al. 2008; Chao 2010; Rashidi, Kirkwood, and Shanley 2012). The kinetics of growth are then

$$\frac{dP_{act}}{dt} = \mu(S)P_{act} - aP_{act}, \qquad\qquad (3.2)$$

$$\frac{dP_{dam}}{dt} = aP_{act}. \qquad\qquad (3.3)$$

It is assumed that once damaged, material can be repaired by a lumped repair process requiring resources and specialized proteins such as chaperones and proteases as 'repair machinery'. Cells have evolved sophisticated mechanisms of repair that can be induced in response to stress (Visick and Clarke 1995; Dougan, Mogk, and Bukau 2002; González-Montalbán et al. 2005; Tyedmers, Mogk, and Bukau 2010; Winkler et al. 2010; Geiler-Samerotte et al. 2011). For example, misfolded proteins can be refolded by ATP-dependent chaperones or failing that degraded by ATP-dependent proteases. Chaperones also prevent misfolding. Oxidatively damaged proteins can be degraded by proteases although the formation of cross-links may impede proteolysis (Tyedmers, Mogk, and Bukau 2010). If the capacity for such repair is exceeded, e.g. during stress, misfolded proteins aggregate temporarily to become later disaggregated and preferentially refolded or alternatively degraded by bi-chaperone systems (Tyedmers, Mogk, and Bukau 2010; Winkler et al. 2010). Elevated expression of proteasome or disaggregase activities can prevent the accumulation of aggregates and hence aging of budding yeast (Andersson et al. 2013). Similarly, elevated expression of superoxide dismutase in *E. coli* reduces formation of protein aggregates below wild type levels (Maisonneuve, Ezraty, and Dukan 2008). Importantly, repair processes, defences against e.g. reactive oxygen species, and their expression levels could evolve to adapt to recurring stresses provided this would increase fitness.

For this reason, details and expression levels of repair and defence processes are not prescribed as we are asking an evolutionary question. What is essential is to consider the costs of repair, and there are two types of cost in UnicellAge: (i) protein dedicated to repair cannot contribute to growth, so that the conversion of substrate into new active biomass, and thus growth rate, becomes reduced in proportion to β, the fraction of protein dedicated to repair (Figure 3.2C); (ii) some material has to be consumed in the repair process to generate the required resources such as energy and building blocks. Refolding requires less energy than proteolysis plus re-synthesis, but even proteolysis will release intact monomers that can be recycled in the synthesis of new polymers. Hence, the efficiency of converting damaged material into new material should be higher than the efficiency of converting a single type of monomer, the growth substrate glucose, into all monomers required (Stouthamer 1979). In summary, the efficiency of repair should be higher than the efficiency of growth (known as the growth yield) on glucose of 44% (Neijssel, de Mattos, and Tempest 1996) but lower than 100%. By default an efficiency of 80% is assumed. Repair and growth machineries are considered to be equally susceptible to damage. For simplicity, the rate of repair, r, is assumed to be proportional to the concentration of damage and proportional to the concentration of repair machinery (Figure 3.2D), and that this rate saturates similar to Michaelis-Menten enzyme kinetics as some maximal rate of repair cannot be exceeded. This all gives

$$\frac{dP_{act}}{dt} = (1 - \beta)\mu(S)P_{act} - aP_{act} + Y_r r(\beta P_{act}, P_{dam}),$$ (3.4)

$$\frac{dP_{dam}}{dt} = aP_{act} - r(\beta P_{act}, P_{dam})$$ (3.5)

where

$$r(\beta P_{act}, P_{dam}) = \frac{\beta P_{act} P_{dam}}{\beta P_{act} + P_{dam}}$$ (3.6)

as the simplest kinetics satisfying these assumptions (compare Equations 3.4 and 3.5 with Equations 3.2 and 3.3). Some previous models have not included repair at all (Chao 2010), while

others have assumed that damage decays with a certain, fixed rate (Erjavec et al. 2008; Rashidi, Kirkwood, and Shanley 2012). The difference between *repair* in UnicellAge and damage *decay* in previous models is twofold: (i) decay is assumed to follow first order kinetics like spontaneous, radioactive decay, i.e. decay is not catalysed by 'repair machinery'; (ii) in decay the material is lost while in repair some of the material is recycled.

3.2.3. Modelling toxicity of damaged material

While it is known that some types of damaged material have some inhibitory or toxic effects (González-Montalbán et al. 2005; Nyström 2005), the empirical evidence for an overall toxic effect of damage is weak. If damage were *inert*, one would expect the specific growth rate of a cell to be proportional to the fraction of catalytically active material it contains. As a corollary, specific growth rate should decline linearly with the fraction of damage, i.e. the age of the cell. Equations 3.2 and 3.4 are then extended to

$$\frac{dP_{act}}{dt} = (1 - \beta)\mu(S)P_{act}\left[\frac{P_{act}}{P_{act}+P_{dam}}\right] - aP_{act} + Y_r r(\beta P_{act}, P_{dam}). \qquad (3.7)$$

The decline of reproductive output or specific growth rate with age appears to be approximately linear in *C. crescentus* (Ackermann, Stearns, and Jenal 2003; Ackermann, Schauerte, et al. 2007) and, albeit to a much lesser extent, in *E. coli* (Stewart et al. 2005; Lindner et al. 2008) and *B. subtilis* (Veening et al. 2008). If damage were *toxic*, one would expect the specific growth rate of the cell to decline more strongly than linear, resulting in a concave quadratic relationship (Figure 3.2A). Such a concave quadratic relationship was found to be statistically significant only in some experiments with *C. crescentus* (Ackermann, Chao, et al. 2007), but the deviation from a linear dependency was rather small. The small deviation from a linear relationship observed could be due to a residual activity of damaged material compensating a stronger toxic effect, or due to efficient repair of the damage masking the true rate of toxic damage accumulation. For these two reasons, toxicity may only appear to be absent. As the evidence is not conclusive, both cases are

compared here: inert versus toxic damage. In previous models, toxicity has either been neglected or included in various ways (Table 3.1).

3.2.4. Modelling time

All processes in UnicellAge occur continuously and concurrently, apart from discrete events such as cell division. As a consequence, any formation of new damage will decrease, and any repair of damage will increase, the specific rate of growth with immediate effect rather than once per generation. Another consequence of continuous time processes is that cells do not have to be divided after a certain, fixed generation time as in (Watve et al. 2006; Ackermann, Chao, et al. 2007). Rather, cells with different amounts of damage will grow at different rates and divide at different times in UnicellAge, as in (Erjavec et al. 2008; Chao 2010; Rashidi, Kirkwood, and Shanley 2012). Recent high precision measurements in *E. coli* confirm the assumption made in UnicellAge that cell division is triggered by cell size rather than a timing mechanism (Robert et al. 2014).

Table 3.4. Estimates of damage accumulation rate under experimental conditions.

The group of Lin Chao has estimated the rate at which *E. coli* cells accumulate damage under a number of experimental conditions. Their parameter λ is broadly equivalent to a in UnicellAge, except that they assume damage accumulation to be constant in time only, whereas in UnicellAge it scales by the active protein available. The first, presented in Chao (2010), is based on an analysis of Stewart et al (2005), where a gene for fluorescent protein was inserted into, and expressed by, cells observed using potentially harmful excitation light. All other estimates are from Rang et al (2012): here the authors estimated the effect of applying streptomycin, an antibiotic known to cause protein mistranslation but no genetic damage.

Assumed cause of damage	λ (h^{-1})	95% Confidence Interval	
Fluorescent protein (*yfp*)	0.4642	0.3208	0.5830
None	-0.1998	-0.3408	0.1998
Streptomycin (1 µg ml^{-1})	0.1098	-0.4596	0.2232
Streptomycin (2 µg ml^{-1})	0.3846	0.2568	0.4680
Streptomycin (3 µg ml^{-1})	0.3972	0.2550	0.4890

Estimation of appropriate values for the damage accumulation rate, a, is difficult due to the (assumed) non-linear effects of repair and toxicity in real microbial cells. Lin Chao and co-workers have given a number of estimates for the damage accumulation rate (denoted by λ in their work: Chao 2010; Rang et al. 2012), which are summarised in Table 3.4. It is worth noting that λ signifies a spontaneous accumulation of damage (i.e. the net rate per cell is λt), rather than a in UnicellAge, which signifies an exponential decay of active protein (i.e. the net rate per cell is aP_{act}). The wide range of values, several of them negative, in Table 3.4 demonstrate the difficulty in fitting parameter values to experimental data of a system so non-linear, as we would argue, as the accumulation and repair of damage by microbial cells.

3.2.5. Modelling cell division

Regarding division of volume, cells are assumed to divide instantly into roughly equally sized daughter cells upon reaching a threshold volume (Figure 3.1B). Limited random variation of daughter cell sizes around the average 50:50 models the imprecision of cell division and leads to desynchronization of cell divisions amongst offspring. Since age-related changes of cell size at division have either not been noticed (Ackermann, Stearns, and Jenal 2003; Ackermann, Chao, et al. 2007; Lindner et al. 2008; Veening et al. 2008; Wang et al. 2010; Bergmiller and Ackermann 2011 for *E. coli*) or if noticed been small (Stewart et al. 2005; Bergmiller and Ackermann 2011 for *Methylobacterium extorquens*), the volume triggering cell division is assumed to be the total volume of the cell regardless of how much of it is active or damaged material. However, this assumption is changed for comparison with the model of Erjavec et al (2008) below in Dependence of predictions on model assumptions.

Regarding damage segregation, the scheme of Erjavec et al (2008) is followed for partitioning active and damaged material between the old-pole and new-pole inheriting daughter cells at division (Figure 3.1B). This scheme employs an asymmetry parameter α that can take any

value between 0 for completely symmetric division (i.e. no damage segregation) leading to identical offspring and 1 for completely asymmetric division where one daughter cell takes all the damage (up to the capacity of the cell). The daughter cell inheriting more of the damage represents the daughter cell inheriting the older cell pole from the mother.

Upon cell division, the post-division protein masses of the old-pole cell are

$$P_{act} = (1 - \theta)P'_{act} - \alpha\theta P'_{dam}, \tag{3.8}$$

$$P_{dam} = (1 - \theta)P'_{dam} + \alpha\theta P'_{dam}, \tag{3.9}$$

and those of the new-pole cell are

$$P_{act} = \theta P'_{act} + \alpha\theta P'_{dam}, \tag{3.10}$$

$$P_{dam} = \theta P'_{dam} - \alpha\theta P'_{dam}, \tag{3.11}$$

where the prime indicates the protein amounts in the pre-division cell. However, when $(1 - \theta)P'_{act} < \alpha\theta P'_{dam}$ and so the old-pole cell would inherit a negative quantity of active protein, the old-pole cell inherits only damaged protein

$$P_{act} = 0, \tag{3.12}$$

$$P_{dam} = (1 - \theta)(P'_{act} + P'_{dam}), \tag{3.13}$$

and the new-pole cell inherits all the active protein plus the remainder of the damaged protein

$$P_{act} = P'_{act}, \tag{3.14}$$

$$P_{dam} = \theta P'_{dam} - (1 - \theta)P'_{act}. \tag{3.15}$$

Complete symmetry, complete asymmetry, and various intermediate asymmetries were all simulated.

In all simulations apart from the lineage study (see Minimal aging below), the Baby Mass Fraction, θ, was the only randomly varied parameter since this was sufficient to avoid unrealistic synchronous growth. This Baby Mass Fraction CV was set to 0.05 for all simulations, which

means that the actual values of θ followed a Gaussian distribution with a mean of 0.5 and SD of 0.025, similar to typically observed variation (c.f. Figure 1D in Aldridge et al. 2012).

3.2.6. Modelling a constant environment

In order to compare UnicellAge more directly with all previous models, which have not included any competition for dynamic resources, a constant environment was implemented. For this case, substrate concentration is kept constant at the half-saturation constant K_S, and the total population size is maintained at 1000 cells by removing an individual at random each time a division occurs (Figure 3.1C). This fulfils the role of extrinsic mortality, which is important since extrinsic mortality is the reason why early reproduction is favoured by natural selection (Medawar 1952). Note that only some models included extrinsic mortality (Table 3.1). Populations were initialized either with 1000 cells of one strategy or with 500 each of two competing strategies. To assess the fitness of a single population following a given strategy in isolation, the mean specific growth rate of all cells in the population was sampled once a day after a stochastic steady state had been reached (over the final 400 days of a 500-day simulation) and the mean of these calculated.

For the lineage simulations replicating the experiments of Lindner et al. (2008), the population was first simulated in a constant environment to mimic inoculation from a pre-culture growing under the same conditions. Parameters used in these simulations were: maximum growth rate μ_{max} = 3 h^{-1} and constant substrate concentration S = 5.64 mg L^{-1} to reflect the experiments. Fifteen cells were randomly selected from the final output of the pre-culture, i.e. at steady state, and the two immediate offspring of each of these fifteen used as progenitors (i.e. thirty progenitor cells) for a simulation with identical parameters but without removal of cells from the population. These simulations ran until the total population reached 8000 to ensure that

all cells underwent at least 6 divisions, from which the lineage trees were constructed. Growth rates were normalized by generation and averaged, as in Lindner et al. (2008).

3.2.7. Modelling a dynamic environment

Since the constant environment is clearly unrealistic, researchers have traditionally used the chemostat to assess experimentally or theoretically the fitness of different strategies competing for the same limiting resource (Smith and Waltman 1995). The chemostat is an open, well-mixed system where fresh resources are supplied, and cells and left over resources are removed, with a constant dilution rate D (Figure 3.1D). As such, the substrate concentration S varies according to

$$\frac{dS}{dt} = D(S_{in} - S) - \sum_{cells}(1 - \beta)Y_\mu^{-1}\mu(S)P_{act} \qquad (3.16)$$

when damage is inert, and

$$\frac{dS}{dt} = D(S_{in} - S) - \sum_{cells}(1 - \beta)Y_\mu^{-1}\mu(S)P_{act}\left[\frac{P_{act}}{P_{act}+P_{dam}}\right] \qquad (3.17)$$

when it is toxic. S_{in} denotes the substrate concentration of the chemostat inflow (Table 3.3).

This system reaches a steady state where growth is balanced by dilution. Since specific growth rate in the chemostat will become equal to the fixed dilution rate in steady state, growth rate cannot be used to assess fitness. Rather, the steady-state substrate concentration can be used to assess the fitness of single strategies in isolation because the ability to grow as fast as the dilution rate at a *lower* substrate concentration confers *higher* fitness (Tilman 1982; Kreft 2009). Populations were seeded either with 2000 cells of one strategy or with 1000 each of two competing strategies. As with mean specific growth rate in the constant environment, substrate concentration was recorded daily after reaching steady state, over the final 400 days of a 500-day chemostat simulation, and averaged. Note that dilution is a form of extrinsic mortality, so both environments feature extrinsic mortality.

3.2.8. Determination of fitness

Specific growth rate in the constant environment, or substrate concentration sustaining sufficient growth rate in the steady state of a chemostat, are important contributing factors to fitness, but ultimately, fitness cannot be determined in single species cultures since it emerges from the interactions between strategies. Therefore, fitness has to be evaluated by competition of two strategies in a given environment, counting how often a strategy becomes extinct or fixed in the population.

The fitnesses of aging strategies were initially ranked based on simulations of single strategies in isolation (Figure 3.3). To verify these rankings we then performed pairwise competitions between strategies next in rank, which most of the time confirmed the initial rankings but not always. A standard test of the null hypothesis that the binomial probability of each of the two competing strategies being washed out was equal, i.e. 50:50, decided competiveness. If this had to be rejected, then the strategy washed out less often was considered to have a significant competitive advantage. Results of all tests are available online (see Software and hardware used). For detecting an effect-size of 10% (i.e. probability of washout 40:60) at a significance level of 5% (two-sided) and a power of 90%, up to 518 pairwise competitions between the strategies were required. If the effect was larger, fewer competitions were simulated. Note that not all competitions led to washout within the 500 day maximum simulated time; these draws were ignored.

The full data set of all competition results is freely available from BMC Biology at http://www.biomedcentral.com/content/supplementary/s12915-014-0052-x-s15.xlsx

Figure 3.3. Fitness is verified by pairwise competition simulations.

For a given set of environmental conditions (constant/dynamic environment, damage accumulation rate) the strategies are first ranked by their fitness in single-strategy simulations. Next, pairwise competition simulations are performed between all immediate neighbours in this ranking: up to 518 simulations were performed for each competition to test the hypothesis that the chance of the lower-ranked strategy being washed out of the system is greater than 0.5. If this null hypothesis can be accepted then the initial ranking holds for this pair. If an alternate hypothesis, that the probability is 0.5 is instead acceptable, then the two strategies are concluded to have equal fitness. Third, if a hypothesis that the probability is less than 0.5 can be accepted, then the rankings are switched for this pair, and competition simulations with their new neighbours performed.

3.3. Results

3.3.1. Repair is fitter than damage segregation

The fitness of damage repair and damage segregation strategies were compared, assuming damage to be either inert or toxic and varying all aging related parameters: the investment in repair, the efficiency of repair, the degree of asymmetry, and the rate of damage accumulation. All strategies were evaluated in two well-mixed environments, with constant or dynamic resources, as well as in isolation (pure culture) and in competition (mixed culture). Apart from very low

damage accumulation rates, the fittest strategy was repair of damage but not damage segregation (Table 3.5).

If damage was inert, fitness differences between strategies were minute (Figure 3.4A, C). Nevertheless, these minute differences were large enough to result in statistically significant differences in competitiveness in most cases, particularly between strategies that repair but differ in damage segregation. Indeed, the only set of conditions under which the fitnesses of the higher-ranked strategies were found to be indistinguishable was the most benign, i.e., when damage was inert and accumulated at the lowest rate of 0.01 h^{-1} in the constant environment. Under all other sets of conditions tested, there was a clearly superior strategy (Table 3.5).

If damage was toxic, the fitness differences between strategies were more apparent, becoming very strong at high damage accumulation rates (Figure 3.4B, D). Nevertheless, there were still a few instances of statistically insignificant differences in competitiveness of lower ranked strategies at low damage accumulation rates (Table 3.5).

Table 3.5. Overview of which strategy is fittest depending on conditions.

Damage accumulation rate and environment were varied for inert and toxic damage being repaired at a certain optimal investment in repair determined beforehand. Fitness was evaluated by competition (Figure 3.3). Strategies were: (N) Non-repairers regardless of the damage segregation strategy when the latter had insignificant effects on fitness; (S) Symmetric (α=0); (O) Optimal repair.

Damage accumulation rate a (h^{-1})	Environment	Damage Inert	Damage Toxic
0.01	Constant	N	SO
	Dynamic	SO	SO
0.05	Constant	SO	SO
	Dynamic	SO	SO
0.10	Constant	SO	SO
	Dynamic	SO	SO
0.15	Constant	SO	SO
	Dynamic	SO	SO
0.20	Constant	SO	SO
	Dynamic	SO	SO
0.25	Constant	SO	SO
	Dynamic	SO	SO
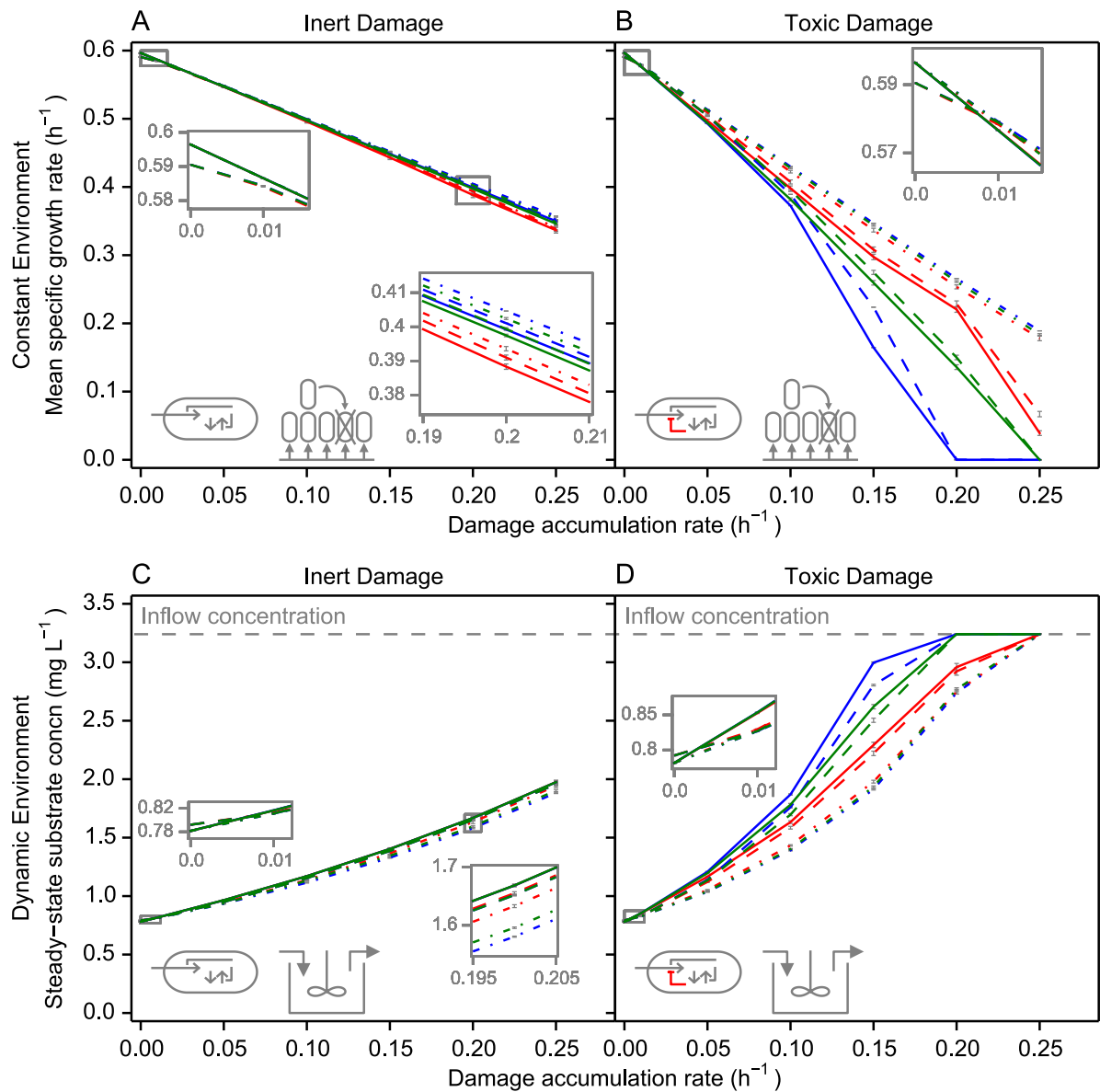
Figure 3.4. Fitness of damage repair and segregation strategies with increasing damage accumulation rates.

The fitness of the completely symmetric (blue), mid-symmetric (green) and completely asymmetric (A, red) damage segregation strategies increased when combined with repair (solid lines with no repair, dashed lines with repair fixed at $\beta = 0.01$ Optimal investment in repair was always fittest (dash-dotted lines), most of all in the absence of segregation. Fitness differences were much smaller when damage was inert **(A, C)** than when it was toxic **(B, D)**. Note that in the constant environment **(A, B)**, single-strategy fitness is determined by specific growth rate, while in the dynamic environment **(C, D)**, it is determined by the ability to persist at the lowest substrate concentration. Error bars show standard deviations (n = 400).

3.3.2. Optimal investment in repair machinery

An optimal investment in repair machinery is expected given that repair is both beneficial, by turning damaged protein into active protein, and costly. This would suggest that strategies become well adapted to their long-term environmental conditions. Indeed, an optimal, positive investment in repair existed for all damage segregation strategies and environments (Figures 3.3 to 3.5). These optima were often quite broad (Figure 3.5) suggesting that investment in repair remains almost optimal in the case of small changes in environmental conditions. The optima were broader for asymmetrically dividing cells and this might give these strategies an advantage if damage accumulation rates fluctuate. One would also expect that the optimal investment in repair increases in proportion to the damage accumulation rate, and this was more or less the case (Figure 3.6). With optimal repair, fitness never declined sharply at high damage accumulation rates (Figure 3.4B) since cells remained rather young even at the highest damage accumulation rate (Figure 3.7B). As mentioned, experimental studies have rarely found growth rate to decline more strongly than linearly, although one would expect this if damage were non-catalytic and toxic. The results presented here suggest that optimal repair, which led to a linear decline of growth rate even if damage was toxic, can effectively mask toxic effects (Figure 3.4B).

3.3.3. Interaction between repair and segregation

Since repair of damage was found to be beneficial, the next question was whether it is best to repair and segregate damage or just repair damage. In both environments and for inert and toxic damage, the fittest strategy was to repair damage optimally but not to segregate it (Figures 3.3 to 3.4). While repair was always beneficial, this benefit was more pronounced if the damage was not also segregated. As a corollary, the less damage was repaired the more beneficial it became to segregate it: if damage was inert and not repaired, asymmetric division became about as fit as symmetric division; if damage was toxic and not repaired, asymmetric division was fitter than symmetric division (Figures 3.3 to 3.4), in line with results of previous models.

3.3.4. Benefits of repair

Another question was why the benefits of repair outweighed the costs. As a consequence of investment in repair being optimal, optimally repairing cells had a higher fraction of active protein than those investing too little in repair (Figure 3.7). Those investing too much in repair had a higher fraction of active protein than those investing optimally. However, optimally-repairing cells did have more active protein *that was dedicated to growth* (recall that repair machinery cannot contribute to growth). If damage was toxic, this led to an additional benefit: optimally repairing cells also contained less damage hindering growth.
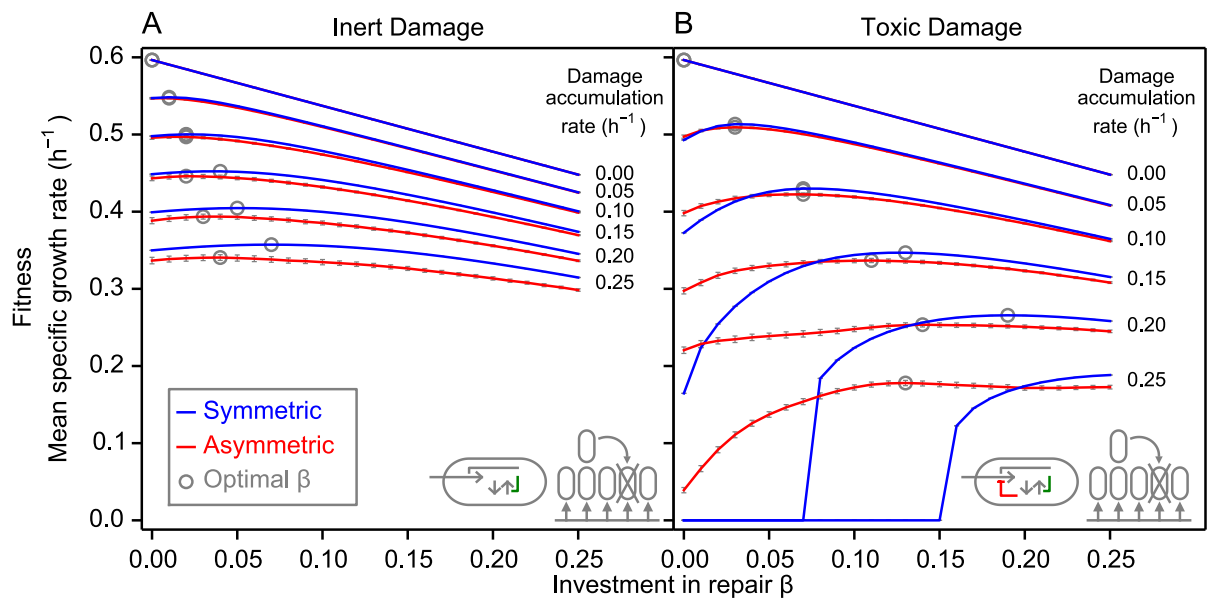
Figure 3.5. Existence of an optimal investment in repair for both symmetric and asymmetric damage segregation strategies.

The dependence of the mean specific growth rate on the level of investment in repair β is shown for completely asymmetric (red) and completely symmetric (blue) segregation strategies over a range of damage accumulation rates. Optimal investment in repair β is indicated by circles. The optimum was at a higher β for symmetric division. Fitness at the optimal β for symmetric division was higher than the fitness at the optimal β for asymmetric division. Repair was more beneficial if damage was not segregated. Damage is assumed to be **(A) inert** or **(B) toxic**. The environment is constant. Error bars show standard deviations (n = 400).
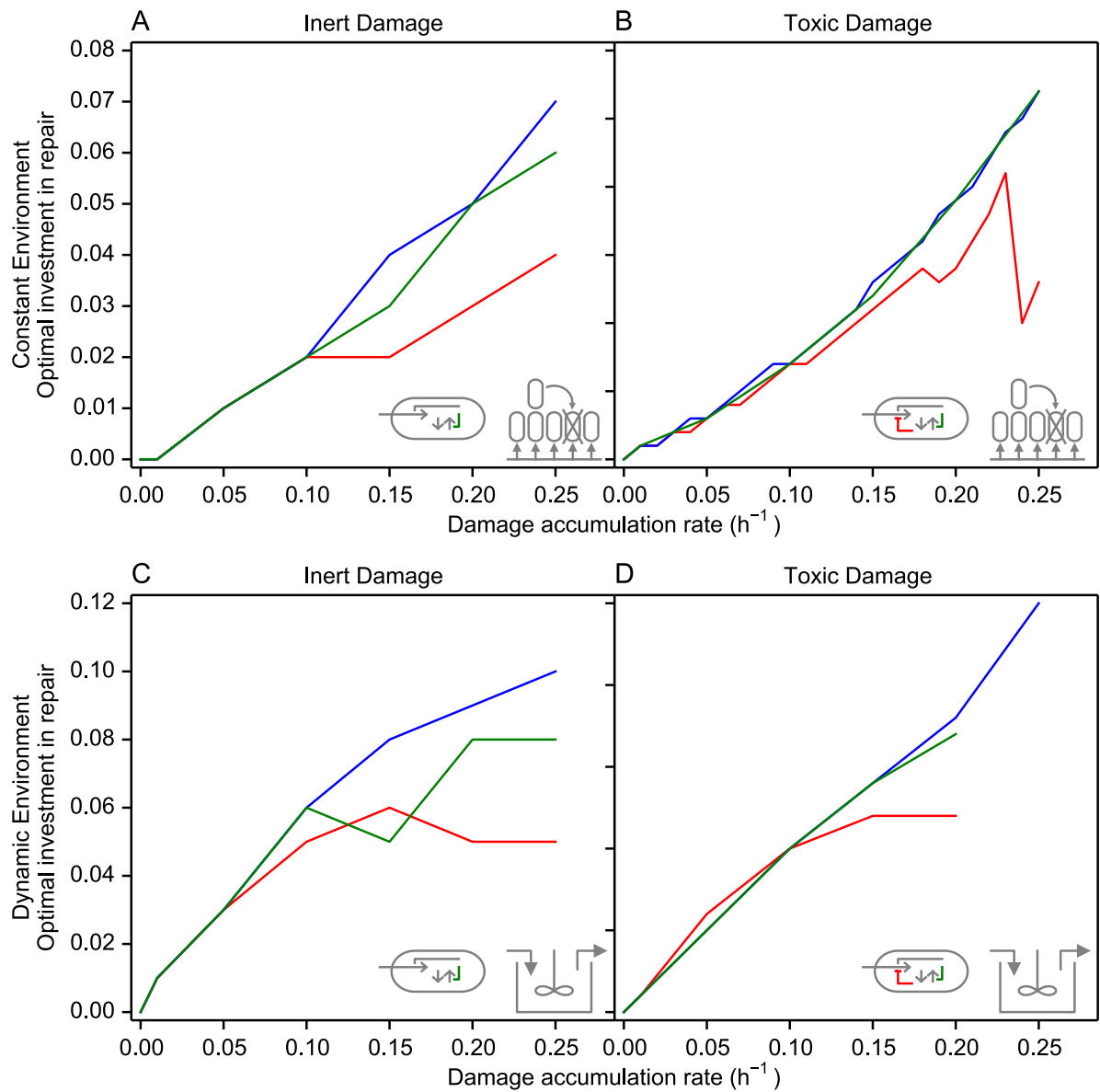
Figure 3.6. The optimal investment in repair β increased with damage accumulation rate.
Asymmetric (red), mid-symmetric (green) and symmetric (blue) damage segregation strategies showed similar trends. Abrupt deviations from a smooth increase were due to older age classes becoming extinct at certain damage accumulation rates and also imprecise determination of optimal values of β due to broad optima. The increase of the optimal investment in repair with damage accumulation rate was much lower for inert damage **(A, C)** than for toxic damage **(B, D)**. Trends were similar within the same environment, whether constant **(A, B)** or dynamic **(C, D)**.
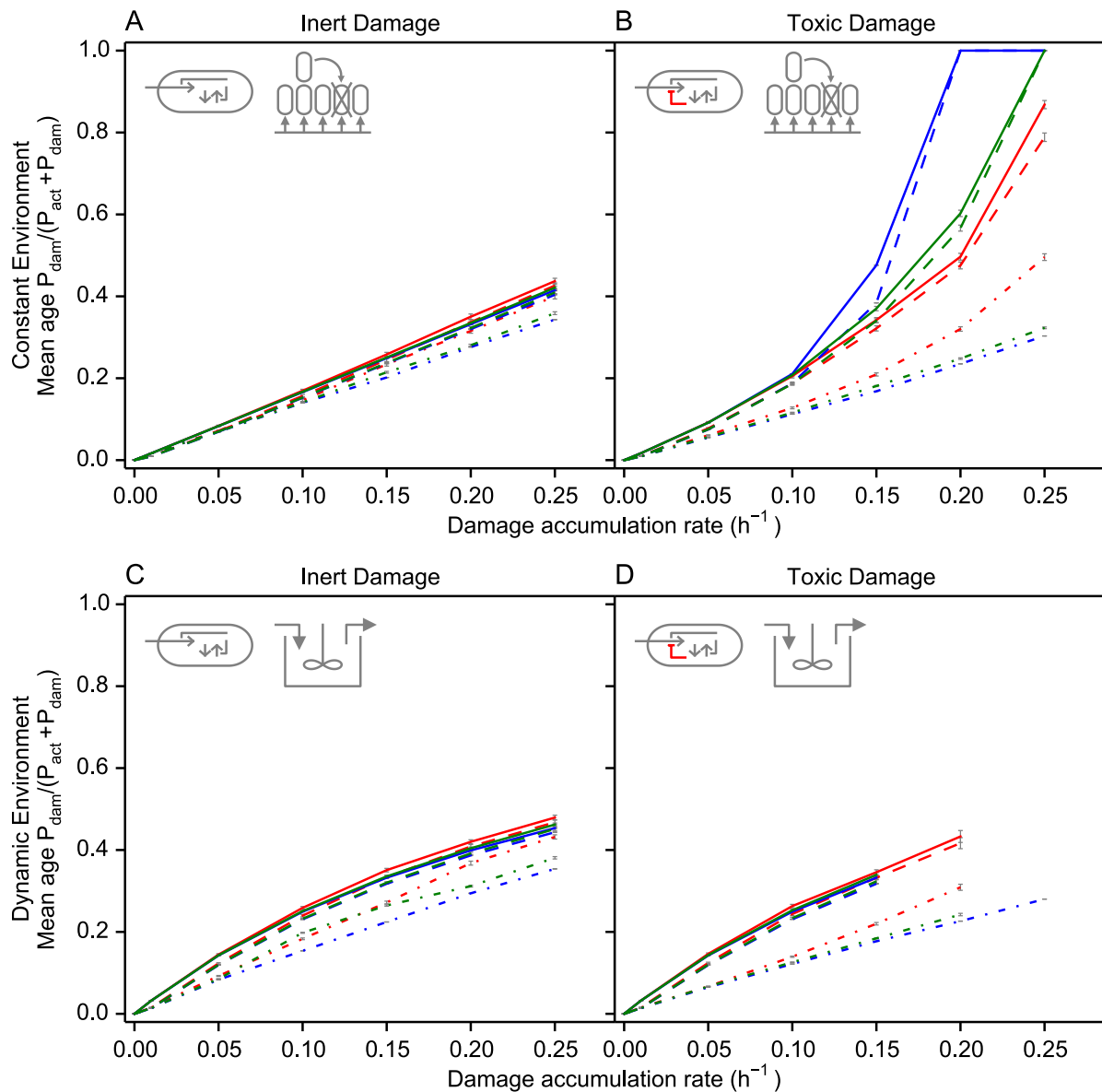
Figure 3.7. Mean age increased with damage accumulation rate.

Age defined as the fraction of damaged protein increased with damage accumulation rate, regardless of whether the environment was constant **(A, B)** or dynamic **(C, D)** or whether damage was inert **(A, C)** or toxic **(B, D)**. Asymmetric (red), mid-symmetric (green) and symmetric (blue) damage segregation strategies showed similar trends, but there were notable differences between repair strategies: strategies without repair (solid lines) were oldest, strategies with fixed repair were intermediate (dashed lines, β fixed at 0.01), and strategies with optimal investment in repair were youngest. Surprisingly, strategies with optimal investment in repair had a lower age when damage was toxic than when it was inert. Note that age cannot exceed one and that populations may become extinct if they are too old to grow fast enough. Error bars show standard deviations (n=400).
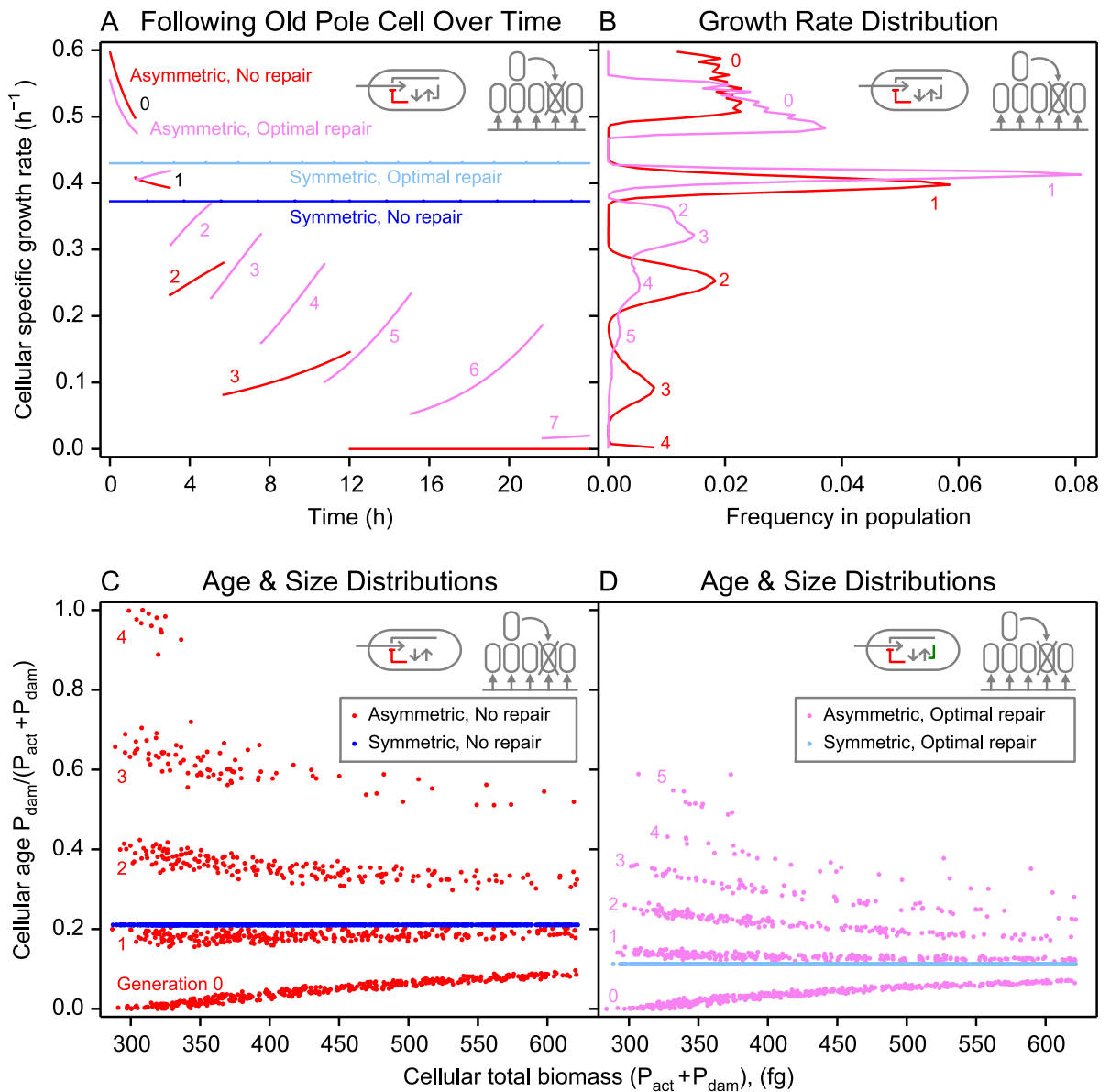
Figure 3.8. Effect of repair on specific growth rate.

(A) Following asymmetrically dividing single cells over consecutive cell divisions, indicated by numbers, in which they repeatedly inherited all damage (old-pole cells) shows that the specific growth rate of a cell without repair (red) starts higher but decreases faster than that of a cell with optimal repair (magenta, β =0.07). Specific growth rates of symmetrically dividing cells do not change at division giving horizontal lines: lower without repair (blue) than with optimal repair (cyan, β =0.07). **(B)** Specific growth rate distribution in steady-state populations of asymmetrically dividing cells. Only new-pole cells grow faster without repair (red) than with optimal repair (magenta). **(C, D)** Snapshots of age and size distributions in the population without repair **(C)** or with optimal repair **(D)**. Each dot represents a cell with a certain mass and age. Age is constant, i.e. in a steady state, in symmetrically dividing cells, and reduced with optimal repair. In asymmetrically dividing cells, young cells grow older during the cell cycle while the damage that older cells have inherited can become diluted by growth, which decreases age

during the cell cycle. Cells are younger with optimal repair. **(A-D)** The environment was constant and damage toxic, accumulating at a rate of 0.1 h^{-1}.

3.3.5. Population age structure

Firstly, a single asymmetrically dividing cell was followed over consecutive divisions. The specific growth rate of an old-pole cell, the cell that inherited all of the damaged protein at each division, declined from generation to generation (Figure 3.8A). In this example, old-pole cells of non-repairers grew at a lower specific growth rate than optimally repairing cells, already after the first cell division. Only the new-pole cells of non-repairers grew at higher specific growth rates than cells repairing damage optimally. Another advantage of repair was that it increased the number of generations over which an old-pole cell remained viable (Figure 3.8A). Note that this benefit of an extended lifespan of the old-pole cell could be reduced by extrinsic mortality as present in the simulations so cells were unlikely to survive into old age (Figure 3.8C, D).

Secondly, the benefits of repair for asymmetrically dividing cells were examined at the population level, i.e. where an ancestor produced a lineage of offspring, leading to a clonal population with age structure (Figure 3.8C, D). The snapshots of the population age structures show several generations and in each generation cells in different phases of their division cycle (from ~300 to ~600 fg dry mass). Age during the division cycle can increase due to damage accumulation, or decrease because of dilution of damage due to growth. The former is more likely if the cell has initially little damage and *vice versa*. Due to extrinsic mortality, there are fewer cells in older generations. With optimal repair, there are more generations and the ages are younger and closer together as the increase of age during the division cycle is reduced. The youngest age cohort of non-repairers was the only one growing at a faster specific rate than optimal repairers. For all other ages, optimal repairers grew faster, and the difference increased the older the cells became (Figure 3.8B).

Symmetrically dividing cells, in contrast, were all of equal age (Figure 3.8C, D), i.e. containing the same fraction of damage, and therefore growing at the same specific growth rate (Figure 3.8A). In this case, the specific growth rate was higher if damage was repaired optimally than if it was not repaired, for all cells (Figure 3.8A). In summary, optimal repair contributed most to fitness, while symmetry provided an additional advantage, in all cases (Figure 3.5).

Table 3.6. Repair efficiency affects which strategy is fittest.

Damage accumulation rate and repair yield (repair efficiency) were varied for inert and toxic damage. Fitness was evaluated by competition in the constant environment. Strategies were: (N) Non-repairers regardless of the damage segregation strategy when the latter had insignificant effects on fitness; (SO) Symmetric with Optimal repair; (AO) Asymmetric with Optimal repair.

Damage accumulation rate (h^{-1})	Repair efficiency 40%		Repair efficiency 60%		Repair efficiency 80%	
	Inert	Toxic	Inert	Toxic	Inert	Toxic
0.05	N	SO	N	SO	SO	SO
0.10	N	AO	N	SO	SO	SO
0.15	N	AO	N	SO	SO	SO
0.20	N	AO	N	AO	SO	SO
0.25	N	AO	N	AO	SO	SO

3.3.6. When repair is not beneficial

In the absence of measurements, it has so far been assumed that 80% of the mass of the damaged material being repaired can be recycled into undamaged material, allowing for a small energy requirement of refolding denatured proteins and a larger energy requirement of degrading and re-synthesising those that are not refolded. The default parameter of 80% comes from assuming that recycling is about twice as efficient as de-novo synthesis from glucose. Since this is only an estimate lower repair efficiencies were also tested.

If damage was inert, the optimal investment in repair fell to zero if the recycling efficiency was reduced to 60% or 40%. In this case, fitness of symmetric or asymmetric damage segregation was not significantly different (Table 3.6). If damage was toxic, the optimal

investment in repair was lower but remained above zero in all cases, even if the efficiency of repair was lower than de-novo synthesis. In combination with optimal repair, symmetric division was fitter at low damage accumulation rates. Damage segregation, in combination with optimal repair, became the fittest strategy at high enough damage accumulation rates (Table 3.6).

3.3.7. *When asymmetry is better than repair*

Looking at results from the perspective of the advantages of asymmetric division rather than the advantages of repair, the range of aging parameters under which asymmetry is advantageous can be made explicit. Damage segregation was beneficial at sufficiently high damage accumulation rates provided that damage was toxic and repair inefficient (Figures 3.3 and 3.4, Tables 3.3 and 3.4. If damage was inert and repair optimal but inefficient, the fitnesses of symmetric and asymmetric damage segregation were not significantly different (Table 3.6).

3.3.8. *Dependence of predictions on model assumptions*

So far, the sensitivity of results to changes of all aging parameters (damage accumulation rate a, investment in repair β, damage segregation α, efficiency of repair Y_r, toxicity of damage) have been evaluated and examined in the two environments. The sensitivity of results towards *structural* changes in the model is now considered, i.e. changing assumptions and equations rather than parameters. In particular, the effect of replacing assumptions with those made in a previous model (Erjavec et al. 2008) that did not include repair and assumed damage to be toxic, but otherwise followed the same approach of letting cells grow and accumulate damage continuously and dividing cells when they reach a threshold size. The approaches of the other models (Watve et al. 2006; Ackermann, Chao, et al. 2007; Chao 2010; Rashidi, Kirkwood, and Shanley 2012) are too different to allow us to re-implement them in the individual-based modelling framework iDynoMiCS, which is based on a growth process where cells take up and consume resources leading to growth in mass and volume and then cell division upon reaching a critical size (Lardon

et al. 2011). For a summary of differences between the models, please see Table 3.1 and Figure 3.14.

Erjavec et al. (2008) presented two sets of dynamics they termed "linear" (Equations 3.18 and 3.20) and "exponential" (Eqs 3.19 and 3.20). They scaled proteins in units of molecules (as opposed to femtograms) and time in arbitrary units (as opposed to hours):

$$\frac{dP_{act}}{dt} = \frac{k_1}{k_s + P_{act} + P_{dam}} - k_2 P_{act} - k_3 P_{act}, \qquad (3.18)$$

$$\frac{dP_{act}}{dt} = \frac{c k_1 P_{act}}{k_s + P_{act} + P_{dam}} - k_2 P_{act} - k_3 P_{act}, \qquad (3.19)$$

$$\frac{dP_{dam}}{dt} = k_3 P_{act} - k_4 P_{dam} \qquad (3.20)$$

where $k_s = 1$, $k_1 = 10^7$, $k_2 = k_4 = \ln(2) \approx 0.69$, and k_3 was varied from 0.1 to 2.2. k_s can be considered an affinity constant of sorts, although there is no nutrient consumption in their model. k_1 is essentially a maximum growth rate. k_2 and k_4 are constants describing the rate of decay of P_{act} and of P_{dam}. k_3 gives the rate of conversion from P_{act} to P_{dam} and so is equivalent to a in UnicellAge. The factor c converts from "linear" to "exponential" as P_{act} is typically of the order of 10^3 (Marija Cvijovic, personal correspondence). Their simulations were seeded with only one cell composed of just one active protein and one damaged protein ($P_{act} = P_{dam} = 1$); cells divided according to Equations 3.8 to 3.11 when their active protein reached the threshold of 1500 molecules; and fitness was measured by the size of the population after one arbitrary time unit rather than at steady-state, so their fitness measure may be time-dependent.

Note that the model of Erjavec et al (2008) does not include repair, but instead includes degradation terms (those involving constants k_2 and k_4). Protein degraded is lost rather than recycled, and degradation is a chemical decay reaction that is not catalysed by any fraction of the active protein, as in repair. Here repair in UnicellAge is replaced repair degradation to discover whether this affects results.

The claim of Erjavec et al in describing the growth term in Equation 3.18 as "linear", or that in Equation 3.19 as "exponential" is highly disputable. Their so-called exponential growth (Equation 3.19) is in practice linear growth with toxic damage since their k_s parameter was set to 1, which is negligible compared to the other terms in the denominator (the cell's protein content is on the order of 10^3 molecules). Equation 3.19 therefore simplifies to a constant growth rate (ck_1) multiplied by one minus the age of the cell $\left[\frac{P_{dam}}{P_{act}+P_{dam}}\right]$, resulting in a growth rate that declines linearly with age, as in our model with toxic damage (c.f. Equation 3.7). Hence, their equations can be simplified and rewritten in our notation to give Equations 3.21 to 3.23, the final, exact forms of the growth dynamics applied in our simulations:

$$\frac{dP_{act}}{dt} = 10^4 \frac{P_{act}}{P_{act}+P_{dam}} - kP_{act} - aP_{act} \qquad (\;3.21\;)$$

$$\frac{dP_{act}}{dt} = 10P_{act} \frac{P_{act}}{P_{act}+P_{dam}} - kP_{act} - aP_{act}, \qquad (\;3.22\;)$$

$$\frac{dP_{dam}}{dt} = aP_{act} - kP_{dam} \qquad (\;3.23\;)$$

where, following Erjavec et al (2008), k takes the value of 0.69 (with degradation) or 0 (without degradation) and a takes a range of values between 0 and 3 inclusive.

No experimental evidence can be found that shows growth rate decreasing with increasing active protein (see A. L. Koch 1996 for a review), as described by their so-called linear growth of Equation 3.18. However, there is some evidence that microbial growth may be bi-phasic linear in some organisms (Mitchison and Nurse 1985; Baumgärtner and Tolić-Nørrelykke 2009; Kempes, Dutkiewicz, and Follows 2012; Horváth et al. 2013) but note that this is debated (Cooper 2013) and so the growth term in Equation 3.21, which we consider to be linear growth with toxic damage, merits further attention.

In UnicellAge it is assumed that the cell does not distinguish active from damaged protein when measuring cell volume, so cell division is triggered by reaching a critical amount of total

protein, rather than a critical amount of active protein as in Erjavec et al (2008). Experimental evidence for these assumptions is inconclusive: *Schizosaccharomyces pombe* increases in size with replicative age (Barker and Walmsley 1999); total volume at division does increase in *Methylobacterium extorquens* (about 15% as estimated from Bergmiller and Ackermann (2011) Fig. 2A); old-pole *E. coli* cells divide at the same size as new-pole cells (Bergmiller and Ackermann 2011). The implications of these two conflicting assumptions are also tested here.

In order to be able to directly compare UnicellAge with the model of Erjavec et al (2008), isolated populations were simulated in a constant environment and the mean specific growth rate at steady-state (the mean value over the final 400 time points in a 500 time-unit simulation) was taken to be the fitness of each strategy. This is in contrast to the fitness measure used in Erjavec et al (2008), where it is defined as the size, after one time unit, of a population seeded by one cell composed of just one active and one damaged protein molecule.

The results for the simulations of what can be correctly called exponential growth with toxic damage (Equations 3.22 and 3.23) are shown in Figure 3.9; Figure 3.10A-D shows results for what can be correctly called linear growth with toxic damage (Equations 3.21 and 3.23), and results of Erjavec et al (2008) are reproduced in Figure 3.10E. The effect of protein degradation (Figure 3.9B, D and Figure 3.10B, D) made no difference to the strategy rankings and so including protein degradation was the least important of the assumptions in Erjavec et al (2008). The assumptions regarding measurement of division size and growth law also seemed to make little qualitative difference except in the combination of linear growth and division being triggered by total protein, which lead to fitness decreasing linearly with increasing damage accumulation rate regardless of the symmetry of damage segregation (Figures 3.8 and 3.9). This suggests that assumptions that one might regard as peripheral can affect conclusions.

The clearest differences between these results (Figures 3.8 and 3.9) and those of Erjavec et al (2008) (shown in Figure 3.10E) derived from the difference in measuring fitness. Both

models show an advantage for asymmetric segregation of damage at division when damage is toxic, but whereas Erjavec et al (2008) find that all strategies reach clonal senescence at the same damage accumulation rate (presumably because they start their simulations with a single cell which does not divide and so segregation strategies are irrelevant), we found that this point differs between strategies in our steady-state approach. Note that repair is excluded here as Erjavec et al (2008) did not include it; asymmetric damage segregation was the best strategy only in the absence of repair.

One of the key results of Erjavec et al. (2008) – that damage segregation is beneficial if the damage accumulation rate is high, the damage toxic, and repair not occurring – has therefore been confirmed here.
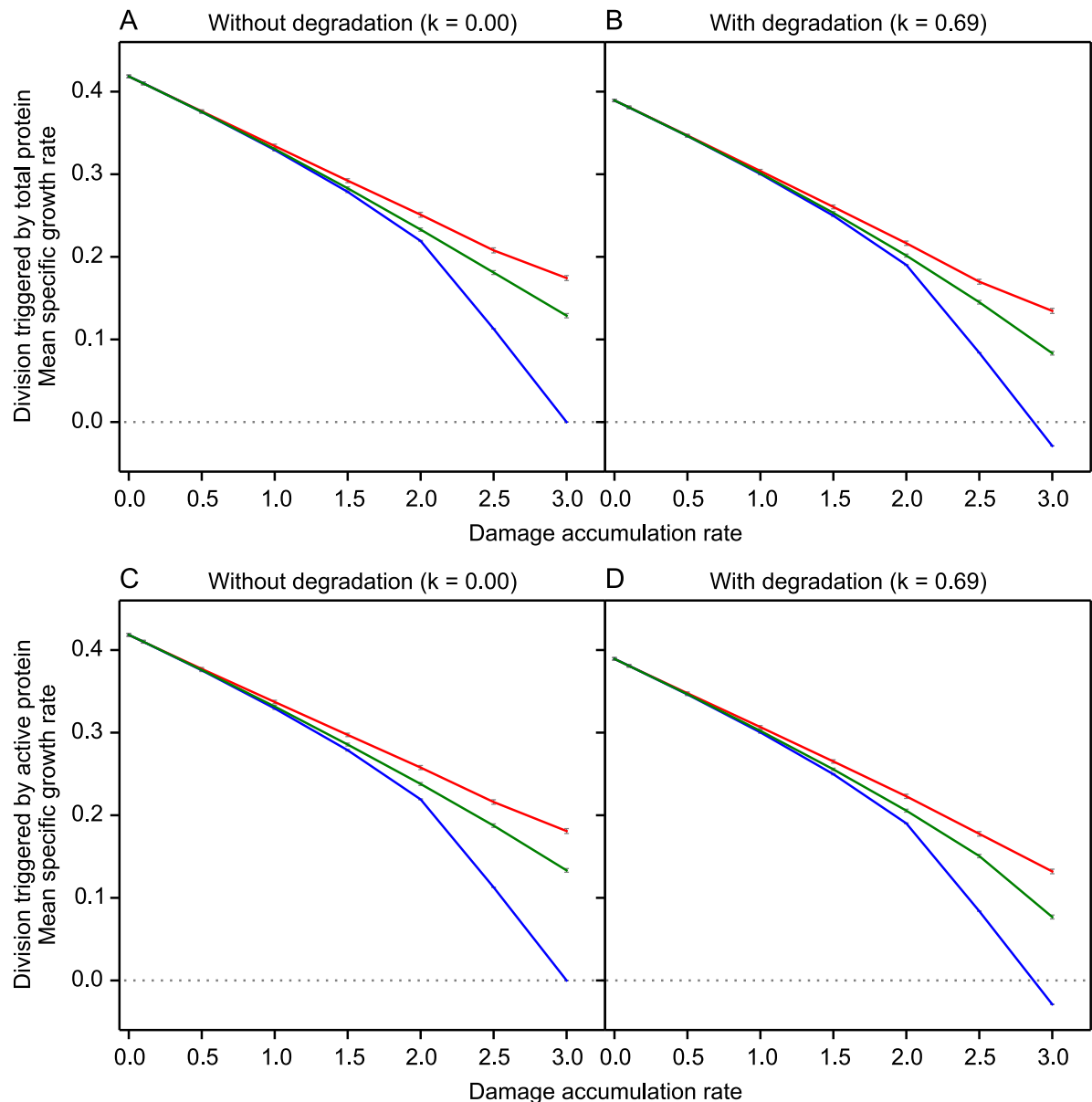
Figure 3.9. Exponential growth with toxic damage in a constant environment without repair.

Mean specific growth rates (per arbitrary time unit) of different damage segregation strategies when growth is exponential (Equations 3.22 and 3.23): asymmetric (red), mid-symmetric (green), and symmetric (blue). **(A, B)** Division is triggered by *total* protein, the default for UnicellAge; **(C, D)** Division is triggered by *active* protein only, as in Erjavec et al. (2008); **(A, C)** without degradation (k= 0.00), the default for UnicellAge; **(B, D)** with degradation (k=0.69), as in Erjavec et al. (2008). Panels **(A-D)** should also be compared with the corresponding panels in Figure 3.10 for linear growth. Conditions and assumptions for panel **(A)** are equivalent (although with different units and parameters) to those made in UnicellAge, see Figure 3.4B. Results for UnicellAge under these conditions are qualitatively the same as the results from the re-implemented model Erjavec et al. (2008). Error bars are standard deviations (n=400).

(FOLLOWING PAGE)

Figure 3.10. Linear growth with toxic damage in a constant environment without repair.

Mean specific growth rates (per arbitrary time unit) of different damage segregation strategies when growth is linear as in Erjavec et al. (2008) (Equations 3.21 and 3.23): asymmetric (red), mid-symmetric (green), and symmetric (blue). **(A, B)** Division is triggered by *total* protein, the default for UnicellAge; **(C, D)** Division is triggered by *active* protein only, as in Erjavec et al. (2008); **(A, C)** without degradation (k= 0.00), the default for UnicellAge; **(B, D)** with degradation (k=0.69), as in Erjavec et al. (2008). **(A, B)** Symmetric division had a minimally but not significantly higher specific growth rate than mid-symmetric division. Panels **(A-D)** should also be compared with the corresponding panels in Figure 3.9 for exponential growth. Error bars are standard deviations (n=400). For comparison with the results of Erjavec et al. (2008), panel **(E)** reproduces their Figure 3A with permission (© 2008 The National Academy of Sciences of the USA). Their parameter *re* (retention of damage) is equivalent to α in UnicellAge, with 0 indicating symmetric division.

A Without degradation (k = 0.00)   B With degradation (k = 0.69)

C Without degradation (k = 0.00)   D With degradation (k = 0.69)

E

re=0.000
re=0.125
re=0.500
re=0.875
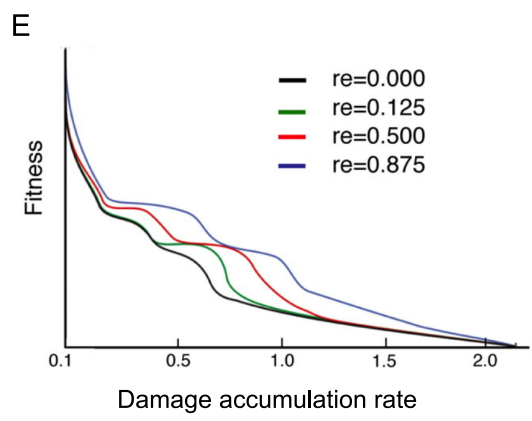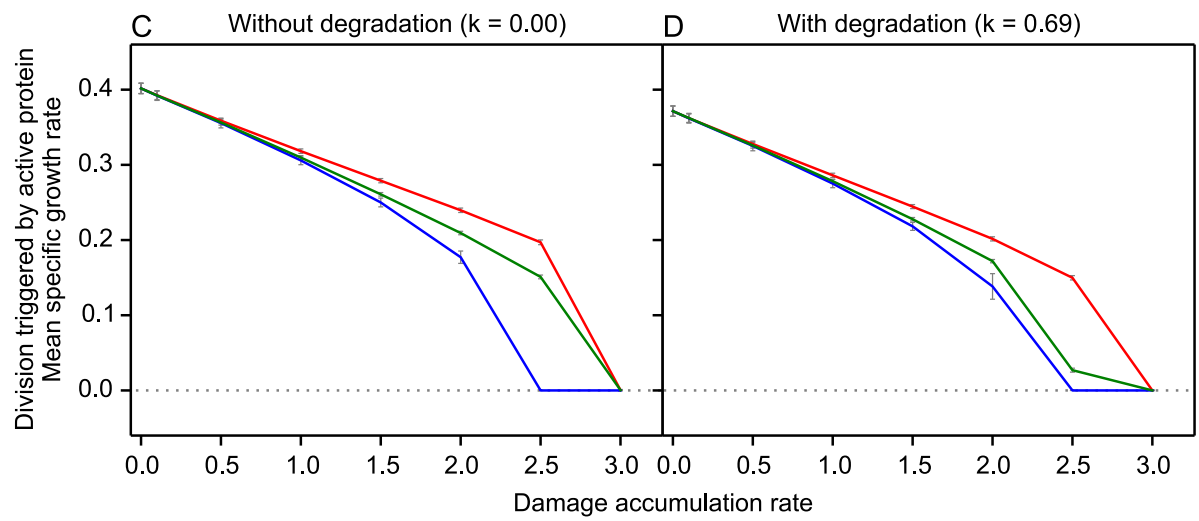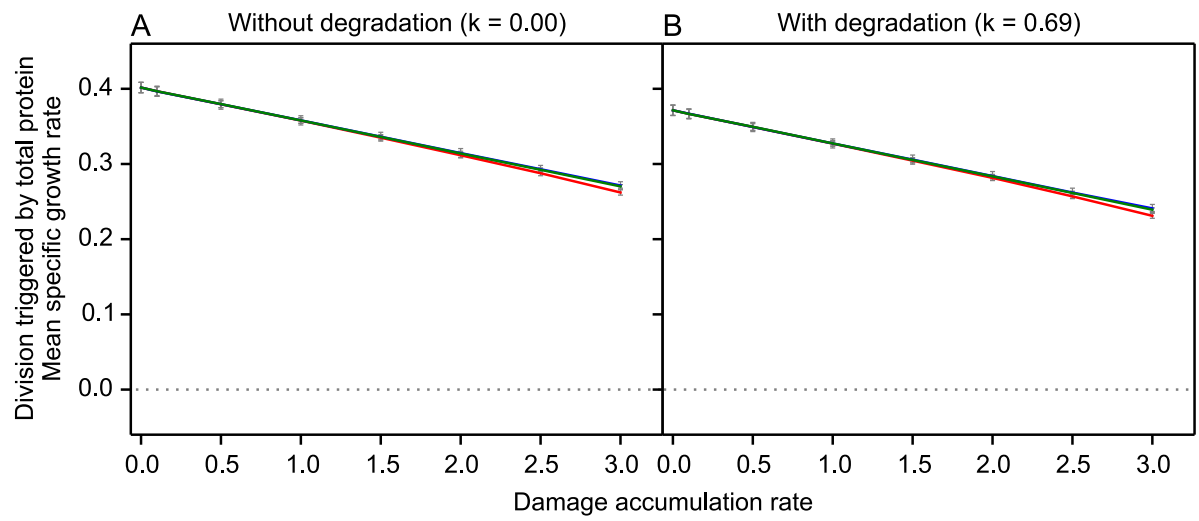
3.3.9. Minimal aging

The results of UnicellAge suggested that all damage should be repaired rather than segregated, if repair is biochemically possible, optimal and sufficiently efficient (Figure 3.5, Table 3.6). Now we compare these predictions with data (Figure 3.11A) that suggest minimal aging does occur in some unicells such as *E. coli*. Note, however, that not all studies found evidence for aging in *E. coli* or some other unicells. Nevertheless, let us assume that, for whatever reason, a fraction of the damage arising may not be repaired before cell division. This should be a small fraction, perhaps about 10% of the total damage accumulated during a generation. For such recalcitrant damage, UnicellAge predicts that it should indeed be completely segregated if it is toxic (see case of zero investment in repair in Figure 3.5). If it were inert, the effect would be very small (Figures 3.3 and 3.4), and presumably impossible to detect experimentally. Let us further assume that not all of this recalcitrant and toxic damage can be as perfectly segregated as it should, e.g. because the segregation of a few large protein aggregates is quite stochastic (Coquel et al. 2013), so asymmetry would be somewhat below perfect.

Figure 3.11B shows that this scenario of largely complete segregation of small amounts of non-repairable, toxic damage can explain the observed specific growth rate reduction of old-pole cells of *E. coli*; compare with Figure 3.11A showing unfiltered data from the study of Lindner et al. (2008). Note that this approach is not fitting the model to the data, since these data do not provide sufficient information for fitting key parameters such as the rates of damage accumulation and repair. Importantly, the alternative scenario shown in Figure 3.11C of minimal segregation of larger amounts of damage can also explain the experimental data, demonstrating that at least two aging scenarios are consistent with these data, while only the first scenario is consistent with predictions of UnicellAge. Comparison of panels B and C of Figure 3.11 highlights the difficulty of reconciling theoretical models with experimental data in biology, particularly when one aims for generality and understandable simplicity (Chapter 1).
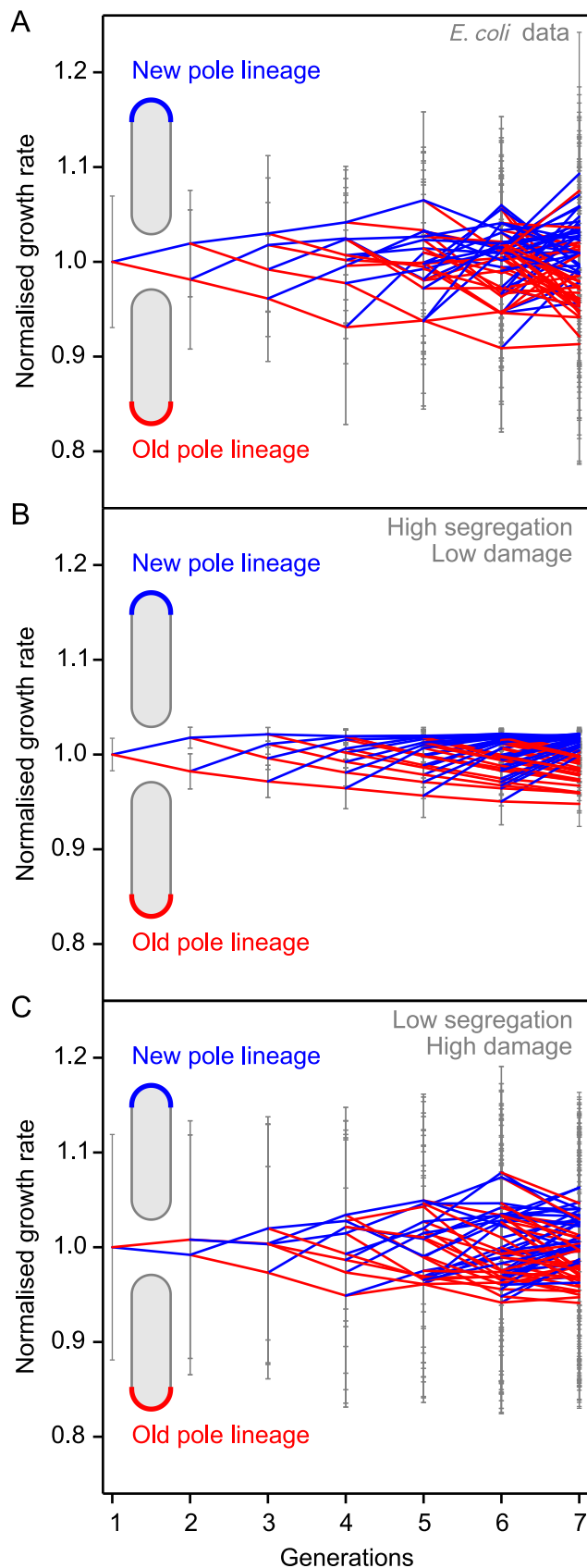
Figure 3.11. Comparison with some experimental results for *E. coli*.

Mean growth rates of new-pole cells (blue) and old-pole cells (red), normalized by generation. Error bars show SD.

(A) Measured growth rates of *E. coli* as published in the paper of Lindner et al. (2008) but without removing rates from lower quality fits (n = 2-30).

(B-C) Results of UnicellAge lineage simulations mimicking the experimental set-up of (A). The Standard Deviation of asymmetry was 0.25 and Coefficients of Variation were 0.05 for both cell radius triggering division and mass fractions of daughter cells. See Figures 3.11 and 3.12 for the effect of changing the extent of stochasticity in these processes.

(B) Simulation assuming high degree of segregation ($\alpha = 0.75$) of low amounts of damage ($a = 0.04$ h^{-1}) (n = 26-30).

(C) Simulation assuming low degree of segregation ($\alpha = 0.05$) of high amounts of damage ($a = 0.35$ h^{-1}) (n = 30).

Both scenarios **(B, C)** are consistent with the data **(A)**, but only **(B)** is consistent with predictions of UnicellAge.

Parameters used in these simulations were: maximum growth rate $\mu_{max} = 3$ h^{-1} and constant substrate concentration S = 5.64 mg L^{-1} to reflect the experiments. Fifteen cells were randomly selected from the final output of the pre-culture, i.e. at steady state, and the two immediate offspring of each of these fifteen used as progenitors (i.e. thirty progenitor cells) for a simulation with identical parameters but without removal of cells from the population. These simulations ran until the total population reached 8000 to ensure that all cells underwent at least 6 divisions, from which the lineage trees were constructed. Growth rates were normalized by generation and averaged, as in Lindner et al. (2008).

Figure 3.12. Effect of stochasticity in damage segregation.

Lineages were simulated using the same method as in Figures 3.10 and 3.12, see also Modelling a constant environment**Error! Reference source not found.**. The standard deviation of the

damage segregation parameter α increases from row to row: **(A, B)** α_{dev} = 0.00; **(C, D)** α_{dev} = 0.25 as in Figure 3.11B-C; **(E, F)** α_{dev} = 0.50. The left column **(A, C, E)** shows the scenario of low segregation of high damage (α = 0.05, a = 0.35 h^{-1}) showing that the spread of mean growth rates and standard deviations increases with increasing α_{dev}. The right column **(B, D, F)** shows the scenario of high segregation of low damage (α = 0.75, a = 0.04 h^{-1}) showing the opposite effect. All other parameters were fixed and the same as in Figure 3.11B-C: Division Radius CV = 0.05, Baby Mass Fraction CV = 0.05. Error bars show standard deviations (n = 17-30).

Parameters used in these simulations were: maximum growth rate μ_{max} = 3 h^{-1} and constant substrate concentration S = 5.64 mg L^{-1} to reflect the experiments. Fifteen cells were randomly selected from the final output of the pre-culture, i.e. at steady state, and the two immediate offspring of each of these fifteen used as progenitors (i.e. thirty progenitor cells) for a simulation with identical parameters but without removal of cells from the population. These simulations ran until the total population reached 8000 to ensure that all cells underwent at least 6 divisions, from which the lineage trees were constructed. Growth rates were normalized by generation and averaged, as in Lindner et al. (2008).

Figure 3.13. Effect of stochasticity in size at division and daughter cell sizes.

Lineages were simulated using the same method as in Figures 3.10 and 3.11, see also Modelling a constant environment. In the top row, the threshold radius triggering division was deterministic (Division Radius CV = 0) **(A)** or allowed to vary (Division Radius CV = 0.1) **(B)**. In the bottom row, the mother's total material is divided deterministically into identically sized daughter cells (Baby Mass Fraction CV = 0) **(C)** or stochastically leading to somewhat differently sized daughter cells (Baby Mass Fraction CV = 0.1) **(D)**. The other CV's had default values of 0.05 as in Figure 3.11C and Figure 3.12C. The effect of stochasticity in size at division and daughter cell sizes was negligible, especially when compared with the effect of varying α_{dev} in Figure 3.12. Error bars show standard deviations (n = 30).

Parameters used in these simulations were: maximum growth rate μ_{max} = 3 h^{-1} and constant substrate concentration S = 5.64 mg L^{-1} to reflect the experiments. Fifteen cells were randomly selected from the final output of the pre-culture, i.e. at steady state, and the two immediate offspring of each of these fifteen used as progenitors (i.e. thirty progenitor cells) for a simulation

with identical parameters but without removal of cells from the population. These simulations ran until the total population reached 8000 to ensure that all cells underwent at least 6 divisions, from which the lineage trees were constructed. Growth rates were normalized by generation and averaged, as in Lindner et al. (2008).
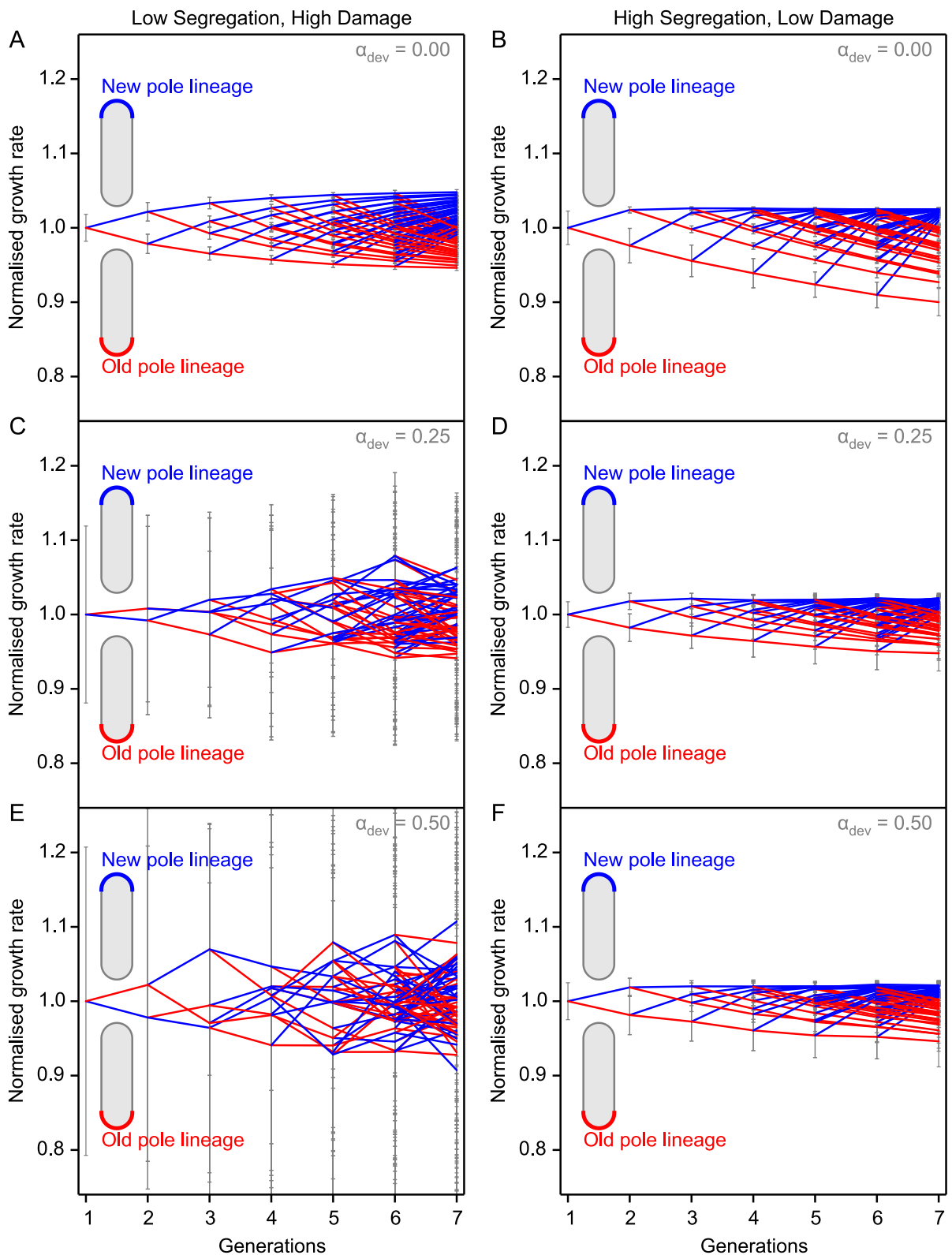
3.4. Discussion

The differences between key results in models demand explanation; to this end, we must examine which models' assumptions and predictions are empirically better supported. Table 3.1 shows the conceptual structure of the various models: the components considered and the processes that produce or remove or interconvert components, apart from the model of Watve *et al.* (2006), which is conceptually too different to be described in this framework Table 3.1 also describes the latter model, and summarizes assumptions and predictions for all.

3.4.1. Repair is beneficial if costs and benefits affect growth immediately

Overall, previous models have supported the notion that repair of damage is not beneficial, but as assumptions vary, results also vary (Table 3.1). If 'repair' has been considered at all, it has either been implemented as removal of damage rather than return to active protein (with or without cost), or conversion of oldest components into newest without any cost (Figure 3.14, Table 3.1). How these differences lead to different predictions is best explained comparing UnicellAge with the conceptually clear and simple model of Ackermann, Chao, et al. (2007). They assumed that 'repair' removes a certain amount of damage from the cell. Since cells in their model are vehicles of damage without size or catalytically active protein, adding or removing damage cannot affect cell growth and division. This means that repair cannot immediately improve growth rate by turning damaged material into active material as in UnicellAge. Instead, benefits of repair are delayed as cells with less damage are more likely to survive after cell division. Costs of repair were implemented by linearly reducing the probability of survival into the next generation with increasing investment in repair (Ackermann, Chao, et al. 2007). They

A Ackermann *et al.* (2007)

Cell divides after fixed time

P_{dam} → ⊣ Probability(survival)

B Erjavec *et al.* (2008)

P_{act} → Growth

P_{dam}

C Chao (2010)

P_{act} → Growth

P_{dam}

D Rashidi *et al.* (2012)

P_{act} → Growth

Energy Budget → ⊣

P_{dam}

if($P_{dam} \geq$ threshold) then Death

E UnicellAge

S → $P_{act} < \begin{matrix}(1-\beta)\\ \beta\end{matrix}$

P_{dam}
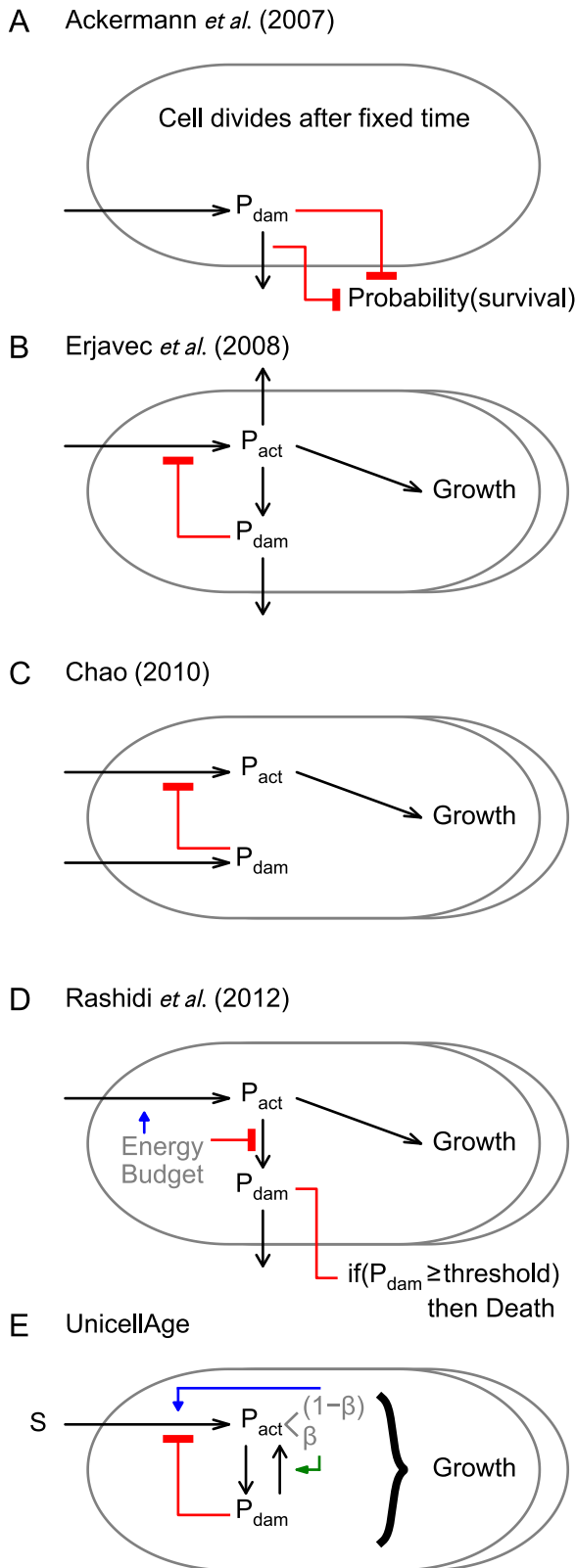
Growth

found that repair is not beneficial if damage can be segregated; the best strategy is complete asymmetry without repair. The absence of an autocatalytic growth process leading to cell division as soon as a critical size is reached prevents the immediate advantage that repair has in UnicellAge.

Note that none of the previous models has implemented 'repair' in such a way that both costs and benefits are realistically accounted for. If 'repair' has no growth rate cost, it is always beneficial (Watve et al. 2006). If 'repair' has no immediate benefit on growth rate, it either does not improve fitness (Ackermann, Chao, et al. 2007), or the bare minimum is employed to avert sudden death (Rashidi, Kirkwood, and Shanley 2012). If 'repair' is simply decay (Erjavec et al. 2008) it has no

Figure 3.14. Comparison of the models.
The components and processes producing, removing, or interconverting the components in various mathematical models, apart from that of Watve et al. (2006), which does not fit into this framework. See Table 3.1 for a description of the assumptions and predictions of these models, including Watve et al. (2006).

fitness benefit, as showed by re-implementing their model (see Dependence of predictions on model assumptions). Only if repair had both immediate benefits and costs as in UnicellAge, there existed an optimal investment in repair machinery that depended on environmental conditions.

Such optimal repair is predicted to improve fitness in the environments tested here, i.e. in long lasting steady state environments with random external mortality with or without resource competition. In essence, the advantage of UnicellAge over previous models is that it considers conditional senescence as part of the aging process, rather than focussing simply on replicative senescence (Box 2).

3.4.2. Evidence supports the prediction that repair is beneficial

Importantly, all organisms studied in this regard have evolved active mechanisms to prevent the formation of, and to repair, various types of non-genetic damage: superoxide dismutases, catalases and reactive oxygen species scavengers prevent oxidative damage, various chaperones prevent misfolding or refold misfolded proteins, bi-chaperone systems disaggregate aggregates of misfolded proteins, and various proteases degrade proteins too damaged to be refolded (Tyedmers, Mogk, and Bukau 2010; Visick and Clarke 1995). Sophisticated defence and repair systems have obviously evolved despite their consumption of ATP and other resources, suggesting that the fitness benefits outweigh the costs, exactly as predicted by UnicellAge. Costs have been reduced in the course of evolution by making the systems inducible (Tyedmers, Mogk, and Bukau 2010) such that their expression is more or less optimal under given environmental conditions. This suggests that the optimal investment in repair identified in UnicellAge will typically be realized *in vivo*.

Further support for the predictions of UnicellAge comes from the following findings: (i) damage reduces fitness in a dosage-dependent manner (Geiler-Samerotte et al. 2011); (ii) repair mutants have reduced fitness (González-Montalbán et al. 2005); a repair mutant shows increased rate of aging (Winkler et al. 2010); overexpression of defence systems (superoxide dismutase)

(Maisonneuve, Ezraty, and Dukan 2008) or overexpression of disaggregase activity reduces the amount of protein aggregates (Andersson et al. 2013). Experimental evidence therefore supports the prediction of UnicellAge that optimal repair evolved to be the major mechanism to deal with damage.

Aging under benign conditions in the laboratory is pronounced in some unicells that inhabit transient environments (Table 3.2). This is further discussed later, but worth mentioning here because it suggests that such unicells invest less in repair than others, such as *E. coli*, that show minimal aging. This highlights that organisms can evolve to deal with damage by segregation or repair, and have done so depending on their ecology. The minimal damage segregation due to sufficient investment in repair observed in *E. coli*, and other unicells living in lasting environments, confirms the prediction of UnicellAge for stable environments.

3.4.3. Damage segregation on top of repair is beneficial under stress

Collectively, previous models have shown damage segregation to be more advantageous than repair, but not always under all conditions (Table 3.1). Note that Erjavec et al. (2008) concluded that damage segregation is fittest when division leads to equally sized offspring, but that symmetry may be advantageous when offspring are smaller, as in the budding yeast. This conclusion is in conflict with evidence of aging in the budding rather than fission yeast and may be a consequence of not including repair as an alternative mechanism of dealing with damage.

Optimal repair plus segregation of damage was found to be the fittest strategy under 'severe' conditions, i.e. if damage was toxic, accumulated at a high rate, whilst repair was inefficient. Under more 'benign' conditions, optimal repair without damage segregation was the best strategy, in the steady state environments examined. Thus, UnicellAge results suggest that unicellular organisms growing in benign and lasting conditions should not age. Aging should be

limited to stressful conditions or short-lived environments. This prediction will now be compared with evidence.

3.4.4. Aging is not for all

Compiling all the evidence on aging in relatively well-studied unicellular organisms, three aspects appear to be crucial for aging: (i) the presence of stress in the experiments, (ii) the cell division mechanism, and (iii) the ecology of the organism (Table 3.2). There appear to be two different life expectancy groups: short-lived and long-lived unicells. The short-lived unicells are *Caulobacter crescentus* and *Saccharomyces cerevisiae*. These are the only unicells that show considerable aging without stress. Their cell biology has little in common, but both produce daughter cells by budding, a process where the non-diffusible components of the daughter cell are made *de novo*. The fission yeast has a similar ecology to the budding yeast but divides by binary fission and does not age in the absence of stress (Coelho et al. 2013).

In short-lived environments early reproduction becomes much more advantageous, also because these environments enable population expansion: early colonisers are likely to have few competitors but the resources may be consumed, or the environment destroyed, before the population can reach a steady state of some kind (Ratcliff et al. 2009). Producing offspring quickly as soon as the habitat has arisen is more beneficial than maintaining cellular function to reproduce late when the environment is short-lived, in contrast to the long-lasting environment assumed in UnicellAge. Figure 3.8 shows that populations of asymmetrically dividing, non-repairing cells contained a fraction of cells that were younger and faster growing than populations of cells that segregated but also repaired damage. The ecology of model organisms is rarely considered, but it turns out to be crucial for understanding why only certain unicells age considerably. A recent analysis of lifespan in birds and mammals came to the similar conclusion that extrinsic mortality, influenced by the ecology and life-history of the organisms, can explain the observed variation in life expectancy (Healy et al. 2014).

3.4.5. Minimal aging in lasting environments

According the predictions of UnicellAge, unicells living in lasting environments are not expected to segregate damage under benign conditions as this would not increase their fitness. Some experimental studies, however, suggest a small degree of damage segregation in long-lived unicells, apparently in the absence of stress. Rang et al. (2012) have argued that studies using fluorescent proteins in fact apply an extrinsic damage agent or stress, and that this is required for aging to be observed. However, many studies using fluorescent proteins have not detected any fitness effects (e.g. Lindner et al. 2008; Wang et al. 2010) so the level of stress may be quite small or, as UnicellAge predicts, effects may be masked by repair processes efficiently dealing with most of the damage. Note that *C. crescentus* (Ackermann, Stearns, and Jenal 2003) and *S. cerevisiae* (Egilmez and Jazwinski 1989) do age even if fluorescent proteins are not used. In any case, the studies showing minimal aging of long-lived unicells under no more than small degrees of stress require further consideration.

Let us first consider the extent to which studies showing minimal aging are consistent with the predictions of UnicellAge. Lindner et al. (2008) is a suitable choice of example because it is a follow-up study of Stewart et al. (2005) revealing the contribution of protein aggregates to the growth rate decline. This study should be representative of all that found a similarly small extent of growth rate decline in: *E. coli* (Stewart et al. 2005), *B. subtilis* (Veening et al. 2008), *Mycobacterium smegmatis* (Aldridge et al. 2012), and the diatom *D. brightwellii* (Laney, Olson, and Sosik 2012). When growth rate does decline with age, it is clear that some damage was not repaired, but inherited by the old-pole cell. UnicellAge predicted that there is an optimal investment into repair provided that repair is sufficiently efficient at returning damaged to active material. This suggests that repair of some damage might not be efficient enough. Indeed, some damage might be too difficult or costly to repair, especially damage that organisms do not usually encounter such as the protein aggregate binding chaperone IbpA fused to the fluorescent protein YFP (Lindner et al.

2008). Moreover, even if the cell has invested into what would normally be the optimal amount of repair machinery, the rate of repair is never infinite so some residual damage will be present during cell division. Results of UnicellAge also suggest that the effect of a small amount of inert damage on the growth rate is too small to be detectable experimentally. Together, this means that any observed extent of aging should be due to the presumably small fraction of non-repaired, toxic damage. Such damage might be associated with protein aggregates which have been shown to localize at the cell poles due to passive Brownian motion combined with size exclusion by the nucleoid, resulting unavoidably in preferential location at the old-pole (Coquel et al. 2013; Winkler et al. 2010). This scenario was simulated in Figure 3.11B, which shows a similar extent of growth rate decline as in the experiments (Figure 3.11A). However, other scenarios not consistent with UnicellAge predictions (Figure 3.11C) can also explain the experimental findings. In summary, the observations of minimal aging in long-lived cells neither contradict nor support the predictions of UnicellAge, while the studies finding no aging support the predictions of UnicellAge (Table 3.2).

3.4.6. Longer term studies

The most decisive studies should be those that have followed old and new-pole cells over the largest number of generations. A recent study by Coelho et al. (2013) of the fission yeast followed old and new-pole cells over more than 30 generations and found fluctuations of growth rate but no clear trend in time under benign conditions. Applying oxidative or heat stress, aging in the sense of an increased time between divisions and probability of death was observed and due to the formation and inheritance of large protein aggregates (Coelho et al. 2013).

Wang et al. (2010) used the same *E. coli* strain with fluorescent protein expression as Stewart et al. (2005), but trapped old-pole cells in a microfluidic cul-de-sac environment following the growth of these cells for about 200 generations. The specific growth rates of these old-pole cells fluctuated but did not decline over time, while the probability of sudden death

increased, although to a low level of 0.02 per cell and per generation. Interestingly, a *lex*A3 SOS stress response mutant had a constant, higher death probability of 0.027 per cell and per generation. Compare undiminished growth over 200 generations to the less than 30 generations of life expectancy of budding yeast where growth rate drops sharply in the last few generations (Egilmez and Jazwinski 1989; Mortimer and Johnston 1959; Lin and Austriaco 2014). Rang et al. (2011) suggested that the old-pole cells tracked by Wang et al. (2010) had reached a steady state age. However, as explained in the Background section, this steady state hypothesis is inconsistent with the observed increase of the probability of death. In summary, the reasons for the various differences between experimental systems remain unclear and it cannot currently be decided whether aging in the group of long-lived unicells only occurs in the presence of external damage agents or whether minimal yet significant aging also occurs under benign conditions. The latter case would suggest that some toxic damage is not efficiently repairable but can instead be 'automatically' segregated by a passive, diffusion-based mechanism.

3.4.7. More evidence supporting the predictions of UnicellAge

There is more empirical backing for the predictions of UnicellAge than the existence of active repair machinery in all organisms studied and the limited extent of aging in some bacteria and fission yeast under benign conditions. Firstly, if aging would in fact be beneficial for all unicellular organisms, either in place of repair or in addition to repair, unicellular organisms dividing by binary fission should have evolved mechanisms for active segregation of damage. However, to our knowledge no active damage segregation mechanisms have been discovered in these organisms, and accumulating evidence is now strongly in favour of passive segregation of protein aggregates in *E. coli* (Winkler et al. 2010; Coquel et al. 2013). This supports the view that active damage segregation mechanisms have not evolved in unicells dividing by binary fission, while budding to facilitate damage segregation is not very common. In budding yeast, damage

segregation is now thought to result from tethering of protein aggregates to organelles (Spokoini et al. 2012; Unruh, Slaughter, and Li 2013).

Secondly, the fact that some unicells show considerably less (if any) aging than *Caulobacter* and the budding yeast under similar stress-free laboratory conditions, implying similar damage accumulation rates, suggests that these minimally aging organisms have invested more into repair than budding cells, in line with expectations from our results for steady state environments.

3.5. Conclusions

Assumptions made in UnicellAge abstract from the details of real unicellular organisms for generality, yet capture the essence of empirical knowledge better than previous models. Most importantly, UnicellAge combines damage segregation and repair, includes realistic costs of repair and allows damage accumulation or repair to have immediate effects on autocatalytic growth. UnicellAge predicts that active repair mechanisms should exist in all unicells but segregation mechanisms should not, or only as a stress response if large amounts of damage accumulate suddenly. Decline of growth rate with age should be absent under benign conditions, or where present, minimal and due to the small amounts of damage that cannot be efficiently repaired whilst segregating passively, due to stochastic rather than active mechanisms. These predictions are much better supported by evidence than previous models' predictions of complete asymmetry and absence of repair. However, some unicells do age considerably without stress. This can be explained by the ecology and cell biology of these organisms: all inhabit short-lived environments and evolved a budding mechanism for cell division that facilitates damage segregation. Distinguishing between (i) benign versus stressful conditions, (ii) inhabiting lasting versus ephemeral environments, and (iii) morphologically symmetric versus budding mechanisms of cell division resolves many of the discrepancies in the literature. Aging is not beneficial for unicellular organisms in well-mixed, lasting and benign environments.Software and hardware used

UnicellAge is free open-source software written in Java™ version 1.6 and based on iDynoMiCS (Lardon et al. 2011) version 1.1, and was run on both a High Performance Computer Cluster (HPCC) and a Dell Precision T1500 PC with 8GB RAM under a Linux operating system. Custom analysis scripts were written in Python (Python Software Foundation 2010) and are included in the UnicellAge repository accessible from www.idynomics.org. All figures were produced using the Python module Matplotlib (Hunter 2007).

CHAPTER 4: ESTIMATING THE RATE OF INTERSPECIES METABOLITE TRANSFER

Competition between microbes is the predominant driving force in their evolution (Foster and Bell 2012); this should be no surprise to anyone familiar with the basics of evolutionary theory. Research on the evolution of cooperation has therefore focussed primarily on the strategies used to exclude "cheaters", i.e. individuals benefitting from the cooperative efforts of others without contributing in return (see, e.g. Damore and Gore 2012). By not paying the costs of cooperation, these individuals would grow and reproduce faster and so their descendants would dominate the population, displacing the cooperative traits. Proposed solutions to this paradox within the world of microorganisms include exchange of genetic material (Juhász et al. 2014), spatial structure (Kreft 2004; Momeni, Waite, and Shou 2013), and even direct attachment between partners (Shimoyama et al. 2009), but the problem is not considered to be solved definitively.

In the shadow of this challenge lies more general research of the cooperation between microbes. While we have been studying the growth of bacterial monocultures for over a century, we still seem to know very little about synergistic interactions between species; authors of one recent review have suggested that as studying isolated microbial cultures is equivalent to the purification and *in vitro* examination of proteins, so we should attempt to knock-out individual species in mixed communities in much the same way that genes encoding proteins of interest are often knocked-out during *in vivo* experiments (Haruta et al. 2009). Yet they, and others, also recognise the contribution that theoretical models have made, and are continuing to make, in this field.

4.1. Background

While "masters of metabolism" when taken as a whole, metabolism by microbial communities often involves cooperative metabolic interactions, particularly among anaerobes (Schink 1992; M. J. McInerney and Gieg 2004; Costa, Pérez, and Kreft 2006). The primary focus of this chapter will be anaerobic methanogenesis, a key process in a number of environments: gastrointestinal

tracts, wastewater treatment plants, freshwater and saline sediments, rice paddies, oil fields, hydrothermal vents, and many more (Schink 1992; Stams 1994; Yuchen Liu and Whitman 2008; Conrad 2009). It has been estimated that around two thirds of global methane production is due to the process (Yuchen Liu and Whitman 2008; Conrad 2009); given the role of atmospheric methane in driving climate change, improved understanding will therefore be of wide interest.

Complex organic polymers are first broken down to simpler molecules, such as lactate or butyrate, by heterotrophic anaerobes. Syntrophic acetogenic bacteria then catabolise these further, releasing metabolites that may include hydrogen, formate and acetate. Local accumulation of these metabolites would make their production thermodynamically unfavourable, but they diffuse away to be consumed by methanogenic archaea. This flow from acetogens, to whom the metabolite is an inhibitory waste product, to methanogens, to whom it is a food source, is a form of syntrophy known as interspecies metabolite transfer (IMT; Stams 1994; Seth and Taga 2014).

It is worth noting that IMT is also significant in the global carbon and nitrogen cycles (Boetius et al. 2000; Costa, Pérez, and Kreft 2006; Popa et al. 2007) and microbial fuel cells (Zeikus 1980; Stams et al. 2006; Yamamuro et al. 2014). Its potential role in disease-causing communities of microbes is only just beginning to emerge (Periasamy and Kolenbrander 2009; Aminov 2013; Zhu et al. 2013; K. H. Tan et al. 2014). Obligate interspecies metabolite transfer is also suspected to play a role in the strong symbiotic relationship seen between partners in phototrophic consortia (Overmann and Schubert 2002), and may well have sparked eukaryotic life (Martin and Müller 1998; López-García and Moreira 2002; Searcy 2003; Dyall, Brown, and Johnson 2004; J. O. McInerney, O'Connell, and Pisani 2014) and the transition from unicellular to multicellular life (J. A. Shapiro 1998; Pfeiffer and Bonhoeffer 2003; Grosberg and Strathmann 2007; Ratcliff et al. 2012).

Estimating the rate of IMT within a simple community metabolising along a linear food chain is straightforward: one needs only measure the rate of consumption of the primary substrate or the rate of production of the ultimate product. Situations this uncomplicated are rarely found in nature however, and it is markedly more difficult to determine the relative contribution of a particular metabolic pathway, or of a particular subset of the microbial community (Dolfing and Bloeman 1985; Knudsen 2007; Zarecki et al. 2014).

Communities performing anaerobic methanogenic degradation are often found in structures such as biofilms or flocs, approximately spherical amalgamations of microbes suspended in liquid, as well as isolated cells (Stams 1994). The shorter distances between syntrophic partners in these structures have been established as facilitating IMT, indeed permitting it outright under certain circumstances (Conrad, Phelps, and Zeikus 1985; Harper and Pohland 1986). Of interest, then, are the relative contributions that communities in these different spatial settings make to the overall rate of IMT; determining this experimentally is complicated by numerous difficulties, but several studies have attempted it (Thiele, Chartrain, and Zeikus 1988; Conrad and Babbel 1989; Goodwin et al. 1991).

The question of which metabolite contributes most to the overall rate of methanogenesis is another source of controversy. While hydrogen has a higher diffusivity than either formate or acetate, restrictive thermodynamic constraints may make one or other of these slower-diffusing molecules a more important intermediary under some circumstances (Thiele and Zeikus 1988; Boone, Johnson, and Liu 1989; Chin and Conrad 1995).

Previous research has estimated the total rate of IMT based on the characteristic distance between syntrophic partner cells and assumptions about concentrations of the metabolite on the surface of each. Use of nearest-neighbour distances is well established in ecology for the purpose of determining whether spatial distributions of individuals are random or not, the classic example being in forestry (see e.g., Clark and Evans 1954; Diggle 1983). This has been successfully applied

to distributions of microbial populations (Jeanson et al. 2011; Raynaud and Nunan 2014) but, to our knowledge, it has never been tested that this statistic can be appropriately employed in estimating IMT.

The aim of this study is to test a number of methods for estimating the total rate of hydrogen transfer, with a view to extending and generalising this approach to other intermediary metabolites, both within anaerobic methanogenic degradation and elsewhere.

4.2. Model description

It has long been recognised that for a syntrophic system to be stable, at least on a short time-scale, the rates of production, of consumption, and of transfer of the metabolite must be equal in magnitude; over longer time-scales the specific growth rates of producers and consumers must also balance (Reilly 1974; G. E. Powell 1984; 1985; 1986; Archer and Powell 1985). As such, the modelling approach described here aims to find the steady-state rate of IMT.

4.2.1. Previous method of estimating rate of IMT

A number of researchers adapted Fick's diffusion law

$$\frac{\partial [H]}{\partial t} = D \cdot \frac{\partial^2 [H]}{\partial x^2} \qquad (4.1)$$

where D denotes the diffusivity of hydrogen under the conditions observed, t time, and x distance, to estimate the total rate of IMT, $J = D \frac{\partial [H]}{\partial x}$, between acetogenic and methanogenic cells at steady-state:

$$J = D \cdot N_A \cdot S_A \left(\frac{H_A - H_B}{d} \right) \qquad (4.2)$$

where N_A denotes the total number of producer cells, S_A the average surface area of a producer cell, H_i the average hydrogen concentration on the surface of a cell of species i, and d the average distance from a producer cell to its nearest neighbouring consumer cell (Cord-Ruwisch, Lovley, and Schink 1998; S. Ishii et al. 2005; 2006; Felchner-Zwirello, Winter, and Gallert 2013).

Since the surface concentrations are not directly measurable, they must also be estimated. Measurements of the hydrogen concentration in the whole system are typically used for H_A, represented here by the average hydrogen concentration $[\overline{H}]$. For H_B, the minimum threshold for consumption, H_{min}, is typically used. Estimates following this approach are compared to the same estimates based on the actual surface concentrations generated numerically.

The definition of 'average' is unfortunately never specified in any more detail, and so it is reasonable to assume that the arithmetic mean has been used. For all parameters in Equation 4.19 except d, this is a perfectly reasonable choice; since we are dividing by d however, it is intuitively more sensible to use the harmonic mean

$$\left(\frac{n}{\frac{1}{d_1}+\frac{1}{d_2}+\cdots+\frac{1}{d_n}}\right)^{-1} = \frac{1}{n}\left(\frac{1}{d_1}+\frac{1}{d_2}+\cdots+\frac{1}{d_n}\right) \tag{4.3}$$

than the arithmetic mean

$$\left(\frac{1}{n}[d_1+d_2+\cdots+d_n]\right)^{-1} \neq \frac{1}{n}\left(\frac{1}{d_1}+\frac{1}{d_2}+\cdots+\frac{1}{d_n}\right). \tag{4.4}$$

For example, if we imagine just two producer-consumer pairs of cells, one with a distance of 1 μm between them, the other with 3 μm between them, and a far greater distance between the pairs, then the total rate of transfer will be proportional to $\frac{1}{1}+\frac{1}{3}=\frac{4}{3}$ μm^{-1}. The arithmetic mean distance between pairs of cells here is $\frac{1}{2}(1+3)=2$ μm, leading to an estimate of the total that is proportional to $2\left(\frac{1}{2}\right)=1$ μm^{-1}; the harmonic mean distance is $\frac{2}{\frac{1}{1}+\frac{1}{3}}=1.5$ μm, leading to an estimate of the total that is proportional to $2\left(\frac{1}{1.5}\right)=\frac{4}{3}$ μm^{-1}.

As such, both methods of calculating the average distance from a producer cell to its nearest consumer are used here for comparison.

Table 4.1. Some reactions involved in methanogenesis via hydrogen transfer.

Standard Gibb's free energy changes are for conditions of pH 7, 1 atm, 25°C. Table adapted from Harper and Pohland (1986) Table 2.

	Substrates		Products	$\Delta G_0{}'$ [kJ/mol]
(4.5)	lactate⁻ + 2H₂O	→	acetate⁻ + HCO₃⁻ + H⁺ + 2H₂	- 4.2
(4.6)	ethanol + H₂O	→	acetate⁻ + H⁺ + 2H₂	+ 9.6
(4.7)	butyrate⁻ + 2H₂O	→	2 acetate⁻ + H⁺ + 2H₂	+ 48.1
(4.8)	propionate⁻ + 3H₂O	→	acetate⁻ + HCO₃⁻ + H⁺ + 3H₂	+ 76.1
(4.9)	4H₂ + HCO₃⁻ + H⁺	→	methane+ 3H₂O	- 135.6

4.2.2. Reaction kinetics of production

For a reaction to be energetically favourable its substrates must be in relative abundance and its products relatively scarce: the change in Gibb's free energy ΔG must be negative, where

$$\Delta G = \Delta G_0' + RT ln\left(\frac{[products]}{[substrates]}\right)$$
(4.10)

with T as the temperature (°K), R as the gas constant (8.314 J K⁻¹ mol⁻¹), and $\Delta G_0'$ as the standard free-energy change (kJ mol⁻¹). As a reaction proceeds, its products may accumulate and cause a decline in the energy obtainable, leading eventually to thermodynamic equilibrium. The commonly used term for this is 'product inhibition' (Hoh and Cord-Ruwisch 1996; Schink 1997).

Following the approach of Hoh and Cord-Ruwisch (1996) and others (e.g., Kleerebezem and Stams 2000), in assuming reversible Michaelis-Menten kinetics (see Equation 2.3 and Table 2.1) with one substrate and one product to be rate-limiting and the maximum rates of forward and reverse reactions to be equal, the rate of a reaction consuming a substrate S and producing hydrogen, H, is

$$r_A([S], [H]) = r_{max,A} \frac{[S] - [H]/K_{eq,A}}{K_S + [S] + [H]/K_{eq,A}} \qquad (\text{ 4.11 })$$

where $[...]$ denotes molar concentration, $r_{max,A}$ is the maximum rate possible, $K_{eq,A}$ the equilibrium constant, and K_S the affinity constant. Here we make the simplifying assumption that the substrate concentration $[S]$ is at steady state in time and constant in space, justified through the production of S by other, un-modelled microbes in the environment and typical concentrations so high that they saturate the consumption kinetics (Conrad, Schink, and Phelps 1986).

Calculating $K_{eq,A}$ is a matter of defining the critical change in free energy, ΔG_{crit} (kJ/mol reaction), above which the reaction may not proceed, and then rearranging Equation 4.6:

$$K_{eq,A} = \frac{[products]^*}{[substrates]^*} = e^{\frac{\Delta G_{crit} - \Delta G_0'}{RT}} \qquad (\text{ 4.12 })$$

where $[...]^*$ denotes concentration at equilibrium. Many researchers have assumed $\Delta G_{crit} = 0$ kJ/mol reaction by default (see e.g., Hoh and Cord-Ruwisch 1996) but subsequent research has suggested that microbial metabolism ceases to function before the metabolites are at exact thermodynamic equilibrium: instead, a ΔG_{crit} of around -10 kJ/mol reaction may be required for transport mechanisms in the cell membrane to operate (Kleerebezem and Stams 2000; Jackson and McInerney 2002).

We may now rearrange Equation 4.7 to

$$r_A([H]) = r_{max,A} \frac{H_{max} - [H]}{K_A + H_{max} + [H]} \qquad (\text{ 4.13 })$$

where

$$H_{max} = [S] K_{eq,A} \qquad (\text{ 4.14 })$$

is the maximum hydrogen threshold, and

$$K_A = K_S K_{eq,A} \qquad (\text{ 4.15 })$$

the effective affinity constant. The rate at which a cell of type A produces hydrogen is proportional to this rate

$$q_A([H]) = Y_A\, r_A([H]) \qquad\qquad (\,4.16\,)$$

where Y_A is the stoichiometric constant.

Estimates for the maximum production rate

$$q_{max,A} = Y_A\, r_{max,A} \qquad\qquad (\,4.17\,)$$

are given in Table 4.2. They vary over only one order of magnitude, from ~2 to ~30 mmol metabolite produced, per g dry mass of cells, per hour. Estimates for the affinity constant K_S are more diverse, ranging from ~2 to 4500 μM substrate (Table 4.3). *In situ* metabolite concentrations reported in (Conrad, Schink, and Phelps 1986) are reproduced in Table 4.4 and an estimate of kinetic saturation is given for those substrates that also feature in Table 4.3.

For these estimates and measurements the corresponding equilibrium parameters $K_{eq,A}$ can be calculated. The maximum hydrogen threshold H_{max} is then estimated by Equation 4.10 and the effective affinity K_A using Equation 4.11 (Table 4.5).

Table 4.2. Estimates of the maximum rate of hydrogen production, $q_{max,A}$.

Estimated values for the maximum rate of hydrogen production are collated from the literature on anaerobic methanogenic degradation.

Substrate	Organism	$q_{max,A}$ (mmol g^{-1} h^{-1})	Source
Lactate	Dechlorinating culture	8.6	(Fennell and Gossett 1998)
Ethanol	Dechlorinating culture	21.9	(Fennell and Gossett 1998)
Butyrate	Dechlorinating culture	4.9	(Fennell and Gossett 1998)
	Butyrate degrader [*]	6.5	(Ahring and Westermann 1987)
	Butyrate degrader [†]	10.3	(Ahring and Westermann 1987)
	Strain IB [§]	28.8	(Jin 2007)
Propionate	Dechlorinating culture	2.2	(Fennell and Gossett 1998)

[*] Long-term chemostat culture result. [†] Batch culture result. [§] Based on results of (Wu, Jain, and Zeikus 1994).

Table 4.3. Estimates of the affinity constant of production K_S.

Estimated values from the literature for a number of different substrates degraded anaerobically to hydrogen and other products via reactions given in Table 4.1.

Substrate	Organism	K_S (µM)	Source
Butyrate	Dechlorinating culture	34.3	(Fennell and Gossett 1998)
	Activated sludge	57	(Lawrence and McCarty 1969)
	Strain SB [*]	65	(Jin 2007)
	Butyrate degrader	76.4	(Ahring and Westermann 1987)
Ethanol	Dechlorinating culture	17	(Fennell and Gossett 1998)
Lactate	Dechlorinating culture	2.5	(Fennell and Gossett 1998)
Propionate	Dechlorinating culture	11.3	(Fennell and Gossett 1998)
	Acclimatised sludge [†]	15.9	(Fukuzaki et al. 1990)
	Digesting sludge	90	(Kaspar and Wuhrmann 1978)
	Activated sludge ('slow' group)	149	(Heyes and Hall 1983)
	Activated sludge	432	(Lawrence and McCarty 1969)
	Activated sludge ('fast' group)	4500	(Heyes and Hall 1983)

[*] Based on results of (Wu, Jain, and Zeikus 1994). [†] Evidence of substrate inhibition kinetics, with K_I = 790 µM propionate. All values given to 2 s.f.

Table 4.4. Estimates of metabolite concentrations based on Conrad, Schink and Phelps (1986) Table 2.

Conrad, Schink and Phelps (1986) measured the conditions present in four anaerobic environments where methanogenesis is known to take place. They are reproduced here in approximate order of richness, from left to right: the sediment taken from Lake Mendota has very low concentrations of metabolites (it is said to be oligotrophic), whereas fetid liquid extracted from the cottonwood tree (*Populus deltoides*) has much higher concentrations (i.e. it is eutrophic).

Values for hydrogen have been converted from partial pressures in Pascal (Pa) to micromolar concentrations (μM) using Henry's Law and *in situ* temperatures. For reference, 1 Pa $\approx$ 0.008 μM at standard conditions. Affinity constants based on Table 4.3 are used to estimate how close to saturation the kinetics of lactate, ethanol, butyrate and propionate degradation (reactions given in Table 4.1) would be in each of the environments, were we to assume Michaelis-Menten kinetics (i.e. [*products*] = 0 μM). Note that bicarbonate (HCO_3^-, predominantly due to dissolved carbon dioxide) is in abundance, typical for anaerobic environments. ND: not determined.

Environment	Lake Mendota sediment	Knaack Lake sediment	Sewage sludge	Fetid liquid of cottonwood
T ($^\circ$C)	10	4	32	20
pH	7.2	6.2	7.2	7.0
H_2 (μM)	0.031	0.042	0.199	0.111
HCO_3^- (μM)	6450	1540	4260	123000
Acetate (μM)	32	151	360	32000
Lactate (μM)	77	138	ND	100
$S/(K_S+S)$ if $K_S = 2.5$ μM	0.97	0.98	ND	0.98
Ethanol (μM)	43	174	113	2500
$S/(K_S+S)$ if $K_S = 17$ μM	0.72	0.91	0.87	0.99
Butyrate (μM)	< 0.2	< 0.2	ND	1000
$S/(K_S+S)$ if $K_S = 55$ μM	< 0.0036	< 0.0036	ND	0.95
Propionate (μM)	0.88	0.3	2.3	2800
$S/(K_S+S)$ if $K_S = 150$ μM	0.0058	0.0020	0.015	0.95

Table 4.5. Estimates of maximum threshold, H_{max}, and of the effective affinity constant, K_A, of hydrogen production.

Estimates are based on the *in situ* temperatures and concentrations given in Table 4.4, varying only the concentration of hydrogen and the critical change in free energy, ΔG_{crit} (kJ/mol reaction), above which the reaction may not proceed (see Equations 4.8, 4.10, 4.11).

Estimates for K_S [µM substrate] are from Table 4.3, and estimates for H_{max} and K_A given here are in units of µM H_2. Substrates can be paired according to their $\Delta G_0'$ values (Table 4.1): the degradation of lactate and of ethanol is energetically neutral at standard conditions ($\Delta G_0' \approx 0$ kJ), whereas the degradation of butyrate and of propionate is much less energetically favourable ($\Delta G_0' \approx +60$ kJ). Furthermore, concentrations of butyrate and propionate measured in the lake sediments and sewage sludge were very low (< 2.5 µM) compared with the other metabolites and in the fetid liquid of cottonwood (32 – 32000 µM, Table 4.4).

All values given to 2 s.f. ND: not determined.

Substrate (K_S)		Lactate (2.5)		Ethanol (17)		Butyrate (55)		Propionate (150)	
Environment	ΔG_{crit}	0	-10	0	-10	0	-10	0	-10
Lake Mendota sediment	H_{max}	32000	3800	110	13	0.35	0.042	0.024	0.0059
	K_A	1000	120	120	5.1	96	11	4.1	1.0
Knaack Lake sediment	H_{max}	11000	1300	26	3.0	0.016	0.0018	0.0055	0.0013
	K_A	200	23	7.4	0.29	4.4	0.51	2.7	0.64
Sewage sludge	H_{max}	ND	ND	97	14	ND	ND	0.049	0.013
	K_A	ND	ND	43	2.0	ND	ND	3.21	0.86
Fetid liquid of cottonwood	H_{max}	260	33	280	3.5	0.035	0.0045	0.019	0.0048
	K_A	6.4	0.82	0.55	0.82	0.0019	0.00025	0.0010	0.00026

Table 4.6. Abbreviations of genus names for methanogenic archaea used in Tables 4.7 to 4.9.

Genus	Abbreviation
Methanobacterium	*Mba.*
Methanobrevibacter	*Mbr.*
Methanococcus	*Mc.*
Methanospirillum	*Ms.*
Methanothermobacter	*Mtb.*

4.2.3. Reaction kinetics of consumption

The same approach can then be followed for determining the rate of the reaction consuming hydrogen by A's syntrophic partner B. As for substrate, S, we assume that the concentration of the product of this reaction, P, is at steady-state in time and constant in time (p. 87). Here, hydrogen is the (variable) substrate of the reaction and P the (fixed) product, methane:

$$r_B([H], [P]) = r_{max,B} \frac{[H] - {[P]}/{K_{eq,B}}}{K_H + [H] + {[P]}/{K_{eq,B}}} \qquad (4.18)$$

becomes

$$r_B([H]) = r_{max,B} \frac{[H] - H_{min}}{K_B + [H] + H_{min}} \qquad (4.19)$$

with

$$H_{min} = \frac{[P]}{K_{eq,B}} \qquad (4.20)$$

as the minimum threshold of hydrogen concentration and $K_B = K_H$ the affinity constant. The rate at which a cell of type B consumes H is proportional to this rate

$$q_B([H]) = Y_B \, r_B([H]) \qquad (4.21)$$

where Y_B is the stoichiometric constant.

Estimates for the maximum rate of hydrogen consumption vary over a greater range than those for production: $-q_{max,B}$ lies between ~6 to ~1800 mmol hydrogen consumed, per g dry mass of cells, per hour (Table 4.7). Table 4.8 gives estimates of ~2 to ~300 μM for the affinity constant K_B. Numerous estimates for the minimum hydrogen concentration threshold, H_{min}, are given in the literature (Table 4.9), but all are in the range of ~0.02 to ~0.08 μM.

Table 4.7. Estimates of the maximum rate, $q_{max,B}$, of hydrogen consumption by methanogenic archaea.

Higher maximum consumption rates are typically observed in thermophilic methanogenic archaea, such as *Methanothermobacter thermoautotrophicus* (formerly known as *Methanobacterium thermoautotrophicum*).

Organism	$-q_{max,B}$ [mmol g^{-1} h^{-1}]	Source
Methanogens [b][nl]	6.6	(Joseph A Robinson and Tiedje 1984)
Ms. hungatei PM-1 [b][nl]	10.8	(Dwyer et al. 1988)
Dechlorinating culture [u]	40	(Fennell and Gossett 1998)
Mba. formicicum T1N [u][w]	54	(Jin 2007)
Mba. formicicum JF-1 [b][lb]	48 – 174	(Schauer, Brown, and Ferry 1982)
Mba. bryantii M.o.H. [b][nl]	83 – 133	(Karadagli and Rittmann 2005)
Mbr. arboriphilus AZ [b][lb]	120	(Kristjansson, Schönheit, and Thauer 1982)
Mtb. thermoautotrophicus [s][c][lb]	131.7	(Ahring and Westermann 1987)
Mtb. thermoautotrophicus [s][b][lb]	141.5	(Ahring and Westermann 1987)
Enrichment culture [b]	426	(Goodwin et al. 1991)
Mtb. thermoautotrophicus Marburg [c][lb]	1725	(Schönheit, Moll, and Thauer 1980)

[b] Batch culture, time series of hydrogen concentration recorded.

[c] Long-term chemostat culture, hydrogen concentration in inflow varied.

[lb] Michaelis-Menten kinetics fitted to data using a Lineweaver-Burk plot.

[nl] Michaelis-Menten kinetics fitted to data using nonlinear regression.

[s] No strain given.

[u] Estimate based on unpublished data.

[w] Based on results of Wu, Jain, and Zeikus (1994).

Table 4.8. Estimates of the affinity constant of hydrogen consumption, K_B.

Many estimates obtained using Lineweaver-Burk plots (also known as double reciprocal plots), and therefore deserving of scepticism (see Section 2.2.1). Estimates obtained using nonlinear regression tend to give lower estimates for the affinity constant, in line with predictions given later (see Results and Discussion).

Organism	K_B [μM]	Source
Methanospirillum sp. [b nl]	2.5	(Joseph A Robinson and Tiedje 1984)
Ms. hungatei PM-1 [b nl]	2.5	(Dwyer et al. 1988)
Rumen fluid [b nl]	4.2 – 9.1	(Joseph A Robinson and Tiedje 1982)
Digestor sludge [b nl]	4.4 – 6.8	(Joseph A Robinson and Tiedje 1982)
Ms. hungatei JF-1 [b nl]	5	(Joseph A Robinson and Tiedje 1984)
Hypereutrophic lake sediment [b nl]	5.6 – 8.6	(Joseph A Robinson and Tiedje 1982)
Mba. formicicum JF-1 [b lb]	6	(Schauer, Brown, and Ferry 1982)
Mba. formicicum [s u]	6.5	(Thiele and Zeikus 1988)
Mbr. arboriphilus AZ [b lb]	6.6	(Kristjansson, Schönheit, and Thauer 1982)
Mtb. thermoautotrophicus [s b]	6.8	(Ahring and Westermann 1987)
Digesting sludge [b lb]	7.8	(Kaspar and Wuhrmann 1978)
Mtb. thermoautotrophicus [s c]	8.5	(Ahring and Westermann 1987)
Mba. bryantii M.o.H. [b nl]	18	(Karadagli and Rittmann 2005)
Mtb. thermoautotrophicus Hveragerdi [d]	55 - 103	(Jud, Schneider, and Bachofen 1997)
Mtb. thermoautotrophicus Marburg [c lb]	108	(Schönheit, Moll, and Thauer 1980)
Mba. formicicum JF-1 [c lb]	290	(Schauer and Ferry 1980)

[b] Batch culture, time series of hydrogen concentration recorded.

[c] Long-term chemostat culture, hydrogen concentration in inflow varied.

[d] Chemostat culture, dilution rate varied to find washout criterion.

[lb] Michaelis-Menten kinetics fitted to data using a Lineweaver-Burk plot.

[non] Michaelis-Menten kinetics fitted to data using nonlinear regression.

[s] No strain given.

[u] Unclear how parameter was estimated.

Table 4.9. Estimates of the minimum threshold for product consumption, H_{min}.

Estimates for the minimum threshold of hydrogen consumption are remarkably consistent across the species and strains of methanogenic archaea reported in the literature.

Organism	H_{min} (µM)	Source
Ms. hungatei M1h	0.017 - 0.022	(Seitz, Schink, and Conrad 1988)
Mba. formicicum DSM 1535	0.021	(Cord-Ruwisch, Seitz, and Conrad 1988)
Ms. hungatei DSM 864	0.022	(Cord-Ruwisch, Seitz, and Conrad 1988)
Enrichment culture	0.028	(Goodwin et al. 1991)
Mba. formicicum MF	0.035	(Boone, Johnson, and Liu 1989)
Mba. formicicum JF-1	0.046	(Lovley 1985)
Mba. bryantii M.o.H.	0.049	(Lovley 1985)
Mc. vannielii DSM 1224	0.056	(Cord-Ruwisch, Seitz, and Conrad 1988)
Mbr. arboriphilus DSM 744	0.067	(Cord-Ruwisch, Seitz, and Conrad 1988)
Ms. hungatei JF-1	0.068	(Lovley 1985)
Mbr. smithii DSM 861	0.073	(Cord-Ruwisch, Seitz, and Conrad 1988)

Table 4.10. Estimates of diffusivity, *D*.

Estimates for the diffusivity of dissolved hydrogen vary by almost one order of magnitude, due to differences in temperature and the viscosity of the medium. The temperature range has been restricted to those similar to *in situ* temperatures in the environments of Table 4.4.

D (10^{-9} m^2 s^{-1})	Temperature (˚C)	Source
1.39	37	(Öztürk et al. 1987)
1.4	37	(Muralidharan et al. 1997)
4.5	25	(Cussler 2009)
4.6	10	(Wise and Houghton 1966)
5.0	20	(Wise and Houghton 1966)
5	25	(Sørensen, Finster, and Ramsing 2001)
7.0	30	(Wise and Houghton 1966)
8.3	40	(Wise and Houghton 1966)

Microbial cells performing methanogenic degradation have cell volumes of the order of 1 μm^3 (S. Ishii et al. 2006; Yuchen Liu and Whitman 2008), meaning a side-length of 1 μm once this cell is idealised as a cube; these are then the characteristic units of volume and of length chosen for the system. Since diffusivities of all products are approximately of the order of magnitude 10^{-9} m^2 s^{-1} = 1 μm^2 ms^{-1} (Table 4.10), 1 ms is a suitable characteristic unit of time.

A satisfactory estimate for the dry mass of a cell with volume 1 μm^3 is 0.36 pg (Donachie and Robinson 1987; Neidhardt and Umbarger 1996), and this particular value allows straightforward conversion of the maximum production and consumption rates, $q_{max,A}$ and $q_{max,B}$. Both are typically around 10 mmol (g dry mass)$^{-1}$ h^{-1} = 10^{-21} mol (0.36 pg)$^{-1}$ ms^{-1} = 1 zmol cell^{-1} ms^{-1} (Tables 4.2 and 4.7). Conveniently, 1 zmol μm^{-3} = 1 μM, and so this becomes the characteristic unit of product concentration.

Since a number of previous models have assumed irreversible Michaelis-Menten kinetics for consumption (i.e. they ignore product inhibition), the effect of this change is tested by taking H_{min} = 0 μM in the sensitivity analysis (Table 4.11). Since many experimentalists have also assumed this, they may have reported overestimates for K_B.

We are also able to ignore all pairs of H_{max} and H_{min} parameter values where H_{max} < H_{min} since the metabolism of neither producers nor consumers could function under such a scenario

4.2.4. Numerical methods

Populations of cells were randomly generated on 100 x 100 grids, with the sole restriction that only one cell may occupy a single grid element (e.g. Figure 4.1A). The open source, multi-physics finite element (FEM) solver Elmer (Lyly, Ruokolainen, and Järvinen 1999) was passed these grids together with files detailing the reaction kinetics, diffusivity, and periodic boundary conditions (to prevent boundary effects, thereby mimicking a larger domain). Given the non-linearity of this

reaction-diffusion (R-D) system, Elmer's steady-state solver failed to find the steady-state solution directly; instead, the time-dependent solver was run for long enough that the relative difference between the total rate of production and the total rate of consumption was less than 10^{-10}. This typically took less than 500 time units, i.e. less than 0.5 seconds of simulation time, and around 20-30 minutes of wall time on a single node of a High Performance Computer Cluster. Elmer returns the hydrogen concentration field (Figure 4.1C) as output, from which the metabolic rates of individual cells are calculated.

The decision to use Elmer, instead of iDynoMiCS, for the numerical solution of the R-D system was made because of the relative advantages of the R-D solvers in each. The R-D solver in iDynoMiCS was chosen for its speed, rather than precision at a fine spatial resolution, since as the biofilm grows in a typical simulation the system will need to be solved many times. Here this is not the case, as we require a precise and finely resolved calculation of the concentration field for just one spatial structure each simulation.

All results were analysed using custom-written Python scripts (Python Software Foundation 2010) and figures generated using the Python module Matplotlib (Hunter 2007).

Table 4.11. Summary and conversion of parameters.

The parameters given in Tables 4.2 to 4.10 are summarised and converted into characteristic units where necessary. The majority of the simulations performed used the default parameters given in the fourth column (Default), but the low and high parameters are explored in the sensitivity analysis.

Parameter	Units	Low	Default	High
D	$m^2 s^{-1}$	1×10^{-9}	3×10^{-9}	10×10^{-9}
	$\mu m^2 ms^{-1}$	1	3	10
$q_{max,A}$	$mmol\ g^{-1}\ h^{-1}$	3	10	30
	$zmol\ cell^{-1}\ ms^{-1}$	0.3	1	3
H_{max}	μM	0.05 [*]	10	3×10^4
K_A	μM	3×10^{-4}	10	1000
$q_{max,B}$	$mmol\ g^{-1}\ h^{-1}$	5	50	2000
	$zmol\ cell^{-1}\ ms^{-1}$	0.5	5	200
H_{min}	μM	0.0 [†]	0.04	1.0 [§]
K_B	μM	3	30	300

[*] Increased from an estimated value of 3×10^{-4} μM to ensure that $H_{max} > H_{min}$. [†] Reduced from an estimated value of 0.02 μM to allow comparison with models assuming Michaelis-Menten kinetics of consumption. [§] Increased from an estimated value of 0.073 μM, as members of the *Methanosarcinales* that can metabolise hydrogen typically have higher minimum thresholds than other orders of methanogenic archaea (Thauer et al. 2008).
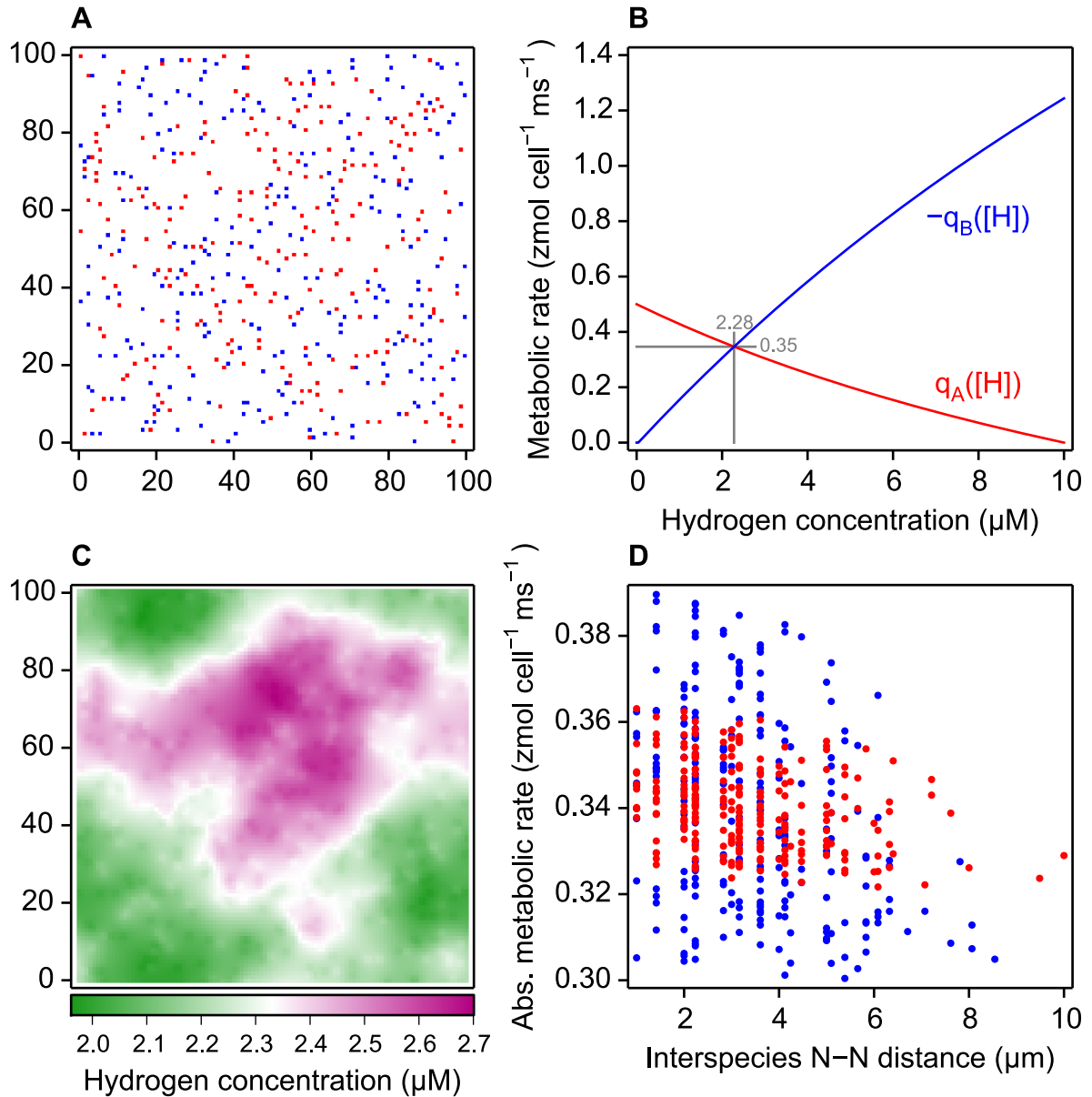
Figure 4.1. An example population distribution and kinetics show the typical degree of heterogeneity.

(A) The positions of an example population randomly distributed over a 100 μm x 100 μm domain. There are 250 producer cells (red) and 250 consumer cells (blue), giving a total density of 0.05 cells μm⁻² ≈ 18 mg m⁻². **(B)** The kinetics of production (Equation 4.8, red) and of consumption (Equation 4.15, blue) used in this example. The parameters used here are the default parameters given in Table 4.11: $q_{max,A} = 1$ zmol cell⁻¹ ms⁻¹, $P_{max} = 10$ μM, $K_A = 10$ μM, $q_{max,B} = 5$ zmol cell⁻¹ ms⁻¹, $P_{min} = 0.04$ μM, $K_B = 30$ μM. **(C)** The spatial distribution of hydrogen resulting from the population distribution shown in (A), the kinetics in (B), and the default diffusivity of hydrogen, $D = 3$ μm² ms⁻¹ (default in Table 4.11). **(D)** Scatter plot showing that the distance from a cell to its nearest neighbour (N-N) of the opposite species has very little effect on the absolute rate at which it metabolises H. Producer cells shown in red, consumer cells in blue. Note the proximity of the hydrogen concentrations (C) and the absolute metabolic rates (D) observed here to the crossover point in (B).

4.3. Results

In addition to the Fickian approach of Equation 4.2, we have considered using the kinetics of production and of consumption for a potential estimator. Figure 4.1B shows the *per cell* kinetics using the default parameters of Table 4.11. The crossover point between the blue and red lines illustrates the outcome, were the obstacle of diffusion limitation somehow removed. This point can be found analytically as the (positive) root of a quadratic, although it is convenient to use a numerical solver. A population consisting of equal numbers of producers and consumers would reach a hydrogen concentration of ~ 2.28 μM, and the total rate of IMT would be 0.35 N_A zmol ms^{-1} (Figure 4.2).

Changing the community composition alters the crossover point of the total population kinetics in a non-linear manner (Figure 4.3). The composition leading to the optimum total rate of IMT may not be of equal number of producers and consumers; when the total population is 500 and default parameters assumed (Table 4.11) the highest total rate occurs where the community is composed of ~ 60% producers and ~ 40% consumers (Figure 4.3).
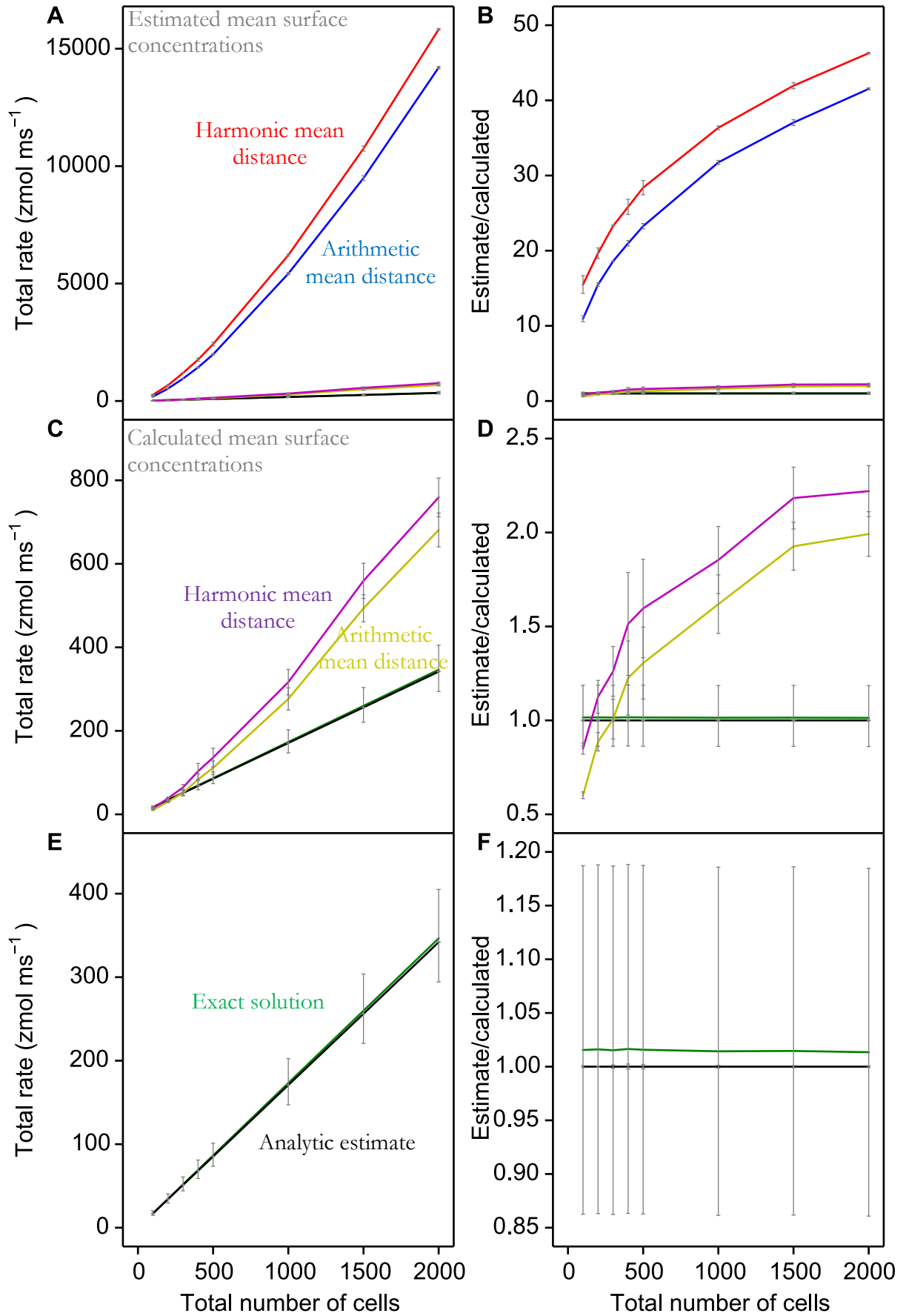
Figure 4.2. Estimates of total exchange as the total number of cells varies.

A number of estimates of the total rate of IMT are compared with the calculated values (black) as the total number of cells in a 100 μm x 100 μm domain is varied. Default parameters are used throughout (Table 4.11). Estimates using the analytic solution to the equalisation of rates are shown in green. The Fickian estimation approach used by previous authors (Equation 4.19) is shown using a number of different assumptions for its parameters: $H_A = [\overline{H}]$, the average hydrogen concentration, and $H_B = H_{min}$, the minimum threshold for consumption (red, blue); H_A and H_B as the average surface concentrations of producers and of consumers (yellow, magenta); d as the arithmetic mean distance from a producer to its nearest consumer (blue, yellow); instead using the harmonic mean distance (red, magenta). (A, C, E) Total rates and estimates of IMT. (B, D, F) Estimates of the total rate divided by the calculated total rate. All estimates are shown in (A, B), but those dependent on $[\overline{H}]$ and H_{min} are excluded in (C, D), and all based on Fick's diffusion law (Equation 4.19) are excluded in (E, F) for clarity. Error bars are standard deviations (n = 3), except for the analytic estimate where error bars show the worst case estimates if uncertainty in all parameters is 1% (see Figure 4.6 for more details).

Figure 4.3. Estimates of total exchange as the composition of the community varies.

A number of estimates of the total rate of IMT are compared with the calculated values (black) as the percentage of producers is varied. Total population is 500, in a 100 μm x 100 μm domain. Default parameters are used throughout (Table 4.11). Estimates using the analytic solution to the equalisation of rates are shown in green. The Fickian estimation approach used by previous authors (Equation 4.19) is shown using a number of different assumptions for its parameters: $H_A = [\overline{H}]$ and $H_B = H_{min}$ (red, blue); H_A and H_B as the average surface concentrations of producers and of consumers (yellow, magenta); d as the arithmetic mean distance from a producer to its nearest consumer (blue, yellow); instead using the harmonic mean distance (red, magenta). (A, C, E) Total rates and estimates of IMT. (B, D, F) Estimates of the total rate divided by the calculated total rate. All estimates are shown in (A, B), but those dependent on $[\overline{H}]$ and H_{min} are excluded in (C, D), and all based on Fick's diffusion law (Equation 4.19) are excluded in (E, F) for clarity. Error bars are standard deviations (n = 3), except for the analytic estimate where error bars show the worst case estimates if uncertainty in all parameters is 1% (see Figure 4.6 for more details).
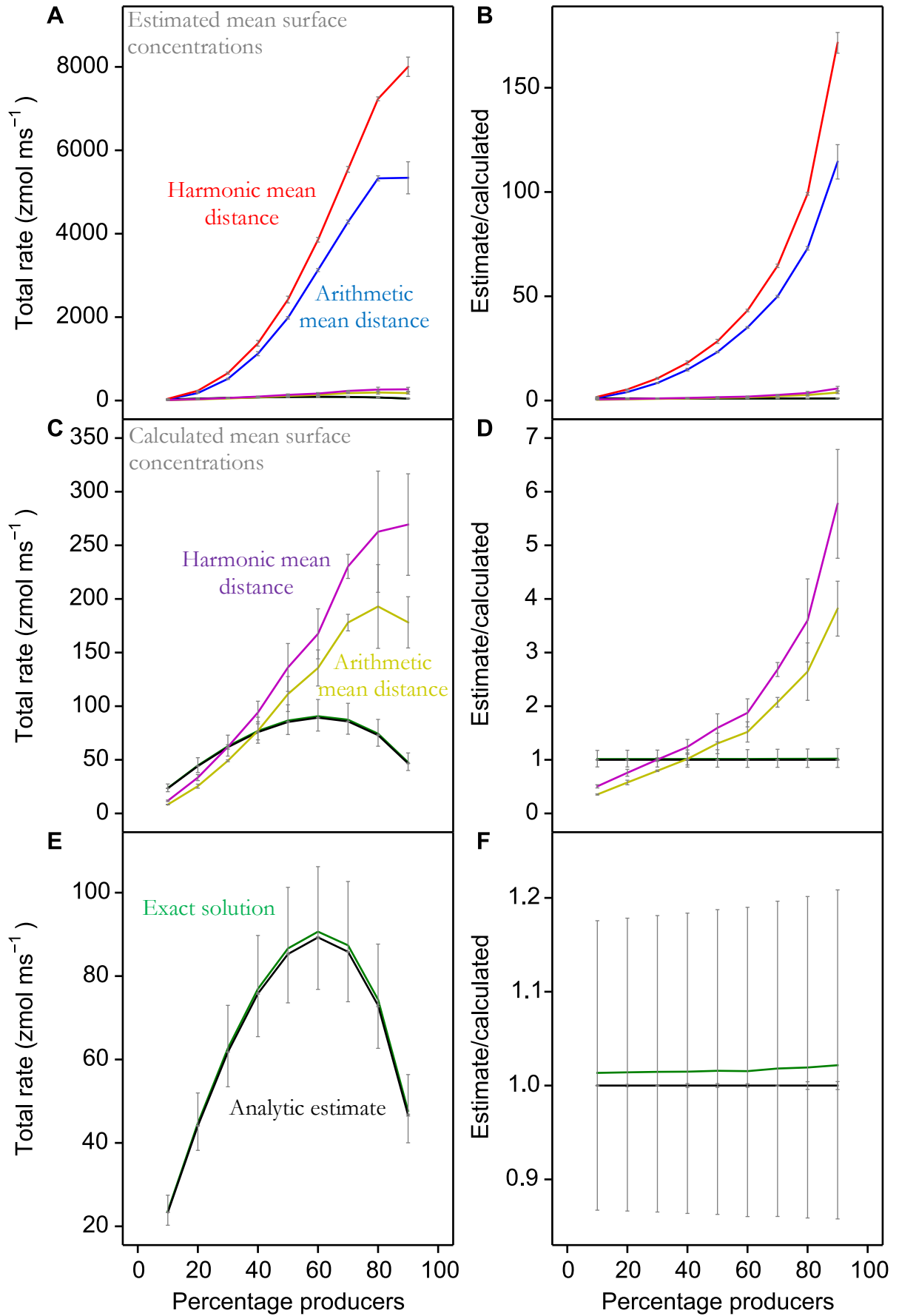
Table 4.12. Effect of varying parameters on estimates of total IMT.

The effect of changing parameter values on the total rate of IMT (zmol ms^{-1}) and on the estimates of this rate. Each parameter is changed individually (i.e. all other parameters set to default) according to the values given in Table 4.11. Total population is 500, with equal numbers of producers and consumers, in all simulation results presented here. Standard deviations (n = 3) are given after the arithmetic mean value, except for the analytic estimate where the error shown is the worst case scenario if uncertainty in all parameters is 1% (see Figure 4.6 for more details)

Parameter changed		Calculated rate	Analytic estimate	Mean concn., arithmetic dist.	Mean concn., harmonic dist.	Surface concn., arithmetic dist.	Surface concn., harmonic dist.
Defaults		85.29 ±0.18	86.63 ±2.80	1983.88 ±30.00	2420.99 ±81.25	111.29 ±16.32	136.11 ±22.33
D	**Low**	83.09 ±0.32	86.63 ±2.80	673.56 ±9.66	821.95 ±26.90	98.39 ±10.32	120.24 ±14.73
	High	86.20 ±0.07	86.63 ±2.80	6568.03 ±99.67	8015.20 ±269.71	118.89 ±20.67	145.46 ±27.82
$q_{max,A}$	**Low**	32.67 ±0.03	32.90 ±1.03	728.15 ±11.86	888.61 ±30.91	43.09 ±6.52	52.70 ±8.89
	High	160.64 ±0.49	164.59 ±5.54	3986.98 ±55.22	4865.31 ±156.68	204.70 ±28.12	250.29 ±38.76
H_{max}	**Low**	0.15 ±0.00	0.16 ±0.02	3.29 ±0.05	4.02 ±0.13	0.19 ±0.03	0.24 ±0.04
	High	249.78 ±0.00	249.79 ±5.03	6747.65 ±116.47	8234.73 ±294.65	338.50 ±55.76	414.07 ±75.43
K_A	**Low**	121.56 ±0.34	124.25 ±3.55	2915.41 ±41.67	3557.71 ±116.27	156.31 ±22.00	191.14 ±30.23
	High	2.45 ±0.00	2.45 ±0.10	53.30 ±0.91	65.05 ±2.32	3.25 ±0.50	3.97 ±0.68
$q_{max,B}$	**Low**	24.31 ±0.01	24.39 ±0.85	6385.86 ±94.49	7792.83 ±259.26	33.66 ±5.97	41.19 ±8.02
	High	120.57 ±0.07	122.87 ±3.75	119.59 ±1.26	145.93 ±4.21	110.85 ±4.51	135.32 ±7.85
H_{min}	**Low**	85.76 ±0.18	87.12 ±2.81	1990.65 ±30.10	2429.26 ±81.52	111.90 ±16.40	136.85 ±22.44
	High	74.24 ±0.15	75.34 ±2.61	1817.55 ±27.54	2218.01 ±74.51	97.21 ±14.40	118.88 ±19.69
K_B	**Low**	115.86 ±0.16	118.33 ±3.63	338.85 ±5.92	413.53 ±14.89	126.19 ±9.61	154.15 ±14.46
	High	28.05 ±0.02	28.18 ±1.04	6060.39 ±89.61	7395.66 ±245.95	38.73 ±6.80	47.39 ±9.15

Figure 4.4. Effect of parameters on the average hydrogen concentration.

As the value of one parameter is changed from the defaults given in Table 4.11, the arithmetic mean hydrogen concentration will also change. The effects of changing parameters listed in Table 4.11 are shown in blue, and displayed in the same order; total population is 500, with equal numbers of producers and consumers, in all these results. For comparison, the effect of changing the total number of cells (as in Figure 4.2) and the population composition (as in Figure 4.3) are shown in red. The effects of different parameter changes are remarkably varied, both in terms of magnitude and of direction; this figure facilitates straightforward comparison, and is considered further in the Discussion. Markers for the total number of cells are not displayed, as the variation between simulations in this case was due more to the random placement of cells than their total number; i.e. the total number of cells makes no difference to the average hydrogen concentration, within the ranges studied here. Concentrations of ~0.2 μM and ~2 μM will be relevant in the Discussion, and so these are marked with grey dotted lines.
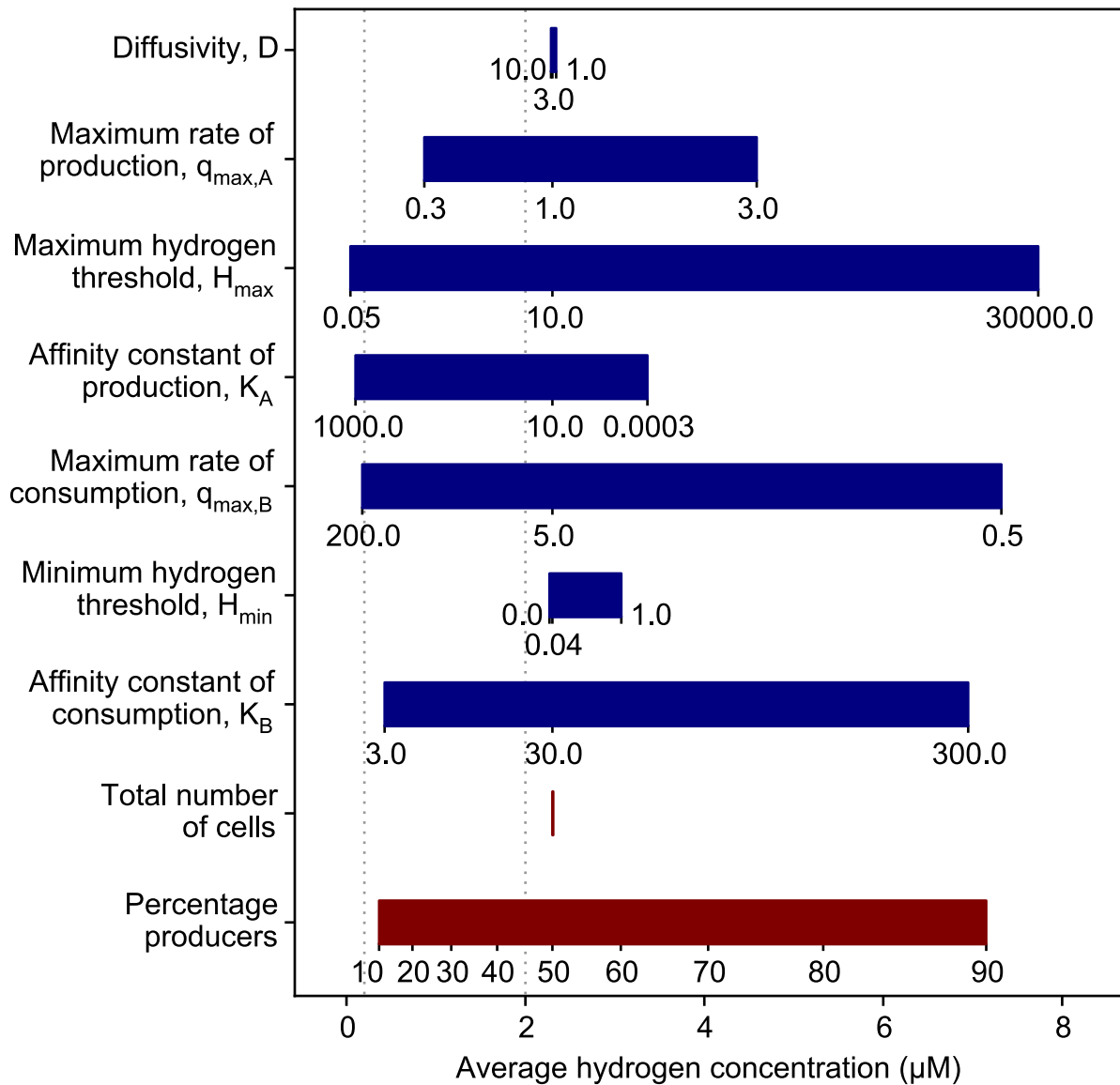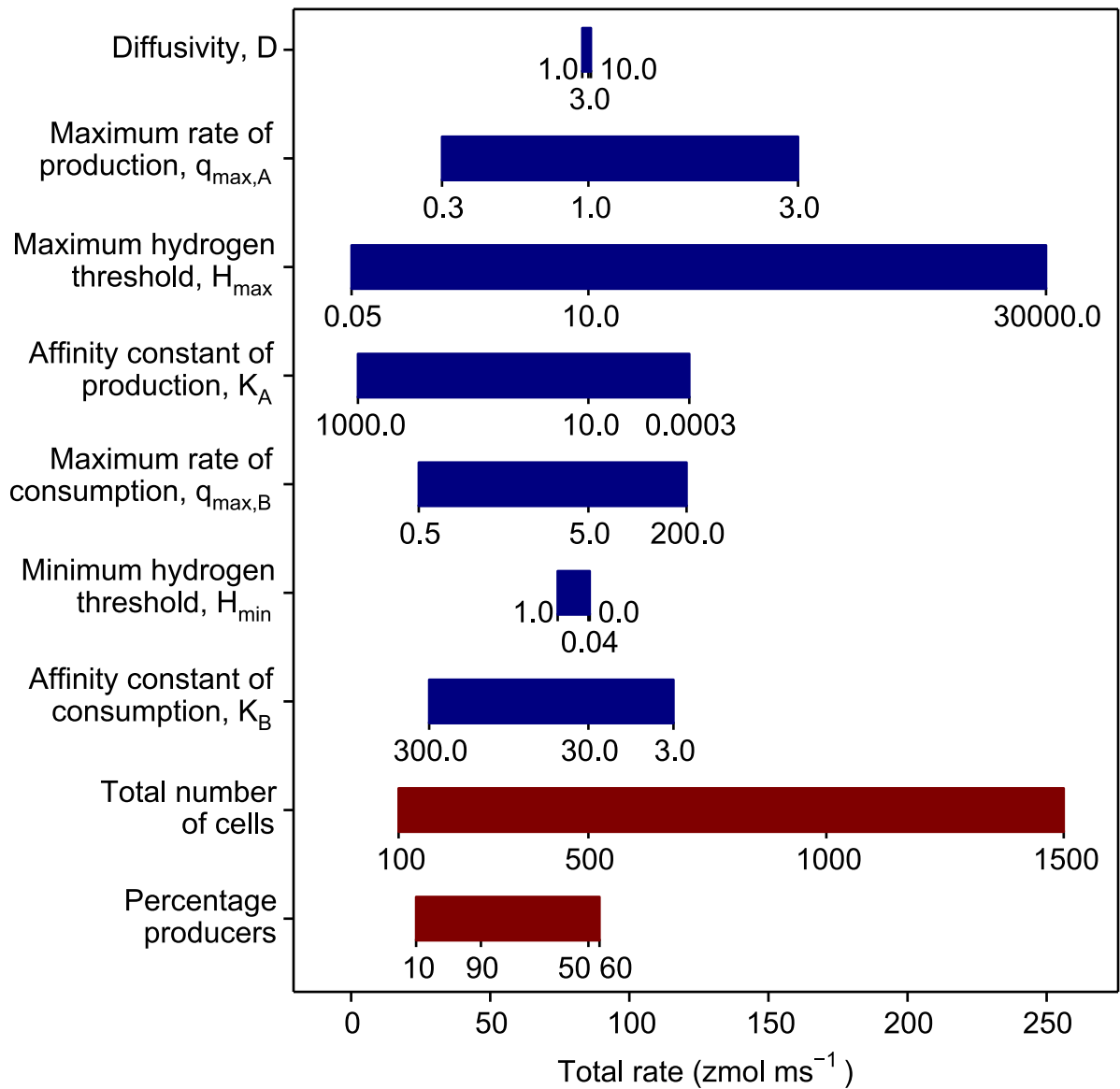
Figure 4.5. Effect of parameters on the total rate of IMT.

As the value of one parameter is changed from the defaults given in Table 4.11, the total rate of IMT will also change. The effects of changing parameters listed in Table 4.11 are shown in blue, and displayed in the same order; total population is 500, with equal numbers of producers and consumers, in all these results. For comparison, the effect of changing the total number of cells (as in Figure 4.2) and the population composition (as in Figure 4.3) are shown in red. The effects of different parameter changes are remarkably varied, both in terms of magnitude and of direction; this figure facilitates straightforward comparison. Of particular interest are the rather modest effect of increasing $q_{max,B}$, especially when compared with $q_{max,A}$, and the influence of K_B, which is considered further in the Discussion. Intermediate markers for the percentage of producers are omitted for clarity.
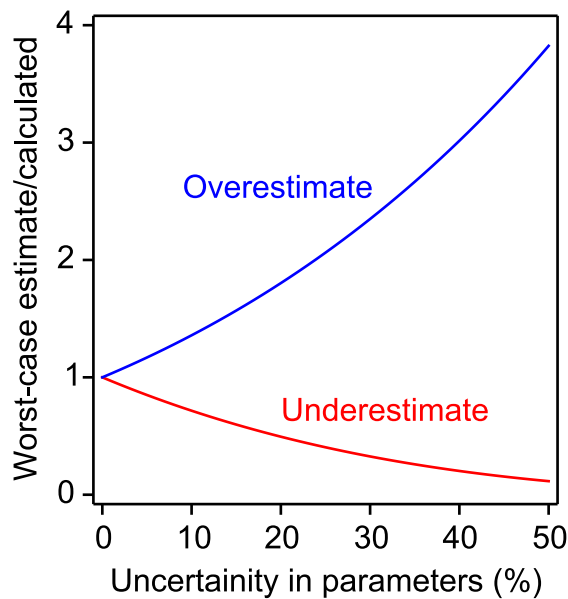
Figure 4.6. Sensitivity of analytic estimation to uncertainty in parameter values.

The analytic solution to the equalisation of kinetic rates, assuming negligible diffusion limitation, is a good estimator of total exchange when there is diffusion (Figures 4.2 and 4.3). However, it requires 8 parameters, all of which will be estimates: $\#(A)$, $q_{max,A}$, H_{max}, K_A, $\#(B)$, $q_{max,B}$, H_{min}, K_B. As the uncertainty in all of these parameters increases, so does the uncertainty in the analytic estimate.

4.4. Discussion

This study provides an effective mechanism for simulating anaerobic methanogenic degradation via the IMT of dissolved hydrogen, and for testing methods for estimating the total rate. The results presented here suggest that estimates based on an analytic treatment of kinetics are far superior to those based on concentrations (Figures 4.2 and 4.3, Table 4.12). However, the analytic estimate suffers from an abundance of parameters, all of which will be estimates and so vulnerable to uncertainty (Figure 4.6). As such, the problem cannot be considered definitely solved, and deserves further investigation. Nonetheless, there are several interesting results worthy of discussion.

Hydrogen concentrations reported *in situ* are typically in the range 0.03 - 0.2 μM, whereas those predicted by simulations using the default parameter values are an order of magnitude greater at ~ 2 μM (Table 4.4, Figure 4.4). This difference cannot be due to the population densities in these environments (Figure 4.4), and is unlikely to be caused by an overabundance of methanogens (consumers). That the methanogens in these environments have a substantially higher maximum hydrogen consumption rate ($q_{max,B}$) than the default value used here also

seems unlikely, as such high maximum consumption rates are more typical in thermophilic methanogenic archaea found in environments such as hydrothermal vents (Thauer et al. 2008) than those in the moderate environments studied by Conrad, Schink and Phelps (1986).

That an unrealistic choice of the maximum hydrogen threshold, H_{max}, or the effective affinity constant of production, K_A, is primarily to blame can also be ruled out: both are proportional to the equilibrium constant of production $K_{eq,A}$ (Equations 4.8, 4.10, 4.11), but while an decrease in H_{max} gives lower hydrogen concentrations, suggesting that $K_{eq,A}$ is too high, an increase in K_A gives a similar result, now suggesting that $K_{eq,A}$ is too low. Diffusivity, D, and the minimum hydrogen threshold, H_{min}, have little effect, and the maximum rate of production, $q_{max,A}$, could not be solely to blame.

While cumulative errors in the estimation of all parameters will have played a role in causing this over-prediction of hydrogen concentration, the affinity constant of consumption, K_B, deserves special attention (Figure 4.4). Reducing this parameter from the default value of 30 μM to 3 μM brings the average hydrogen concentration into the appropriate range (Figure 4.4) and increases the total transfer rate by around 40% (Table 4.12, Figure 4.5). A number of researchers have also suggested that this parameter has been frequently overestimated in the anaerobic methanogenesis literature (Boone, Johnson, and Liu 1989; Giraldo-Gómez, Goodwin, and Switzenbaum 1992), and estimation of affinity constants by Lineweaver-Burk plots (the method used by many of the sources in Table 4.8) has long been known to be error-prone (Dowd and Riggs 1965; Cornish-Bowden 2004).

It should be noted however, that those authors arguing that affinity constants have been overestimated in methanogenic archaea have argued that diffusion limitation has not been accounted for correctly. Boone, Johnson, and Liu (1989) studied low population densities where cells were typically 10 μm or more from their nearest neighbour, a situation not modelled here.

Giraldo-Gómez, Goodwin, and Switzenbaum (1992) assumed Michaelis-Menten kinetics for both production and consumption of dissolved hydrogen, neglecting the inhibitory effect that hydrogen has on its production.

On the other hand, other modelling studies agree with the prediction of this model that diffusion limitation is irrelevant, at least in mesothermal environments. Muralidharan and coworkers (1997) modelled flocs as concentric spheres, with a single methanogen at the centre surrounded by hydrogen producers. Hydrogen consumption (i.e. methanogenesis) is assumed to follow Michaelis-Menten kinetics, but while the authors acknowledge the inhibition of hydrogen on its production, the kinetics are unspecified. Instead, the authors used experimental measurements to predict hydrogen concentration profiles: they suggest that hydrogen concentration is essentially constant under mesophilic (37°C) scenarios but that there is a sharp gradient around the methanogen in thermophilic (85°C) scenarios.

Should this research be continued, it would be of great interest to further explore the parameter space where smaller values of K_B are taken as default. Also of interest are the other intermediary metabolites implicated in anaerobic methanogenic degradation, formate and acetate, and other microbial ecosystems where IMT plays a role. Testing the sensitivity of the numerical model to structural changes is also desirable: comparing simulations in two and three dimensions (possible using the numerical methods presented), and taking a finer spatial resolution, may increase confidence in the predictions of this research. Finally, biasing the distribution of cells to mimic the semi-random structures observed in nature may yield even more useful predictions: cells may cluster (group together) or adopt a more regular spacing, both within and between species.

4.5. Conclusions

The method of estimating the rate of interspecies metabolite transfer based on Fickian diffusion may be vulnerable to poor estimation of the surface concentrations of the syntrophic partner cells. Taking the harmonic mean distance between cells rather than the arithmetic mean is largely irrelevant in light of this. An alternate method of estimation, based on the kinetics of metabolism, appears to yield more reliable estimates but is reliant on many more parameters, increasing uncertainty in its predictions.

The numerical method developed during this research is an effective framework for exploring interspecies metabolite transfer between populations of randomly distributed individuals, to our knowledge the first ever described. The results presented here hint at the importance of reliable estimates for the affinity constant of consumption, an issue that has also been raised by others.

CHAPTER 5: CONCLUSIONS & FUTURE PROSPECTS

The general theme of the work presented here is that of theoretical models in population microbiology. This area of research draws on a wide range of more traditional scientific backgrounds for knowledge and techniques: mathematics, computer science, physical chemistry, biochemistry and, of course, microbiology itself.

The Synopsis outlined an unfortunate trend in biology of separating evolution and ecology; while it would be presumptuous to claim that the research presented has addressed this directly, awareness of the problem has guided the thinking behind it. More encouraging is the growing acceptance of theoretical models throughout biology, as biologists benefit from the benefits that such models can offer while modellers explore a fascinating and fertile realm of science.

5.1. Key findings

The primary purpose of the second chapter was to discuss the methods of modelling microbes as individual cells, pointing out the clarity this approach offers as well as the risks of simplifications that must be made. A minor advance in methodology was also presented, which will improve consistency between simulations where spatial structure is included.

The evolutionary origin of aging was tackled in the third chapter. While long thought to be capable of immortality, recent observations have suggested that microorganisms may suffer finite lifespans. Theoretical studies since have suggested that this is a desirable sacrifice to make, with the benefits to offspring outweighing the costs to the individual; however, these studies neglected the role of repair in slowing the aging process, and of ecological interactions between competing aging strategies. Repair is so universal to life (excluding viruses) that, with hindsight, it seems bizarre that anyone could suggest it should be selected out of existence. The work presented in this chapter, also published in the journal *BMC Biology*, serves to overturn a decade's thinking on the subject.

The fourth chapter looked at the ecology of anaerobic methanogenic degradation, aiming to test methods of estimating the rate of interspecies metabolite transfer. In this it has been partially successful, hindered largely by the difficulties in obtaining reliable estimates of parameter values. Results presented here suggest that the effect of diffusion limitation has been overestimated in the past, but this is sensitive to estimates of the affinity constant of consumption. The model developed during this study is a solid base for further exploration of the topic, which it is expected will yield more conclusive results in future.

5.2. Lessons on modelling

A second, unexpected theme of the work presented here is the seductive ease of modelling too simply. To quote the physicist Albert Einstein,

> "It can scarcely be denied that the supreme goal of all theory is to make the irreducible basic elements as simple and as few as possible without having to surrender the adequate representation of a single datum of experience."
> (Einstein 1934).

While simplification is necessary in modelling complex systems, too much and the conclusions become detached from reality. Equating microbial cells with enzymes of interest is a simplification that demands caution. Assuming that repair has no immediate benefit to growth, or that surface concentrations will take a certain value, may not obey this need for "adequate representation".

The ideal solution to this predicament is first to model the system in minute detail, then simplify iteratively until the results diverge from observations. But such an approach requires such time and effort that only rare instances could be accommodated in the pressures of academic science (Brooks and Tobias 1996), or indeed in our decidedly finite lifespans.

At this point the science of modelling strays into the territory of the humanities. Modellers must take care to justify the simplifying assumptions they make, appealing to observational evidence, sensitivity analysis of model parameters and structure, and to an honest

admission of any limitations. An honest assessment of one's own research is to be encouraged in all academic pursuits, but I would argue that within the sciences the greatest need is in theoretical modelling. We observe reality ultimately through our senses, and in this regard physical models have the advantage of taking a similar form to that which they represent. Statistical models are means of finding or confirming patterns within data gathered from reality-based evidence. Theoretical models, however, do not model reality directly, but our understanding of reality. The task of the theoretical modeller in persuading peers is therefore twofold: justification of the mental model and accurate translation into a theoretical model. The former is usually the more difficult of the two, and often neglected.

Blame for this neglect cannot be heaped solely on the researcher. Transparency can be interpreted as weakness, tempting the researcher to avoid undue criticism by less-than-perfect transparency. This situation serves no one: hype eventually leads to disillusionment once deficiencies are revealed, either through thorough analysis of the model or through faulty predictions. To break this cycle, we need to foster more modest, balanced expectations of what theoretical models, or rather theoretical modellers, can realistically achieve.

5.3. Future prospects

The research constituting this thesis is by no means to be considered complete. Some questions asked have not yet been answered, while more questions have presented themselves along the way. What this thesis does describe, however, is a solid foundation for further research. In particular, the work presented in Chapter 4 is ripe for further investigation: the value taken by the parameter K_B is of great interest. Another topic of interest is the relationship between maximum forward and reverse reaction rates of the enzyme kinetics covered in Chapter 2. Development of the theoretical models presented here drew upon models of previous researchers, be they pioneers of enzyme kinetics Leonor Michaelis and Maud Menten or larger, more recent

collaborations developing open-source software such as iDynoMiCS or Elmer. All such endeavours involve far more in the way of literature review, planning, and bug-hunting, than is ever apparent in the final product. With these issues resolved, there is much scope for progress in the topics of primary interest.

BIBLIOGRAPHY

Ackermann, Martin. 2013. "Microbial Individuality in the Natural Environment." *ISME Journal* 7 (3): 465–67.

Ackermann, Martin, Lin Chao, Carl T Bergstrom, and Michael Doebeli. 2007. "On the Evolutionary Origin of Aging." *Aging Cell* 6 (2): 235–44.

Ackermann, Martin, Alexandra Schauerte, Stephen C Stearns, and Urs Jenal. 2007. "Experimental Evolution of Aging in a Bacterium." *BMC Evolutionary Biology* 7: 126.

Ackermann, Martin, Stephen C Stearns, and Urs Jenal. 2003. "Senescence in a Bacterium with Asymmetric Division." *Science* 300 (5627): 1920.

Adami, C. 2002. "What Is Complexity?" *Bioessays* 24 (12): 1085–94.

Adams, J. 2004. "Microbial Evolution in Laboratory Environments." *Research in Microbiology* 155 (5): 311–18.

Adamson, M W, and A Yu Morozov. 2013. "When Can We Trust Our Model Predictions? Unearthing Structural Sensitivity in Biological Systems." *Proceedings of the Royal Society A* 469 (2149): 20120500.

Ahring, Birgitte Kiær, and Peter Westermann. 1987. "Kinetics of Butyrate, Acetate, and Hydrogen Metabolism in a Thermophilic, Anaerobic, Butyrate-Degrading Triculture." *Applied and Environmental Microbiology* 53 (2): 434–39.

Aldridge, Bree B, Marta Fernandez-Suarez, Danielle Heller, Vijay Ambravaneswaran, Daniel Irimia, Mehmet Toner, and Sarah M Fortune. 2012. "Asymmetry and Aging of Mycobacterial Cells Lead to Variable Growth and Antibiotic Susceptibility." *Science* 335 (6064): 100–104.

Aminov, Rustam I. 2013. "Role of Archaea in Human Disease." *Frontiers in Cellular and Infection Microbiology*, 42.

Andersson, Veronica, Sarah Hanzén, Beidong Liu, Mikael Molin, and Thomas Nyström. 2013. "Enhancing Protein Disaggregation Restores Proteasome Activity in Aged Cells." *Aging* 5 (11): 802–12.

Angert, Esther R. 2005. "Alternatives to Binary Fission in Bacteria." *Nature Reviews Microbiology* 3 (3): 214–24.

Archer, David B, and Godfrey E Powell. 1985. "Dependence of the Specific Growth Rate of Methanogenic Mutualistic Cocultures on the Methanogen." *Archives of Microbiology* 141 (2): 133–37.

Barberán, Albert, Emilio O. Casamayor, and Noah Fierer. 2014. "The Microbial Contribution to Macroecology." *Evolutionary and Genomic Microbiology* 5: 203.

Barker, M G, and R M Walmsley. 1999. "Replicative Ageing in the Fission Yeast *Schizosaccharomyces Pombe*." *Yeast* 15 (14): 1511–18.

Baumgärtner, Stephan, and Iva M Tolić-Nørrelykke. 2009. "Growth Pattern of Single Fission Yeast Cells Is Bilinear and Depends on Temperature and DNA Synthesis." *Biophysical Journal* 96 (10): 4336–47.

Benton, Tim G, Martin Solan, Justin M J Travis, and Steven M Sait. 2007. "Microcosm Experiments Can Inform Global Ecological Problems." *Trends in Ecology & Evolution* 22 (10): 516–21.

Bergmiller, Tobias, and Martin Ackermann. 2011. "Pole Age Affects Cell Size and the Timing of Cell Division in *Methylobacterium Extorquens* AM1." *Journal of Bacteriology* 193 (19): 5216–21.

Boetius, Antje, Katrin Ravenschlag, Carsten J Schubert, Dirk Rickert, Friedrich Widdel, Armin Gieseke, Rudolf Amann, Bo Barker Jørgensen, Ursula Witte, and Olaf Pfannkuche. 2000.

"A Marine Microbial Consortium Apparently Mediating Anaerobic Oxidation of Methane." *Nature* 407 (6804): 623–26.

Bonner, John Tyler. 1998. "The Origins of Multicellularity." *Integrative Biology* 1 (1): 27–36.

Boone, David R, Richard L Johnson, and Yitai Liu. 1989. "Diffusion of the Interspecies Electron Carriers H_2 and Formate in Methanogenic Ecosystems and Its Implications in the Measurement of K_m for H_2 or Formate Uptake." *Applied and Environmental Microbiology* 55 (7): 1735–41.

Boucher, Yan, C.J. Douady, R.T. Papke, D.A. Walsh, M.E. Boudreau, C.L. Nesbo, R.J. Case, and W.F. Doolittle. 2003. "Lateral Gene Transfer and the Origins of Prokaryotic Groups." *Annual Review of Genetics* 37:283-328.: 283–328.

Briggs, George Edward, and John Burdon Sanderson Haldane. 1925. "A Note on the Kinetics of Enzyme Action." *Biochemical Journal* 19 (2): 338.

Briggs, William L, Van Emden Henson, and Stephen Fahrney McCormick. 2000. *A Multigrid Tutorial*. 2nd ed. Philadelphia: Society for Industrial and Applied Mathematics.

Brooks, R J, and A M Tobias. 1996. "Choosing the Best Model: Level of Detail, Complexity, and Model Performance." *Mathematical and Computer Modelling* 24 (4): 1–14.

Button, D K. 1978. "On the Theory of Control of Microbial Growth Kinetics by Limiting Nutrient Concentrations." *Deep Sea Research* 25 (12): 1163–77.

———. 1983. "Differences between the Kinetics of Nutrient Uptake by Micro-Organisms, Growth and Enzyme Kinetics." *Trends in Biochemical Sciences* 8 (4): 121–24.

———. 2000. "Abandon Michaelis-Menten?" *ASM News* 66 (9): 510.

Cavender-Bares, Jeannine, Kenneth H Kozak, Paul V A Fine, and Steven W Kembel. 2009. "The Merging of Community Ecology and Phylogenetic Biology." *Ecology Letters* 12 (7): 693–715.

Chang, Raymond. 1977. *Physical Chemistry with Applications to Biological Systems*. Macmillan.

Chao, Lin. 2010. "A Model for Damage Load and Its Implications for the Evolution of Bacterial Aging." *PLoS Genetics* 6 (8): e1001076.

Chen, William W, Mario Niepel, and Peter K Sorger. 2010. "Classic and Contemporary Approaches to Modeling Biochemical Reactions." *Genes & Development* 24 (17): 1861–75.

Chin, Kuk-Jeong, and Ralf Conrad. 1995. "Intermediary Metabolism in Methanogenic Paddy Soil and the Influence of Temperature." *FEMS Microbiology Ecology* 18 (2): 85–102.

Clark, Philip J, and Francis C Evans. 1954. "Distance to Nearest Neighbor as a Measure of Spatial Relationships in Populations." *Ecology* 35 (4): 445–53.

Clegg, Robert J, Rosemary J Dyson, and Jan-Ulrich Kreft. 2014. "Repair rather than Segregation of Damage Is the Optimal Unicellular Aging Strategy." *BMC Biology* 12 (1): 52.

Coelho, Miguel, Aygül Dereli, Anett Haese, Sebastian Kühn, Liliana Malinovska, Morgan E. DeSantis, James Shorter, Simon Alberti, Thilo Gross, and Iva M Tolić-Nørrelykke. 2013. "Fission Yeast Does Not Age under Favorable Conditions, but Does so after Stress." *Current Biology*.

Cohen, Joel E. 2004. "Mathematics Is Biology's next Microscope, Only Better; Biology Is Mathematics' next Physics, Only Better." *PLoS Biology* 2 (12): e439.

Conrad, Ralf. 2009. "The Global Methane Cycle: Recent Advances in Understanding the Microbial Processes Involved." *Environmental Microbiology Reports* 1 (5): 285–92.

Conrad, Ralf, and Monika Babbel. 1989. "Effect of Dilution on Methanogenesis, Hydrogen Turnover and Interspecies Hydrogen Transfer in Anoxic Paddy Soil." *FEMS Microbiology Letters* 62 (1): 21–27.

Conrad, Ralf, T J Phelps, and J G Zeikus. 1985. "Gas Metabolism Evidence in Support of the Juxtaposition of Hydrogen-Producing and Methanogenic Bacteria in Sewage Sludge and Lake Sediments." *Applied and Environmental Microbiology* 50 (3): 595–601.

Conrad, Ralf, Bernhard Schink, and T J Phelps. 1986. "Thermodynamics of H_2-Consuming and H_2-Producing Metabolic Reactions in Diverse Methanogenic Environments under in Situ Conditions." *FEMS Microbiology Letters* 38 (6): 353–60.

Cooper, Stephen. 2013. "*Schizosaccharomyces Pombe* Grows Exponentially during the Division Cycle with No Rate Change Points." *FEMS Yeast Research* 13 (7): 650–58.

Coquel, Anne-Sophie, Jean-Pascal Jacob, Mael Primet, Alice Demarez, Mariella Dimiccoli, Thomas Julou, Lionel Moisan, Ariel B Lindner, and Hugues Berry. 2013. "Localization of Protein Aggregation in *Escherichia Coli* Is Governed by Diffusion and Nucleoid Macromolecular Crowding Effect." *PLoS Computational Biology* 9 (4): e1003038.

Cordero, Otto X, and Martin F Polz. 2014. "Explaining Microbial Genomic Diversity in Light of Evolutionary Ecology." *Nature Reviews Microbiology* 12 (4): 263–73.

Cord-Ruwisch, Ralf, Derek R Lovley, and Bernhard Schink. 1998. "Growth of *Geobacter Sulfurreducens* with Acetate in Syntrophic Cooperation with Hydrogen-Oxidizing Anaerobic Partners." *Applied and Environmental Microbiology* 64 (6): 2232–36.

Cord-Ruwisch, Ralf, Hans-Jürgen Seitz, and Ralf Conrad. 1988. "The Capacity of Hydrogenotrophic Anaerobic Bacteria to Compete for Traces of Hydrogen Depends on the Redox Potential of the Terminal Electron Acceptor." *Archives of Microbiology* 149 (4): 350–57.

Cornish-Bowden, Athel. 2004. *Fundamentals of Enzyme Kinetics*. 3rd ed. London: Portland.

Costa, Engràcia, Julio Pérez, and Jan-Ulrich Kreft. 2006. "Why Is Metabolic Labour Divided in Nitrification?" *Trends in Microbiology* 14 (5): 213–19.

Cussler, E L. 2009. *Diffusion : Mass Transfer in Fluid Systems*. 3rd ed. Cambridge: Cambridge University Press.

Dabes, J N, R K Finn, and C R Wilke. 1973. "Equations of Substrate-Limited Growth: The Case for Blackman Kinetics." *Biotechnology and Bioengineering* 15 (6): 1159–77.

Damore, James A., and Jeff Gore. 2012. "Understanding Microbial Cooperation." *Journal of Theoretical Biology*, Evolution of Cooperation, 299 (April): 31–41.

Darwin, Charles. 1859. *On the Origin of Species by Means of Natural Selection, or the Preservation of Favoured Races in the Struggle for Life*. 1st ed. London: John Murray.

Davidson, Carla J, and Michael G Surette. 2008. "Individuality in Bacteria." *Annual Review of Genetics* 42: 253–68.

Dawkins, Richard. 1988. *The Blind Watchmaker*. London: Penguin.

Dens, E J, K Bernaerts, A R Standaert, and J F Van Impe. 2005. "Cell Division Theory and Individual-Based Modeling of Microbial Lag: Part I. The Theory of Cell Division." *International Journal of Food Microbiology* 101 (3): 303–18.

Diggle, Peter. 1983. *Statistical Analysis of Spatial Point Patterns*. Mathematics in Biology. Academic Press.

Dobzhansky, Theodosius. 1964. "Biology, Molecular and Organismic." *American Zoologist* 4 (4): 443–52.

———. 1973. "Nothing in Biology Makes Sense except in the Light of Evolution." *The American Biology Teacher* 35 (3): 125–29.

Dolfing, Jan, and Wim G B M Bloeman. 1985. "Acitivity Measurements as a Tool to Characterize the Microbial Composition of Methanogenic Environments." *Journal of Microbiological Methods* 4 (1): 1–12.

Donachie, William D, and Arthur C Robinson. 1987. "Cell Division: Parameter Values and the Process." In Escherichia Coli *and* Salmonella Typhimurium*: Cellular and Molecular Biology*, edited by Frederick C Neidhardt, John L Ingraham, K. Brooks Low, Boris Magasanik, Moselio Schaechter, and H. Edwin Umbarger, 1st ed., 2:1578–93. Washington, D.C: American Society for Microbiology.

Dougan, D A, A Mogk, and B Bukau. 2002. "Protein Folding and Degradation in Bacteria: To Degrade or Not to Degrade? That Is the Question." *Cellular and Molecular Life Sciences* 59 (10): 1607–16.

Dowd, John E, and Douglas S Riggs. 1965. "A Comparison of Estimates of Michaelis-Menten Kinetic Constants from Various Linear Transformations." *Journal of Biological Chemistry* 240 (2): 863–69.

Dwyer, Daryl F, Els Weeg-Aerssens, Daniel R Shelton, and James M Tiedje. 1988. "Bioenergetic Conditions of Butyrate Metabolism by a Syntrophic, Anaerobic Bacterium in Coculture with Hydrogen-Oxidizing Methanogenic and Sulfidogenic Bacteria." *Applied and Environmental Microbiology* 54 (6): 1354–59.

Dyall, Sabrina D, Mark T Brown, and Patricia J Johnson. 2004. "Ancient Invasions: From Endosymbionts to Organelles." *Science* 304 (5668): 253–57.

Egilmez, N K, and S M Jazwinski. 1989. "Evidence for the Involvement of a Cytoplasmic Factor in the Aging of the Yeast *Saccharomyces Cerevisiae*." *Journal of Bacteriology* 171 (1): 37–42.

Egli, T., U. Lendenmann, and M. Snozzi. 1993. "Kinetics of Microbial Growth with Mixtures of Carbon Sources." *Antonie van Leeuwenhoek International Journal of General and Molecular Microbiology* 63 (3-4): 289–98.

Einstein, Albert. 1934. "On the Method of Theoretical Physics." *Philosphy of Science* 1 (2): 163–69.

Elena, Santiago F, and Richard E Lenski. 2003. "Evolution Experiments with Microorganisms: The Dynamics and Genetic Bases of Adaptation." *Nature Reviews Genetics* 4 (6): 457–69.

Erjavec, Nika, Marija Cvijovic, Edda Klipp, and Thomas Nyström. 2008. "Selective Benefits of Damage Partitioning in Unicellular Systems and Its Effects on Aging." *Proceedings of the National Academy of Sciences of the United States of America* 105 (48): 18764–69.

Evans, Matthew R, Mike Bithell, Stephen J Cornell, Sasha R X Dall, Sandra Díaz, Stephen Emmott, Bruno Ernande, et al. 2013. "Predictive Systems Ecology." *Proceedings of the Royal Society B* 280 (1771): 20131452.

Evans, Matthew R, Volker Grimm, Karin Johst, Tarja Knuuttila, Rogier de Langhe, Catherine M Lessells, Martina Merz, et al. 2013a. "Do Simple Models Lead to Generality in Ecology?" *Trends in Ecology & Evolution* 28 (10): 578–83.

———. 2013b. "Do Simple Models Lead to Generality in Ecology?" *Trends in Ecology & Evolution* 28 (10): 578–83.

Felchner-Zwirello, Monika, Josef Winter, and Claudia Gallert. 2013. "Interspecies Distances between Propionic Acid Degraders and Methanogens in Syntrophic Consortia for Optimal Hydrogen Transfer." *Applied Microbiology and Biotechnology* 97 (20): 9193–9205.

Feldgarden, M, D M Stoebel, D Brisson, and D E Dykhuizen. 2003. "Size Doesn't Matter: Microbial Selection Experiments Address Ecological Phenomena." *Ecology* 84 (7): 1679–87.

Fell, David A. 1992. "Metabolic Control Analysis: A Survey of Its Theoretical and Experimental Development." *Biochemical Journal* 286: 313–30.

Fennell, Donna E, and James M Gossett. 1998. "Modeling the Production of and Competition for Hydrogen in a Dechlorinating Culture." *Environmental Science & Technology* 32 (16): 2450–60.

Ferenci, Thomas. 1999. "'Growth of Bacterial Cultures' 50 Years on: Towards an Uncertainty Principle instead of Constants in Bacterial Growth Kinetics." *Research in Microbiology* 150 (7): 431–38.

Ferrer, Jordi, Clara Prats, and Daniel Lopez. 2008. "Individual-Based Modelling: An Essential Tool for Microbiology." *Journal of Biological Physics* 34 (1-2): 19–37.

Flemming, Hans-Curt, and Jost Wingender. 2010. "The Biofilm Matrix." *Nature Reviews Microbiology* 8 (9): 623–33.

Foster, Kevin R, and Thomas Bell. 2012. "Competition, Not Cooperation, Dominates Interactions among Culturable Microbial Species." *Current Biology* 22 (19): 1845–50.

Fukuzaki, Satoshi, Naomichi Nishio, Manabu Shobayashi, and Shiro Nagai. 1990. "Inhibition of the Fermentation of Propionate to Methane by Hydrogen, Acetate, and Propionate." *Applied and Environmental Microbiology* 56 (3): 719–23.

Galli-Taliadoros, L A, J D Sedgwick, S A Wood, and H Körner. 1995. "Gene Knock-out Technology: A Methodological Overview for the Interested Novice." *Journal of Immunological Methods* 181 (1): 1–15.

Geiler-Samerotte, Kerry A, Michael F Dion, Bogdan A Budnik, Stephanie M Wang, Daniel L Hartl, and D Allan Drummond. 2011. "Misfolded Proteins Impose a Dosage-Dependent Fitness Cost and Trigger a Cytosolic Unfolded Protein Response in Yeast." *Proceedings of the National Academy of Sciences of the United States of America* 108 (2): 680–85.

Giraldo-Gómez, Eugenio, Steve Goodwin, and Michael S Switzenbaum. 1992. "Influence of Mass Transfer Limitations on Determination of the Half Saturation Constant for Hydrogen Uptake in a Mixed-Culture CH_4-Producing Enrichment." *Biotechnology and Bioengineering* 40 (7): 768–76.

Godin, Michel, Francisco Feijó Delgado, Sungmin Son, William H Grover, Andrea K Bryan, Amit Tzur, Paul Jorgensen, et al. 2010. "Using Buoyant Mass to Measure the Growth of Single Cells." *Nature Methods* 7 (5): 387–90.

González-Montalbán, Nuria, M Mar Carrió, Sergi Cuatrecasas, Anna Arís, and Antonio Villaverde. 2005. "Bacterial Inclusion Bodies Are Cytotoxic in Vivo in Absence of Functional Chaperones DnaK or GroEL." *Journal of Biotechnology* 118 (4): 406–12.

Goodwin, Steve, Eugenio Giraldo-Gomez, Bruce Mobarry, and Michael S Switzenbaum. 1991. "Comparison of Diffusion and Reaction Rates in Anaerobic Microbial Aggregates." *Microbial Ecology* 22 (1): 161–74.

Goto, Ken, and Chalinda K Beneragama. 2010. "Circadian Clocks and Antiaging: Do Non-Aging Microalgae like *Euglena* Reveal Anything?." *Ageing Research Reviews* 9 (2): 91–100.

Gottschalk, Gerhard. 1979. *Bacterial Metabolism.* 2nd ed. Springer Series in Microbiolgy. New York: Springer.

Grimm, Volker, Uta Berger, Finn Bastiansen, Sigrunn Eliassen, Vincent Ginot, Jarl Giske, John Goss-Custard, et al. 2006. "A Standard Protocol for Describing Individual-Based and Agent-Based Models." *Ecological Modelling* 198 (1-2): 115–26.

Grosberg, Richard K, and Richard R Strathmann. 2007. "The Evolution of Multicellularity: A Minor Major Transition?" *Annual Review of Ecology, Evolution, and Systematics* 38 (1): 621–54.

Gunawardena, Jeremy. 2012. "Some Lessons about Models from Michaelis and Menten." *Molecular Biology of the Cell* 23 (4): 517–19.

———. 2013. "Biology Is More Theoretical than Physics." *Molecular Biology of the Cell* 24 (12): 1827–29.

———. 2014a. "Time-Scale Separation – Michaelis and Menten's Old Idea, Still Bearing Fruit." *FEBS Journal* 281 (2): 473–88.

———. 2014b. "Models in Biology: 'accurate Descriptions of Our Pathetic Thinking.'" *BMC Biology* 12 (1): 29.

Hales, D, J Rouchier, and B Edmonds. 2003. "Model-to-Model Analysis." *Journal of Artificial Societies and Social Simulation* 6 (4): 5.

Hales, Thomas C. 1992. "The Sphere Packing Problem." *Journal of Computational and Applied Mathematics* 44 (1): 41–76.

Harcombe, William R, William J Riehl, Ilija Dukovski, Brian R Granger, Alex Betts, Alex H Lang, Gracia Bonilla, et al. 2014. "Metabolic Resource Allocation in Individual Microbes Determines Ecosystem Interactions and Spatial Dynamics." *Cell Reports* 7 (4): 1104–15.

Harper, Stephen R, and Frederick G Pohland. 1986. "Recent Developments in Hydrogen Management during Anaerobic Biological Wastewater Treatment." *Biotechnology and Bioengineering* 28 (4): 585–602.

Haruta, Shin, Souichiro Kato, Kyosuke Yamamoto, and Yasuo Igarashi. 2009. "Intertwined Interspecies Relationships: Approaches to Untangle the Microbial Network." *Environmental Microbiology* 11 (12): 2963–69.

Hayflick, Leonard. 2007. "Entropy Explains Aging, Genetic Determinism Explains Longevity, and Undefined Terminology Explains Misunderstanding Both." *PLoS Genetics* 3 (12): e220.

Healy, Kevin, Thomas Guillerme, Sive Finlay, Adam Kane, Seán B. A. Kelly, Deirdre McClean, David J. Kelly, Ian Donohue, Andrew L. Jackson, and Natalie Cooper. 2014. "Ecology and Mode-of-Life Explain Lifespan Variation in Birds and Mammals." *Proceedings of the Royal Society B: Biological Sciences* 281 (1784): 20140298.

Heyes, R H, and R J Hall. 1983. "Kinetics of Two Subgroups of Propionate-Using Organisms in Anaerobic Digestion." *Applied and Environmental Microbiology* 46 (3): 710–15.

Hilbert, David. 1902. "Mathematical Problems." *Bulletin of the American Mathematical Society* 8 (10): 437–79.

Hoh, Choon-Yee, and Ralf Cord-Ruwisch. 1996. "A Practical Kinetic Model That Considers Endproduct Inhibition in Anaerobic Digestion Processes by Including the Equilibrium Constant." *Biotechnology and Bioengineering* 51 (5): 597–604.

Horváth, Anna, Anna Rácz-Mónus, Peter Buchwald, and Akos Sveiczer. 2013. "Cell Length Growth in Fission Yeast: An Analysis of Its Bilinear Character and the Nature of Its Rate Change Transition." *FEMS Yeast Research* 13 (7): 635–49.

Hughes, W Howard. 1955. "The Inheritance of Differences in Growth Rate in *Escherichia Coli*." *Journal of General Microbiology* 12 (2): 265–68.

Hunter, John D. 2007. "Matplotlib: A 2D Graphics Environment." *Computing in Science Engineering* 9 (3): 90–95.

Ishii, Nobuyoshi, Martin Robert, Yoichi Nakayama, Akio Kanai, and Masaru Tomita. 2004. "Toward Large-Scale Modeling of the Microbial Cell for Computer Simulation." *Journal of Biotechnology* 113 (1–3): 281–94.

Ishii, Shun'ichi, Tomoyuki Kosaka, Katsutoshi Hori, Yasuaki Hotta, and Kazuya Watanabe. 2005. "Coaggregation Facilitates Interspecies Hydrogen Transfer between *Pelotomaculum Thermopropionicum* and *Methanothermobacter Thermautotrophicus*." *Applied and Environmental Microbiology* 71 (12): 7838–45.

Ishii, Shun'ichi, Tomoyuki Kosaka, Yasuaki Hotta, and Kazuya Watanabe. 2006. "Simulating the Contribution of Coaggregation to Interspecies Hydrogen Fluxes in Syntrophic Methanogenic Consortia." *Applied and Environmental Microbiology* 72 (7): 5093–96.

Jackson, Bradley E, and Michael J McInerney. 2002. "Anaerobic Microbial Metabolism Can Proceed close to Thermodynamic Limits." *Nature* 415 (6870): 454–56.

Jeanson, S, J Chadœuf, M N Madec, S Aly, J Floury, T F Brocklehurst, and S Lortal. 2011. "Spatial Distribution of Bacterial Colonies in a Model Cheese." *Applied and Environmental Microbiology* 77 (4): 1493–1500.

Jensen, Johan L W V. 1906. "Sur Les Fonctions Convexes et Les Inégalités Entre Les Valeurs Moyennes." *Acta Mathematica* 30 (1): 175–93.

Jessup, Christine M, Rees Kassen, Samantha E Forde, Ben Kerr, Angus Buckling, Paul B Rainey, and Brendan J M Bohannan. 2004. "Big Questions, Small Worlds: Microbial Model Systems in Ecology." *Trends in Ecology & Evolution* 19 (4): 189–97.

Jin, Qusheng. 2007. "Control of Hydrogen Partial Pressures on the Rates of Syntrophic Microbial Metabolisms: A Kinetic Model for Butyrate Fermentation." *Geobiology* 5 (1): 35–48.

Johnson, Marc T J, and John R Stinchcombe. 2007. "An Emerging Synthesis between Community Ecology and Evolutionary Biology." *Trends in Ecology & Evolution* 22 (5): 250–57.

Jud, G, K Schneider, and R Bachofen. 1997. "The Role of Hydrogen Mass Transfer for the Growth Kinetics of *Methanobacterium Thermoautotrophicum* in Batch and Chemostat Cultures." *Journal of Industrial Microbiology and Biotechnology* 19 (4): 246–51.

Juhász, János, Attila Kertész-Farkas, Dóra Szabó, and Sándor Pongor. 2014. "Emergence of Collective Territorial Defense in Bacterial Communities: Horizontal Gene Transfer Can Stabilize Microbiomes." *PLoS ONE* 9 (4): e95511.

Karadagli, Fatih, and Bruce E Rittmann. 2005. "Kinetic Characterization of *Methanobacterium Bryantii* M.o.H." *Environmental Science & Technology* 39 (13): 4900–4905.

Karr, Jonathan R, Jayodita C Sanghvi, Derek N Macklin, Miriam V Gutschow, Jared M Jacobs, Benjamin Bolival Jr, Nacyra Assad-Garcia, John I Glass, and Markus W Covert. 2012. "A Whole-Cell Computational Model Predicts Phenotype from Genotype." *Cell* 150 (2): 389–401.

Kaspar, H F, and K Wuhrmann. 1978. "Kinetic Parameters and Relative Turnovers of Some Important Catabolic Reactions in Digesting Sludge." *Applied and Environmental Microbiology* 36 (1): 1–7.

Kempes, Christopher P, Stephanie Dutkiewicz, and Michael J Follows. 2012. "Growth, Metabolic Partitioning, and the Size of Microorganisms." *Proceedings of the National Academy of Sciences of the United States of America* 109 (2): 495–500.

Kirkwood, Thomas B L. 2005. "Understanding the Odd Science of Aging." *Cell* 120 (4): 437–47.

Kirkwood, Thomas B L, and Thomas Cremer. 1982. "Cytogerontology since 1881: A Reappraisal of August Weismann and a Review of Modern Progress." *Human Genetics* 60 (2): 101–21.

Kleerebezem, Robbert, and Alfons J M Stams. 2000. "Kinetics of Syntrophic Cultures: A Theoretical Treatise on Butyrate Fermentation." *Biotechnology and Bioengineering* 67 (5): 529–43.

Knudsen, Guy R. 2007. "Quantifying the Metabolic Activity of Soil- and Plant-Associated Microbes." In *Manual of Environmental Microbiology*, edited by C J Hurst, R L Crawford, J L Garland, D A Lipson, A L Mills, and L D Stetzenbach, 3rd ed., 697–703. Washington, DC: ASM Press.

Koch, Arthur L. 1993. "The Growth Kinetics of *B. Subtilis*." *Antonie van Leeuwenhoek* 63 (1): 45–53.

———. 1996. "What Size Should a Bacterium Be? A Question of Scale." *Annual Review of Microbiology* 50 (1): 317–48.

Koch, Arthur L, and Houston C Wang. 1982. "How close to the Theoretical Diffusion Limit Do Bacterial Uptake Systems Function?" *Archives of Microbiology* 131: 36–42.

Koch, Christof. 2012. "Modular Biological Complexity." *Science* 337 (6094): 531–32.

Kovárová-Kovar, Karin, and Thomas Egli. 1998. "Growth Kinetics of Suspended Microbial Cells: From Single-Substrate-Controlled Growth to Mixed-Substrate Kinetics." *Microbiology and Molecular Biology Reviews* 62 (3): 646–66.

Kreft, Jan-Ulrich. 2004. "Biofilms Promote Altruism." *Microbiology* 150 (8): 2751–60.

———. 2009. "Mathematical Modeling of Microbial Ecology: Spatial Dynamics of Interactions in Biofilms and Guts." In *Food-Borne Microbes: Shaping the Host Ecosystem*, edited by Lee Ann Jaykus, Hua H Wang, and Larry S Schlesinger, 347–77. Washington, DC: ASM Press.

Kreft, Jan-Ulrich, and S Bonhoeffer. 2005. "The Evolution of Groups of Cooperating Bacteria and the Growth Rate versus Yield Trade-Off." *Microbiology* 151 (3): 637–41.

Kreft, Jan-Ulrich, Ginger Booth, and Julian W T Wimpenny. 1998. "BacSim, a Simulator for Individual-Based Modelling of Bacterial Colony Growth." *Microbiology* 144: 3275–87.

Kreft, Jan-Ulrich, Cristian Picioreanu, Julian W T Wimpenny, and Mark C M van Loosdrecht. 2001. "Individual-Based Modelling of Biofilms." *Microbiology* 147 (11): 2897–2912.

Kreft, Jan-Ulrich, Caroline M Plugge, Volker Grimm, Clara Prats, Johan H J Leveau, Thomas Banitz, Stephen Baines, et al. 2013. "Mighty Small: Observing and Modeling Individual Microbes Becomes Big Science." *Proceedings of the National Academy of Sciences of the United States of America* 110 (45): 18027–28.

Kristjansson, Jakob K, Peter Schönheit, and Rudolf K Thauer. 1982. "Different K_s Values for Hydrogen of Methanogenic Bacteria and Sulfate Reducing Bacteria: An Explanation for the Apparent Inhibition of Methanogenesis by Sulfate." *Archives of Microbiology* 131 (3): 278–82.

Krone, S.M., R. Lu, R. Fox, H. Suzuki, and E.M. Top. 2007. "Modelling the Spatial Dynamics of Plasmid Transfer and Persistence." *Microbiology* 153 (1350-0872 (Print)): 2803–16.

Kurland, Charles G, B Canback, and O G Berg. 2003. "Horizontal Gene Transfer: A Critical View." *Proceedings of the National Academy of the Sciences of the United States of America* 100 (17): 9658–62.

Laney, Samuel R, Robert J Olson, and Heidi M Sosik. 2012. "Diatoms Favor Their Younger Daughters." *Limnology and Oceanography* 57 (5): 1572–78.

Lardon, Laurent A, Brian V Merkey, Sónia Martins, Andreas Dötsch, Cristian Picioreanu, Jan-Ulrich Kreft, and Barth F Smets. 2011. "iDynoMiCS: Next-Generation Individual-Based Modelling of Biofilms." *Environmental Microbiology* 13 (9): 2416–34.

Lawrence, Alonzo W, and Perry L McCarty. 1969. "Kinetics of Methane Fermentation in Anaerobic Treatment." *Journal Water Pollution Control Federation* 41 (2): R1–17.

Lele, Uttara N, Ulfat I Baig, and Milind G Watve. 2011. "Phenotypic Plasticity and Effects of Selection on Cell Division Symmetry in *Escherichia Coli*." *PLoS ONE* 6 (1): e14516.

Lencastre Fernandes, R, M Nierychlo, L Lundin, A E Pedersen, P E Puentes Tellez, A Dutta, M Carlquist, et al. 2011. "Experimental Methods and Modeling Techniques for Description of Cell Population Heterogeneity." *Biotechnology Advances* 29 (6): 575–99.

Lendenmann, Urs, Mario Snozzi, and Thomas Egli. 1999. "Growth Kinetics of *Escherichia Coli* with Galactose and Several Other Sugars in Carbon-Limited Chemostat Culture." *Canadian Journal of Microbiology* 46 (1): 72–80.

Levenspiel, Octave. 1980. "The Monod Equation: A Revisit and a Generalization to Product Inhibition Situations." *Biotechnology and Bioengineering* 22 (8): 1671–87.

Levin, Bruce R. 2010. "Nasty Viruses, Costly Plasmids, Population Dynamics, and the Conditions for Establishing and Maintaining CRISPR-Mediated Adaptive Immunity in Bacteria." *PLoS Genetics* 6 (10): e1001171.

Levins, Richard. 1966. "The Strategy of Model Building in Population Biology." *American Scientist*, 421–31.

Lindner, Ariel B, and Alice Demarez. 2009. "Protein Aggregation as a Paradigm of Aging." *Biochimica et Biophysica Acta* 1790 (10): 980–96.

Lindner, Ariel B, Richard Madden, Alice Demarez, Eric J Stewart, and François Taddei. 2008. "Asymmetric Segregation of Protein Aggregates Is Associated with Cellular Aging and Rejuvenation." *Proceedings of the National Academy of Sciences of the United States of America* 105 (8): 3076–81.

Lineweaver, Hans, and Dean Burk. 1934. "The Determination of Enzyme Dissociation Constants." *Journal of the American Chemical Society* 56 (3): 658–66.

Lin, Su-Ju, and Nicanor Austriaco. 2014. "Aging and Cell Death in the Other Yeasts, *Schizosaccharomyces Pombe* and *Candida Albicans*." *FEMS Yeast Research* 14 (1): 119–35.

Liu, Yu. 2006. "A Simple Thermodynamic Approach for Derivation of a General Monod Equation for Microbial Growth." *Biochemical Engineering Journal* 31 (1): 102–5.

———. 2007. "Overview of Some Theoretical Approaches for Derivation of the Monod Equation." *Applied Microbiology and Biotechnology* 73 (6): 1241–50.

Liu, Yuchen, and William B Whitman. 2008. "Metabolic, Phylogenetic, and Ecological Diversity of the Methanogenic Archaea." *Annals of the New York Academy of Sciences* 1125 (1): 171–89.

Lonergan, Mike. 2014. "Data Availability Constrains Model Complexity, Generality, and Utility: A Response to Evans *et Al.*" *Trends in Ecology & Evolution* 29 (6): 301–2.

López-García, P, and D Moreira. 2002. "The Syntrophy Hypothesis for the Origin of Eukaryotes." In *Symbiosis*, edited by Joseph Seckbach, 131–46. Cellular Origin, Life in Extreme Habitats and Astrobiology 4. Springer Netherlands.

Lovley, Derek R. 1985. "Minimum Threshold for Hydrogen Metabolism in Methanogenic Bacteria." *Applied and Environmental Microbiology* 49 (6): 1530–31.

Lyly, Mikko, Juha Ruokolainen, and Esko Järvinen. 1999. *Elmer - Open Source Finite Element Software for Multiphysical Problems*. Espoo, Finland: CSC. http://www.csc.fi/.

Maisonneuve, Etienne, Benjamin Ezraty, and Sam Dukan. 2008. "Protein Aggregates: An Aging Factor Involved in Cell Death." *Journal of Bacteriology* 190 (18): 6070–75.

Marcus, Ian M, Hailey A Wilder, Shanin J Quazi, and Sharon L Walker. 2013. "Linking Microbial Community Structure to Function in Representative Simulated Systems." *Applied and Environmental Microbiology* 79 (8): 2552–59.

Marr, Allen G, R J Harvey, and W C Trentini. 1966. "Growth and Division of *Escherichia Coli.*" *Journal of Bacteriology* 91 (6): 2388–89.

Marr, Allen G, E H Nilson, and D J Clark. 1963. "The Maintenance Requirement of *Escherichia Coli.*" *Annals of the New York Academy of Sciences* 102 (3): 536–48.

Martin, William, and Miklós Müller. 1998. "The Hydrogen Hypothesis for the First Eukaryote." *Nature* 392 (6671): 37–41.

Mathews, C K. 1993. "The Cell-Bag of Enzymes or Network of Channels?" *Journal of Bacteriology* 175 (20): 6377–81.

Maynard Smith, John, Noel H Smith, Maria O'Rourke, and Brian G Spratt. 1993. "How Clonal Are Bacteria?" *Proceedings of the National Academy of Sciences of the United States of America* 90 (10): 4384–88.

Maynard Smith, John, and Eörs Szathmáry. 1995. *The Major Transitions in Evolution*. Oxford: Freeman.

McInerney, James O, Mary J O'Connell, and Davide Pisani. 2014. "The Hybrid Nature of the Eukaryota and a Consilient View of Life on Earth." *Nature Reviews Microbiology* 12 (6): 449–55.

McInerney, Michael J, and Lisa M Gieg. 2004. "An Overview of Anaerobic Metabolism." In *Strict and Facultative Anaerobes: Medical and Environmental Aspects*, edited by Michiko M Nakano and Peter Zuber, 27–66. Wymondham, UK: CRC Press.

Medawar, Peter Brian. 1952. *An Unsolved Problem of Biology*. University College London: H K Lewis & Co.

Merkey, Brian V, Laurent A Lardon, Jose M Seoane, Jan-Ulrich Kreft, and Barth F Smets. 2011. "Growth Dependence of Conjugation Explains Limited Plasmid Invasion in Biofilms: An Individual-Based Modelling Study." *Environmental Microbiology* 13 (9): 2435–52.

Michaelis, Leonor, and Maud L Menten. 1913. "Die Kinetik Der Invertinwirkung." *Biochemische Zeitschrift* 49 (333-369): 352.

Miller, Lance D, Jennifer J Mosher, Amudhan Venkateswaran, Zamin K Yang, Anthony V Palumbo, Tommy J Phelps, Mircea Podar, Christopher W Schadt, and Martin Keller.

2010. "Establishment and Metabolic Analysis of a Model Microbial Community for Understanding Trophic and Electron Accepting Interactions of Subsurface Anaerobic Environments." *BMC Microbiology* 10 (1): 149.

Mir, Mustafa, Zhuo Wang, Zhen Shen, Michael Bednarz, Rashid Bashir, Ido Golding, Supriya G Prasanth, and Gabriel Popescu. 2011. "Optical Measurement of Cycle-Dependent Cell Growth." *Proceedings of the National Academy of Sciences of the United States of America* 108 (32): 13124–29.

Mitchison, John Murdoch, and P Nurse. 1985. "Growth in Cell Length in the Fission Yeast *Schizosaccharomyces Pombe.*" *Journal of Cell Science* 75 (1): 357–76.

Momeni, Babak, Adam James Waite, and Wenying Shou. 2013. "Spatial Self-Organization Favors Heterotypic Cooperation over Cheating." *eLife* 2: e00960.

Monk, Jonathan, and Bernhard O Palsson. 2014. "Predicting Microbial Growth." *Science* 344 (6191): 1448–49.

Monod, Jacques. 1949. "The Growth of Bacterial Cultures." *Annual Review of Microbiology* 3 (1): 371–94.

Mortimer, Robert K, and John R Johnston. 1959. "Life Span of Individual Yeast Cells." *Nature* 183 (4677): 1751–52.

Mösche, Marek, and Hans-Joachim Jördening. 1999. "Comparison of Different Models of Substrate and Product Inhibition in Anaerobic Digestion." *Water Research* 33 (11): 2545–54.

Moser, Anton. 1985. "Rate Equations for Enzyme Kinetics." In *Fundamentals of Biochemical Engineering*, edited by Heinz Brauer, 2:819. Biotechnology : A Comprehensive Treatise. Weinheim: Verlag Chemie.

Muralidharan, V, K D Rinker, I S Hirsh, E J Bouwer, and R M Kelly. 1997. "Hydrogen Transfer between Methanogens and Fermentative Heterotrophs in Hyperthermophilic Cocultures." *Biotechnology and Bioengineering* 56 (3): 268–78.

Neidhardt, Frederick C, and H Edwin Umbarger. 1996. "Chemical Composition of *Escherichia Coli.*" In *Escherichia Coli and Salmonella Typhimurium: Cellular and Molecular Biology*, edited by Frederick C Neidhardt and John L Ingraham, 2nd ed., 1:13–16. Washington, DC: American Society for Microbiology.

Neijssel, O M, M J T de Mattos, and D W Tempest. 1996. "Growth Yield and Energy Distribution." In Escherichia Coli *and* Salmonella Typhimurium*: Cellular and Molecular Biology*, edited by F C Neidhardt, R Curtiss III, J L Ingraham, E C C Lin, K Brooks Low, B Magasanik, W S Reznikoff, M Riley, M Schaechter, and H E Umbarger, 2:1683–92. Washington, D. C.: ASM Press.

Nyström, Thomas. 2005. "Role of Oxidative Carbonylation in Protein Quality Control and Senescence." *EMBO Journal* 24 (7): 1311–17.

Oberhardt, Matthew, and Eytan Ruppin. 2013. "Taming the Complexity of Large Models." *EMBO Reports* 14 (10): 848.

Overmann, Jörg, and Karin Schubert. 2002. "Phototrophic Consortia: Model Systems for Symbiotic Interrelations between Prokaryotes." *Archives of Microbiology* 177: 201–8.

Öztürk, Sadettin S, Bernhard O Palsson, Jurgen H Thiele, and J Gregory Zeikus. 1987. "Modeling of Interspecies Hydrogen Transfer in Microbial Flocs." In *Biotechnology Processes: Scale-up and Mixing*, edited by Chester S Ho and James Y Oldshue, 142. New York, NY, USA: American Institute of Chemical Engineers.

Periasamy, Saravanan, and Paul E Kolenbrander. 2009. "Mutualistic Biofilm Communities Develop with *Porphyromonas Gingivalis* and Initial, Early, and Late Colonizers of Enamel." *Journal of Bacteriology* 191 (22): 6804–11.

Pfeiffer, Thomas, and Sebastian Bonhoeffer. 2003. "An Evolutionary Scenario for the Transition to Undifferentiated Multicellularity." *Proceedings of the National Academy of Sciences of the United States of America* 100 (3): 1095–98.

Picioreanu, Cristian, Jan-Ulrich Kreft, and Mark C M van Loosdrecht. 2004. "Particle-Based Multidimensional Multispecies Biofilm Model." *Applied and Environmental Microbiology* 70 (5): 3024–40.

Pirt, S J. 1965. "The Maintenance Energy of Bacteria in Growing Cultures." *Proceedings of the Royal Society B* 163 (991): 224–31.

Popa, Radu, Peter K Weber, Jennifer Pett-Ridge, Juliette A Finzi, Stewart J Fallon, Ian D Hutcheon, Kenneth H Nealson, and Douglas G Capone. 2007. "Carbon and Nitrogen Fixation and Metabolite Exchange in and between Individual Cells of *Anabaena Oscillarioides*." *ISME Journal* 1 (4): 354–60.

Powell, E O. 1956. "Growth Rate and Generation Time of Bacteria, with Special Reference to Continuous Culture." *Journal of General Microbiology* 15 (3): 492–511.

———. 1958. "An Outline of the Pattern of Bacterial Generation Times." *Journal of General Microbiology* 18 (2): 382–417.

Powell, E O, and F P Errington. 1963. "Generation Times of Individual Bacteria: Some Corroborative Measurements." *Journal of General Microbiology* 31 (2): 315–27.

Powell, Godfrey E. 1984. "Equalisation of Specific Growth Rates for Syntrophic Associations in Batch Culture." *Journal of Chemical Technology and Biotechnology* 34 (2): 97–100.

———. 1985. "Stable Coexistence of Syntrophic Associations in Continuous Culture." *Journal of Chemical Technology and Biotechnology* 35B: 46–50.

———. 1986. "Stable Coexistence of Synthrophic Chains in Continuous Culture." *Theoretical Population Biology* 30 (1): 17–25.

Price, N C. 1985. "The Determination of K_m Values from Lineweaver-Burk Plots." *Biochemical Education* 13 (2): 81.

Pross, Addy, and Robert Pascal. 2013. "The Origin of Life: What We Know, What We Can Know and What We Will Never Know." *Open Biology* 3 (3).

Python Software Foundation. 2010. *Python: Version 2.7.* http://www.python.org/.

Rang, Camilla U, Annie Y Peng, and Lin Chao. 2011. "Temporal Dynamics of Bacterial Aging and Rejuvenation." *Current Biology* 21 (21): 1813–16.

Rang, Camilla U, Annie Y Peng, Art F Poon, and Lin Chao. 2012. "Ageing in *Escherichia Coli* Requires Damage by an Extrinsic Agent." *Microbiology* 158 (6): 1553–59.

Rashidi, Armin, Thomas B L Kirkwood, and Daryl P Shanley. 2012. "Evolution of Asymmetric Damage Segregation: A Modelling Approach." In *Aging Research in Yeast*, edited by Michael Breitenbach, S Michal Jazwinski, and Peter Laun, 57:315–30. Amsterdam: Springer Verlag.

Ratcliff, William C, R Ford Denison, Mark Borrello, and Michael Travisano. 2012. "Experimental Evolution of Multicellularity." *Proceedings of the National Academy of Sciences of the United States of America.*

Ratcliff, William C, Peter Hawthorne, Michael Travisano, and R Ford Denison. 2009. "When Stress Predicts a Shrinking Gene Pool, Trading Early Reproduction for Longevity Can Increase Fitness, Even with Lower Fecundity." *PLoS ONE* 4 (6): e6055.

Raynaud, Xavier, and Naoise Nunan. 2014. "Spatial Ecology of Bacteria at the Microscale in Soil." *PLoS ONE* 9 (1): e87217.

Reilly, Peter J. 1974. "Stability of Commensalistic Systems." *Biotechnology and Bioengineering* 16 (10): 1373–92.

Reshes, Galina, Sharon Vanounou, Itzhak Fishov, and Mario Feingold. 2008. "Cell Shape Dynamics in *Escherichia Coli*." *Biophysical Journal* 94 (1): 251–64.

Robert, Lydia, Marc Hoffmann, Nathalie Krell, Stéphane Aymerich, Jérôme Robert, and Marie Doumic. 2014. "Division in *Escherichia Coli* Is Triggered by a Size-Sensing rather than a Timing Mechanism." *BMC Biology* 12 (1): 17.

Robinson, J A, and James M Tiedje. 1983. "Nonlinear Estimation of Monod Growth Kinetic Parameters from a Single Substrate Depletion Curve." *Applied and Environmental Microbiology* 45 (5): 1453–58.

Robinson, Joseph A, and James M Tiedje. 1982. "Kinetics of Hydrogen Consumption by Rumen Fluid, Anaerobic Digestor Sludge, and Sediment." *Applied and Environmental Microbiology* 44 (6): 1374–84.

———. 1984. "Competition between Sulfate-Reducing and Methanogenic Bacteria for H_2 under Resting and Growing Conditions." *Archives of Microbiology* 137 (1): 26–32.

Roff, Derek A. 2008. "Defining Fitness in Evolutionary Models." *Journal of Genetics* 87 (4): 339–48.

Rosselló-Mora, Ramon, and Rudolf Amann. 2001. "The Species Concept for Prokaryotes." *FEMS Microbiology Reviews* 25 (1): 39–67.

Russell, James B, and Gregory M Cook. 1995. "Energetics of Bacterial Growth: Balance of Anabolic and Catabolic Reactions." *Microbiological Reviews* 59 (1): 48–62.

Schaechter, M, Joan P Williamson, J R Hood, and Arthur L Koch. 1962. "Growth, Cell and Nuclear Divisions in Some Bacteria." *Journal of General Microbiology* 29 (3): 421–34.

Schauer, Neil L, David P Brown, and James G Ferry. 1982. "Kinetics of Formate Metabolism in *Methanobacterium Formicicum* and *Methanospirillum Hungatei.*" *Applied and Environmental Microbiology* 44 (3): 549–54.

Schauer, Neil L, and James G Ferry. 1980. "Metabolism of Formate in *Methanobacterium Formicicum.*" *Journal of Bacteriology* 142 (3): 800–807.

Schink, Bernhard. 1992. "Syntrophism among Prokaryotes." In *The Prokaryotes*, edited by A T Ballows, Martin Dworkin, and Karl-Heinz Schleifer, 2nd ed., 276–99. New York: Springer.

———. 1997. "Energetics of Syntrophic Cooperation in Methanogenic Degradation." *Microbiology and Molecular Biology Reviews* 61 (2): 262–80.

Schönheit, Peter, Johanna Moll, and Rudolf K Thauer. 1980. "Growth Parameters (K_S, M_{max}, Y_S) of *Methanobacterium Thermoautotrophicum.*" *Archives of Microbiology* 127 (1): 59–65.

Searcy, Dennis G. 2003. "Metabolic Integration during the Evolutionary Origin of Mitochondria." *Cell Research* 13 (4): 229–38.

Seitz, Hans-Jürgen, Bernhard Schink, and Ralf Conrad. 1988. "Thermodynamics of Hydrogen Metabolism in Methanogenic Cocultures Degrading Ethanol or Lactate." *FEMS Microbiology Letters* 55 (2): 119–24.

Senn, Heinrich, Urs Lendenmann, Mario Snozzi, Geoffrey Hamer, and Thomas Egli. 1994. "The Growth of *Escherichia Coli* in Glucose-Limited Chemostat Cultures: A Re-Examination of the Kinetics." *Biochimica et Biophysica Acta (BBA) - General Subjects* 1201 (3): 424–36.

Seth, Erica Christine, and Michiko E Taga. 2014. "Nutrient Cross-Feeding in the Microbial World." *Frontiers in Microbiology* 5: 350.

Shapiro, James A. 1998. "Thinking about Bacterial Populations as Multicellular Organisms." *Annual Reviews in Microbiology* 52 (1): 81–104.

Shapiro, Lucy, H H McAdams, and R Losick. 2009. "Why and How Bacteria Localize Proteins." *Science* 326 (5957): 1225–28.

Shimoyama, Takefumi, Souichiro Kato, Shun'ichi Ishii, and Kazuya Watanabe. 2009. "Flagellum Mediates Symbiosis." *Science* 323 (5921): 1574–1574.

Shuler, M L, S Leung, and C C Dick. 1979. "A Mathematical Model for the Growth of a Single Bacterial Cell." *Annals of the New York Academy of Sciences* 326 (1): 35–52.

Smith, Hal L, and Paul Waltman, eds. 1995. *The Theory of the Chemostat*. Cambridge Studies in Mathematical Biology 13. Cambridge University Press.

Sørensen, K. B., K. Finster, and N. B. Ramsing. 2001. "Thermodynamic and Kinetic Requirements in Anaerobic Methane Oxidizing Consortia Exclude Hydrogen, Acetate, and Methanol as Possible Electron Shuttles." *Microbial Ecology* 42 (1): 1–10.

Soyer, Orkun S, and Maureen A O'Malley. 2013. "Evolutionary Systems Biology: What It Is and Why It Matters." *BioEssays*.

Spokoini, Rachel, Ofer Moldavski, Yaakov Nahmias, Jeremy L England, Maya Schuldiner, and Daniel Kaganovich. 2012. "Confinement to Organelle-Associated Inclusion Structures Mediates Asymmetric Inheritance of Aggregated Protein in Budding Yeast." *Cell Reports* 2 (4): 738–47.

Stams, Alfons J M. 1994. "Metabolic Interactions between Anaerobic Bacteria in Methanogenic Environments." *Antonie van Leeuwenhoek* 66 (1-3): 271–94.

Stams, Alfons J M, Frank A M De Bok, Caroline M Plugge, Miriam H A Van Eekert, Jan Dolfing, and Gosse Schraa. 2006. "Exocellular Electron Transfer in Anaerobic Microbial Communities." *Environmental Microbiology* 8 (3): 371–82.

Stewart, Eric J, Richard Madden, Gregory Paul, and François Taddei. 2005. "Aging and Death in an Organism That Reproduces by Morphologically Symmetric Division." *PLoS Biology* 3 (2): e45.

Stouthamer, A H. 1979. "The Search for Correlation between Theoretical and Experimental Growth Yields." In *International Review of Biochemistry*, edited by J R Quayle, 21:1–47. Baltimore: University Park Press.

Tan, Kheng H, Christine A Seers, Stuart G Dashper, Helen L Mitchell, James S Pyke, Vincent Meuric, Nada Slakeski, et al. 2014. "*Porphyromonas Gingivalis* and *Treponema Denticola* Exhibit Metabolic Symbioses." *PLoS Pathogens* 10 (3): e1003955.

Tan, Yunhu, Zhi-Xin Wang, René P Schneider, and Kevin C Marshall. 1994. "Modeling Microbial-Growth - a Statistical Thermodynamic Approach." *Journal of Biotechnology* 32: 97–106.

Thauer, Rudolf K, Anne-Kristin Kaster, Henning Seedorf, Wolfgang Buckel, and Reiner Hedderich. 2008. "Methanogenic Archaea: Ecologically Relevant Differences in Energy Conservation." *Nature Reviews Microbiology* 6 (8): 579–91.

Thiele, Jurgen H, M Chartrain, and J Gregory Zeikus. 1988. "Control of Interspecies Electron Flow during Anaerobic Digestion: Role of Floc Formation in Syntrophic Methanogenesis." *Applied and Environmental Microbiology* 54 (1): 10–19.

Thiele, Jurgen H, and J Gregory Zeikus. 1988. "Control of Interspecies Electron Flow during Anaerobic Digestion: Significance of Formate Transfer versus Hydrogen Transfer during Syntrophic Methanogenesis in Flocs." *Applied and Environmental Microbiology* 54 (1): 20–29.

Tilman, David. 1982. *Resource Competition and Community Structure*. New Jersey: Princeton University Press.

Turner, R D, E C Ratcliffe, R Wheeler, R Golestanian, J K Hobbs, and S J Foster. 2010. "Peptidoglycan Architecture Can Specify Division Planes in *Staphylococcus Aureus*." *Nature Communications* 1: 26.

Tyedmers, Jens, Axel Mogk, and Bernd Bukau. 2010. "Cellular Strategies for Controlling Protein Aggregation." *Nature Reviews Molecular Cell Biology* 11 (11): 777–88.

Unruh, Jay R, Brian D Slaughter, and Rong Li. 2013. "Quality Control: Putting Protein Aggregates in a Bind." *Current Biology* 23 (2): R74–76.

Van Sylke, Donald D, and Glenn E Cullen. 1914. "The Mode of Action of Urease and of Enzymes in General." *Journal of Biological Chemistry* 19 (2): 141–80.

Veening, Jan-Willem, Eric J Stewart, Thomas W Berngruber, François Taddei, Oscar P Kuipers, and Leendert W Hamoen. 2008. "Bet-Hedging and Epigenetic Inheritance in Bacterial Cell Development." *Proceedings of the National Academy of Sciences of the United States of America* 105 (11): 4393–98.

Visick, Jonathan E, and Steven Clarke. 1995. "Repair, Refold, Recycle: How Bacteria Can Deal with Spontaneous and Environmental Damage to Proteins." *Molecular Microbiology* 16 (5): 835–45.

Visscher, William M, and M Bolsterli. 1972. "Random Packing of Equal and Unequal Spheres in Two and Three Dimensions." *Nature* 239 (5374): 504–7.

Wang, Ping, Lydia Robert, James Pelletier, Wei Lien Dang, Francois Taddei, Andrew Wright, and Suckjoon Jun. 2010. "Robust Growth of *Escherichia Coli*." *Current Biology* 20: 1099–1103.

Watson, J D, and F H C Crick. 1953. "Molecular Structure of Nucleic Acids: A Structure for Deoxyribose Nucleic Acid." *Nature* 171 (4356): 737–38.

Watve, Milind, Sweta Parab, Prajakta Jogdand, and Sarita Keni. 2006. "Aging May Be a Conditional Strategic Choice and Not an Inevitable Outcome for Bacteria." *Proceedings of the National Academy of Sciences of the United States of America* 103 (40): 14831–35.

Winkler, Juliane, Anja Seybert, Lars König, Sabine Pruggnaller, Uta Haselmann, Victor Sourjik, Matthias Weiss, Achilleas S Frangakis, Axel Mogk, and Bernd Bukau. 2010. "Quantitative and Spatio-Temporal Features of Protein Aggregation in *Escherichia Coli* and Consequences on Protein Quality Control and Cellular Ageing." *EMBO Journal* 29 (5): 910–23.

Wirtz, Kai W. 2002. "A Generic Model for Changes in Microbial Kinetic Coefficients." *Journal of Biotechnology* 97 (2): 147–62.

Wise, D L, and G Houghton. 1966. "The Diffusion Coefficients of Ten Slightly Soluble Gases in Water at 10–60°C." *Chemical Engineering Science* 21 (11): 999–1010.

Wu, Wei-Min, Mahendra K Jain, and J Gregory Zeikus. 1994. "Anaerobic Degradation of Normal- and Branched-Chain Fatty Acids with Four or More Carbons to Methane by a Syntrophic Methanogenic Triculture." *Applied and Environmental Microbiology* 60 (7): 2220–26.

Yamamuro, Ayaka, Atsushi Kouzuma, Takashi Abe, and Kazuya Watanabe. 2014. "Metagenomic Analyses Reveal the Involvement of Syntrophic Consortia in Methanol/electricity Conversion in Microbial Fuel Cells." *PLoS ONE* 9 (5): e98425.

Yoshida, Takehito, Laura E Jones, Stephen P Ellner, Gregor F Fussmann, and Nelson G Hairston. 2003. "Rapid Evolution Drives Ecological Dynamics in a Predator–prey System." *Nature* 424 (6946): 303–6.

Zarecki, Raphy, Matthew A Oberhardt, Keren Yizhak, Allon Wagner, Ella Shtifman Segal, Shiri Freilich, Christopher S Henry, Uri Gophna, and Eytan Ruppin. 2014. "Maximal Sum of Metabolic Exchange Fluxes Outperforms Biomass Yield as a Predictor of Growth Rate of Microorganisms." *PLoS ONE* 9 (5): e98372.

Zeikus, J G. 1980. "Chemical and Fuel Production by Anaerobic Bacteria." *Annual Review of Microbiology* 34 (1): 423–64.

Zhu, Ying, Stuart G Dashper, Yu-Yen Chen, Simon Crawford, Nada Slakeski, and Eric C Reynolds. 2013. "*Porphyromonas Gingivalis* and *Treponema Denticola* Synergistic Polymicrobial Biofilm Development." *PLoS ONE* 8 (8): e71727.